Oxidation and Emission of Volatile Organic Compounds Indoors

By

Caleb M. Arata

A dissertation submitted in partial satisfaction of the
requirements for the degree of
Doctor of Philosophy
in
Chemistry
In the
Graduate Division
Of the
University of California, Berkeley

Committee in charge:

Professor Allen H. Goldstein
Professor Ronald C. Cohen
Professor Evan Williams
Professor Joshua Apte

Summer 2020

Abstract

Oxidation and Emission of Volatile Organic Compounds Indoors

By

Caleb M. Arata

Doctor of Philosophy in Chemistry

University of California, Berkeley

Professor Allen H. Goldstein, Co-Chair
Professor Ronald C. Cohen, Co-Chair

The vast majority of earth's atmosphere is outside, yet humans spend ~90% of their time indoors so the air they breathe is dominantly indoor air. Indoor air differs substantially from outdoor air in terms of its organic chemical composition and transformation processes, driven by key features including lower oxidant levels, less intense sunlight, higher surface area to volume environment, and more direct human influence While this dissertation looks at indoor air at a variety of scales, a consistent focus is that the human occupant is a defining feature of indoor air. This dissertation investigates how human activity affects indoor oxidant levels, how the human body directly influences the composition of indoor volatile organic compounds (VOCs), and how human activities control the emission of VOCs into the indoor environment.

Chapter 1 introduces the motivation for this work, provides a brief overview of key issues in atmospheric chemistry associated with the study of indoor air, reviews key prior knowledge of indoor air VOCs and oxidants that set the groundwork for the following chapters. A brief description of the instrumentation used to measure indoor VOCs is discussed, and a roadmap to this dissertation is provided.

In Chapter 2 we present direct indoor measurements of the nitrate radical (NO_3) and dinitrogen pentoxide (N_2O_5) produced from combustion cooking emissions in a residential kitchen. The presence and importance of NO_3 indoors had been hypothesized as early as 1986, however this chapter presents the first ever direct measurement made indoors. When indoor ozone (O_3) concentration was low (~4 ppbv), nitric oxide (NO) emitted from gas-stove combustion suppressed NO_3 formation. However, at moderate O_3 levels (~40 ppbv), measured NO_3 concentrations reached 3 to 4 pptv, and the indoor NO_3 reactivity loss rate coefficient reached 0.8 s^{-1}. A box model of known chemistry agrees with the reactivity estimate and shows that moderate O_3 levels led to a nitrate radical production rate of 7 ppbv h^{-1}. These indoor NO_3 production rates and reactivities are much higher than is typical outdoors. At low O_3 levels indoor combustion suppresses nitrate radical chemistry, but when sufficient O_3 enters residences from outdoors or is emitted directly from indoor sources, gas stove combustion emissions promote indoor NO_3 chemistry. Therefore in polluted regions with high levels of ozone, indoor NO_3 chemistry will take on a greater importance.

Chapter 3 presents a laboratory study of the ozonolysis of squalene, a major component of human skin oil. Rather than directly study skin oil, oxidation experiments are carried out on pure squalene particles passing through a flow tube reactor, allowing for the quantification of gas phase products from a single starting material with varying conditions of water vapor and O_3. Previous work examining the condensed-phase products of pure squalene particle ozonolysis in a flow tube reactor found that an increase in water vapor concentration led to lower concentrations of secondary ozonides, increased concentrations of carbonyls, and smaller particle diameter, suggesting that water changes the fate of the Criegee intermediate. To determine if this loss of volume corresponds to an increase in gas-phase products, we measured gas-phase VOC concentrations via proton transfer reaction time of flight mass spectrometry (PTR-TOF-MS). Studies were conducted at atmospherically relevant O_3 exposure levels (5-30 ppb h).

An increase in water vapor concentration led to strong enhancement of gas-phase oxidation products at all tested O_3 exposures. An increase in water vapor from ~0% to 70% relative humidity (RH) at high O_3 exposure increased the total mass concentration of gas-phase VOCs by a factor of three. The observed fraction of carbon in the gas phase correlated well with the fraction of particle volume lost. Experiments involving O_3 oxidation of shirts soiled with skin oil confirms that the RH dependence of gas-phase reaction product generation occurs similarly on surfaces containing skin oil under realistic indoor conditions. Relative humidity changes the fate of the Criegee intermediates and the volatility of the oxidation products, resulting in a RH dependence of the product distribution and amount of gas-phase VOCs emitted from ozonolysis of unsaturated carbon bonds in skin oil. Similar behavior is expected for O_3 reactions with surface bound organics containing unsaturated carbon bonds.

Chapter 4 presents VOC emission profiles from scripted cooking, cleaning and human occupancy experiments performed during the HOMEChem study at the University of Texas, Austin test house. Quantifying indoor VOC speciation and emissions is critical to understanding and modeling the processes controlling indoor concentration dynamics, human exposure, and the chemistry of indoor air. Much of previous research on indoor VOCs has utilized broad surveys of different structures with low time resolution measurements of concentrations for specific target compounds. Such studies necessarily average over the dynamics driven by events and processes controlling variability in concentrations, and focus on the resulting concentrations rather than the actual emission rates. This study was designed to quantify VOC emission profiles from the building and its contents, and from the scripted experiments with multiple replicates. Measurements of VOCs were performed with a PTR-TOF-MS which continuously measured the time-resolved mass spectrum of indoor and outdoor air. Continuous tracer releases enabled determination of air change rates (ACR) and thus calculation of speciated, time resolved net VOC emissions. The building and its contents were the dominant emission source into the house, with large emissions of acetic acid, methanol, and formic acid. Cooking emissions are greater than cleaning emissions, and comprised mainly of ethanol. Bleach cleaning leads to high emissions of reactive chlorinated compounds, while cleaning with a natural product emits predominantly monoterpenes and terpenoids. Emissions from occupancy experiments show large enhancements of siloxanes from personal care products in the morning which are nearly depleted by the afternoon when the products had already mostly evaporated. These results are used to construct VOC emissions for a hypothetical 24 hours, and show emissions from the house and its contents make up nearly half of the indoor VOC emissions, while the rest come from occupants and their typical activities.

In Chapter 5 we provide preliminary evidence that indoor emissions escaping to outdoors are an increasingly important fraction of the fuel for outdoor air pollution in urban areas of developed countries, and suggest this as a promising new research direction for the field of atmospheric chemistry and air pollution control.

Dedication and Acknowledgments

Allen, I could not imagine a better advisor or advocate. Marlene, this is yours as much as it is mine; I'll never forget you married a graduate student. My lab mates, I cannot wait until we can have lunch again. Robin, you always make it happen and show infinite patience for my bumbling and rambling. Kathy and David, you taught me to find a passion. Jane and Bob, you made that possible. Dylan and Lauren, I was never alone in the Bay Area. Matt and AJ, you taught me the meaning of scholarship. Finally, a heartfelt acknowledgment to all of my coauthors and collaborators.

Table of Contents

1. INTRODUCTION 1

1.1. Indoor oxidants 1
1.2. Indoor VOCs 2
1.3. The nitrate radical indoors 3
1.4. Effects of humidity on the oxidation products of skin oil 4
1.5. Indoor VOC emissions from occupancy and activities 4
1.6. References 5

2. MEASUREMENT OF NO_3 AND N_2O_5 IN A RESIDENTIAL KITCHEN 10

2.1. Abstract 10
2.2. Introduction 10
2.3. Materials and Methods 11
2.4. Results and Discussion 12
2.5. Acknowledgments 18
2.6. References 18
2.7. Supporting Information 21

3. HETEROGENEOUS OZONOLYSIS OF SQUALENE: GAS-PHASE PRODUCTS DEPEND ON WATER VAPOR CONCENTRATION 23

3.1. Abstract 23
3.2. Introduction 23
3.3. Experimental Methods 24
3.4. Results and Discussion 26
3.5. Acknowledgements 35
3.6. References 36
3.7. Supporting Information 40

4. VOLATILE ORGANIC COMPOUND EMISSIONS DURING HOMECHEM 49

4.1. Abstract 49
4.2. Introduction 49
4.3. Methods 51
4.4. Results and Discussion 54
4.5. Conclusion 67
4.6. Acknowledgements 68
4.7. References 68
4.8. Supporting Information 72

5. FUTURE WORK 99

5.1. Indoor Air as Outdoor Pollutant 99
5.2. Continued Work Indoors 103
5.3. References ..... **Error! Bookmark not defined.**

1. Introduction

Prior to ~8 years ago, atmospheric chemistry and indoor air largely existed as independent fields. Atmospheric chemists had built high tech instrumentation and models to probe the chemistry of the troposphere and stratosphere, and indoor air scientists had a sophisticated understanding of the dynamics of indoor air and its relationship to buildings and occupants, with modest knowledge of chemical emissions and dynamic behavior. Beginning in 2013, the Sloan Foundation's Chemistry of Indoor Environments program sought to "bring atmospheric chemistry home," pairing atmospheric chemists and their sophisticated instrumentation with indoor scientists and their knowledge of indoor systems. This dissertation represents early work in this ongoing collaboration between these fields with the goal of blurring the line between the two.

Humans spend approximately 90% of their lives indoors.[1] This fact, evoked at the beginning of each chapter (and in many of the works cited) is used to emphasize our level of exposure to indoor air. Perhaps less obvious, though, is the implication that humans are nearly as defining a feature of the indoors as walls and a roof. With this in mind, the following chapters explore the composition and chemistry of indoor air. We begin with a brief overview of oxidants and volatile organic compounds (VOCs) as they relate to indoor spaces. Chapter 2 shows how combustion cooking emissions combine with ozone from the outdoors to alter the indoor oxidative environment. Chapter 3 probes the effect of humidity on the chemistry of heterogenous oxidation using a component of human skin oil as the model reactant. And in Chapter 4 speciated indoor VOC emissions from human occupancy and activity are compared to "background" emissions from a house and its contents.

Indoor air is an important route of pollution exposure. A major concern for air pollution indoors is elevated concentrations of VOCs.[2–4] The VOC composition of indoor air is governed by infiltration of outdoor air, indoor emissions, physical loss processes, and indoor chemical transformations. Understanding indoor oxidant concentration and composition is critical to understanding indoor chemical transformations.

1.1. Indoor oxidants

Indoor air chemical transformations, i.e. the making and breaking of bonds, begins with the oxidation of indoor organic compounds. While there are likely more than 100,000 unique organic compounds in the atmosphere, there are only three main oxidants: the nitrate radical (NO_3), ozone (O_3), and the hydroxy radical (OH).[5] Additionally, new research suggests reactive Cl species may play an important role in indoor oxidation following bleach cleaning.[6,7]

The NO_3 radical is produced from the reaction of O_3 with nitrogen dioxide (NO_2). Outdoors and during the daytime, NO_3 is quickly lost to photolysis but at nighttime concentrations can build and NO_3 begins to oxidize VOCs. The prominence of this oxidant in the absence of sunlight led to speculation of its importance indoors.[8] Nazaroff and Cass (1986) developed a mathematical model of indoor air pollution in an art gallery, predicting NO_3 concentrations of 2-5 ppt

depending on model parameters.[9] Chapter 2 of this dissertation reports an indoor NO_3 concentration of 3-4 ppt, the first direct NO_3 measurement indoors, only 32 years later.

Easily measured, O_3 is the most broadly studied indoor oxidant. The dominant source of indoor O_3 is transport from the outdoors though some appliances such as photocopiers, laser printers, or air purifiers can emit O_3.[10–12] Indoor O_3 concentrations are commonly 20-70% of outdoor levels depending on the building air-change-rate (ACR), air handling system, and the nature of indoor surfaces.[10] Compared to NO_3 or OH, O_3 is relatively unreactive allowing for its transport indoors as well as much higher indoor concentrations and longer lifetimes. Although the reaction of O_3 with most indoor organic compounds is thermodynamically favorable, only the oxidation of unsaturated carbon-carbon bonds is fast enough to compete with removal air exchange with the outdoors.[10] This selectivity means that O_3 loss from homogenous reactions with gas-phase VOCs is typically small compared to loss from heterogenous surface reactions. Indoor environments have a surface-area-to-volume ratio much greater than outdoors, so it is no surprise that heterogenous reactions take on an increased prominence.[13,14]

Indoor OH is generated by ozonolysis reactions, air cleaners, or the photolysis of HONO.[15–18] The photolysis of O_3 by sunlight, a major outdoor OH production pathway, does not generally occur indoors as windows attenuate the wavelengths of light necessary for this reaction.[19] The short lifetime of OH (< 1s) prevents significant transport to the indoors. Predicted indoor concentrations of OH typically fall between 1-5 x 10^5 molecules cm^{-3}, about an order of magnitude lower than outdoor midday concentrations but still greater than outdoor nighttime OH levels.[15,16,20,21] Indoor OH measurements are somewhat scarce, and typically involve manipulation to overcome detection limits. In a commercial building with elevated (but realistic) monoterpene and O_3, Weschler and Shields (1997) report an indoor OH concentration of 7 x 10^5 molecules cm^{-3}.[16] Carslaw *et al.* (2017) find indoor OH levels at or below a 6.5 x 10^5 molecules cm^{-3} limit of detection, but the use of an ozone generating air "cleaner" can raise concentrations as high as 2 x 10^7 molecules cm^{-3}.[17] Alvarez *et al.* (2013) report OH concentrations up to 1.8 x 10^6 molecules cm^{-3} in a classroom.[18] Additionally, they show that production of OH from ozonolysis of alkenes is insufficient to reach the observed concentrations and indoor photolysis of nitrous acid (HONO) is an important source of OH.

1.2. Indoor VOCs

Volatile organic compounds enter the gas phase in a reduced state. Over one or more generations of oxidation VOCs are eventually oxidized to CO_2 or functionalized to a low enough volatility that it is deposited on particles or surfaces.[5]

Sources of indoor VOCs include infiltration from the outdoors, chemical production, or emissions indoors. VOC concentrations are generally much higher indoors than out, suggesting infiltration is typically a minor source.[2,4,22–24] Emissions can be split into two categories: primary emissions, the physical emission of a compound into indoor air (such as ethanol evaporating from a surface), and secondary emissions, emissions due to a chemical transformation (such as a compound formed from heterogenous oxidation that is subsequently volatilized). An area of specific concern is emissions from occupants themselves.[25] Whether through primary or secondary emissions, occupants influence the chemistry of indoor air.

Due to analytical constraints of sampling and typical chromatographic methods, many prior VOC emission studies of buildings, building materials, and furnishings have focused on a target set of compounds, such as formaldehyde or BTEX (benzene, toluene, ethylbenzene, and xylene).[26–28] Recent advances in chemical ionization mass spectrometry allow for real-time, speciated measurements of tens to hundreds of indoor VOCs.[2,4,29–33] Proton transfer reaction time-of-flight mass spectrometry (PTR-TOF-MS) is one such technique. PTR is a chemical ionization technique with minimal fragmentation using H_3O^+ as the reagent ion. PTR-TOF-MS provides mixing ratio measurements of VOCs with a gas basicity greater than that of water, namely alkenes and oxygenated VOCs as well as some halogenated species. It is not sensitive to most alkanes due to their low proton affinity. The mass measuring accuracy of PTR-TOF-MS allows for unambiguous assignment of chemical formulae, however the compound assignment is often not unique as isomeric compounds cannot be differentiated (20 ppm mass accuracy, unambiguous formula assignment up to ~120 Da). An advantage of PTR-TOF-MS over other forms of chemical ionization is the low variability of the rate constant for the proton transfer reaction with VOCs: choosing a default value of 2.5×10^{-9} cm^3 s^{-1} allows for the conversion of counts per second to ppb for a vast array of detectable species with an accuracy of +/- 50%.[34]

1.3. The nitrate radical indoors

Chapter 2 presents measurements of the NO_3 radical and N_2O_5 in a residential kitchen. Nøjgaard (2010) had previously measured the sum of these compounds in an office building, but here is provided the first speciated indoor measurement.[35] Perhaps more important than quantifying the concentration of NO_3 is the limitations found on its indoor production: ozone levels must be sufficiently high to convert nearly all NO to NO_2, as well as produce NO_3 from NO_2. The NO_3 radical can react with NO to form NO_2, or react with VOCs to form oxidation products. It is the competition between these two reactions that determines the influence of NO_3 as an indoor oxidant.[18]

Unventilated combustion from the stove used in the experiment produced large amounts of NO which quickly titrated out O_3 and prevented the formation of NO_3. The NO_3 radical could only be detected when a commercial ozone generator was used to simulate continuous infiltration of polluted air (~40 ppb O_3). The implications for indoor oxidant levels is that NO_3 chemistry is most likely significant when either 1) Infiltration of outdoor NO, NO_2, and O_3 are in sufficient quantities to produce NO_3, or 2) Infiltration of outdoor O_3 is sufficient to titrate out combustion emitted NO and still react with NO_2 to form NO_3. Interestingly, the first scenario may occur mostly during nighttime, mimicking the nocturnal cycle of outdoor NO_3 chemistry.

In addition to measurements of NO_3 and N_2O_5, a box model is constructed to determine the production rate of NO_3 and compare the various loss processes of the reactive nitrogen. Nazaroff and Weschler (2004) identified potentially large amounts of NO_3 oxidation of terpenoid compounds emitted from cleaning products, so limonene was added to the model to match the monoterpene levels found in the kitchen during the stove experiments.[36] Additional VOC reactivity was added to the model until the steady state concentration of NO_3 matched the experimental value. Indoor nitrate reactivity was found to be 0.8 s^{-1}, an order of maginitude larger than seen in outdoor, urban influenced air.[37] Model results indicated that once NO was sufficiently titrated, 80-90% of NO_3 loss was through the oxidation of VOCs. Additionally, NO_3 oxidation of limonene outpaced O_3 oxidation of the terpene.

1.4. Effects of humidity on the oxidation products of skin oil

Human skin secretes unsaturated lipids and oils that react with O_3 to form volatile products. In cases of high occupancy this heterogenous reaction with skin, hair, and skin oil infused clothing can be the dominant indoor sink for O_3.[38] Additionally, the volatile products released from these reactions can comprise a significant fraction of indoor VOCs, some of which are known irritants.[39–42]

Chapter 3 presents a flow tube oxidation study of squalene, an unsaturated compound that comprises 10% of the mass of human skin lipids and 50% of the unsaturated bonds.[43] A previous study of oxidation of pure squalene particles showed that changes in humidity did not change reaction kinetics but did change the resulting product composition.[44] In the model developed by Heine *et al.* (2017), increased water vapor concentration promoted the formation of volatile carbonyl compounds over the production of less volatile secondary ozonides. Chapter 3 reports measurements of the gas phase compounds emitted from the heterogeneous ozonolysis of pure squalene particles, showing that increases in humidity from ~0% to 70% RH increase gas phase products 3 fold. Further confirming the results, the increased amount of C observed as gas phase VOC products correlates well with the particle volume lost as humidity increases.

To confirm the results of the flow tube experiment, T-shirts soiled with skin oil were exposed to ozone in an environmental chamber with varying levels of humidity. Consistent with the flow tube results, increases in humidity lead to increases in VOC skin oxidation products. Humidity is already known to influence indoor VOC concentrations, but few studies have assessed how it influences ozonolysis.[45–49] The results presented in Chapter 3 suggest that water vapor concentration can significantly alter the composition of indoor air through altering the fate of ozone reactions with surface bound organic molecules. While these results are from experiments with squalene, the underlying mechanism could apply to any unsaturated compounds, with gas-phase consequences largest for compounds with carbon-carbon double bonds separating small moieties.

1.5. Indoor VOC emissions from occupancy and activities

Chapter 4 reports VOC emissions from occupant activities (cooking, cleaning), occupancy, and the building and its contents. Scripted activities were performed at the University of Texas at Austin's UTest house, a 110 m^2 manufactured home modified for indoor experiments.[50] Multiple replicates of cooking, cleaning, and varying occupancy provides robust speciated emission profiles. A day of uninterrupted vacancy provides "background" VOC emissions from the building and its contents.

Activities show distinct chemical emissions: cooking is dominated by ethanol, bleach cleaning by chlorinated compounds, and "natural" product cleaning by terpenoids. While cooking events had the largest emissions, 250 mg VOC per event, the dominant species (ethanol, acetic acid, and methanol) are not particularly reactive. Bleach cleaning emits 38 mg of VOC per event, of which 32 mg are chloramine compounds. These secondary emissions, formed by the oxidation of nitrogen containing compounds, are known respiratory irritants with links to asthma.[51–54] Cleaning with a "natural" based cleaner emits 12 mg of monoterpenes per event. We find the

loss rate of these terpenes to be consistent with transport outdoors, rather than chemical loss indoors. Once outdoors, they become precursors to photochemical smog and secondary organic aerosol (SOA).

Occupancy experiments were designed to vary the level of personal care product (PCP) usage. In cases of high occupancy, such as a classroom, occupants with their associated personal care products (PCP) can be the dominant source of VOCs.[55] We find PCP usage can drastically change the total VOC emissions per person, but perhaps more important is the time since last application: by the afternoon most products applied in the morning had been completely depleted from occupants.

Total emissions from the unoccupied house were 49 mg h^{-1}, with acetic acid, methanol, and formic acid making up half of the emissions and 219 distinct ion signals comprising the other half. Compared to occupancy and activity emissions, unoccupied emissions are quite large. Taking the emissions reported in Chapter 4 and constructing a hypothetical day of cooking 3 meals, mopping once with bleach, and an occupancy level of 3 people, a total of 2600 mg of VOC is emitted into the house. The house and its contents contribute 45% of these emissions, the largest single source.

These VOC emissions are at least partially transported to the outdoors. This dissertation concludes in Chapter 5 by providing preliminary data addressing the effect of indoor emissions being transported to the outdoors, and laying out the logical next steps for this research. VOC fluxes from the indoors to the outdoors are presented, showing that the total VOC flux from a house can match biogenic emissions from a pine forest on a per area basis. Time resolved measurements of the emission of OH reactivity to the outdoors show that occupant activities substantially increase emitted reactivity. In future research, the VOC measurements reported in Chapter 4, along with previous measurements at two normally occupied northern California homes will be used to build an estimation of OH reactivity transported from indoors to outdoors. Field experiments measuring urban VOCs using car-based platforms, flux towers, and aircraft will be compared to these bottom up estimates.

1.6. References

1. Klepeis NE, Nelson WC, Ott WR, Robinson JP, Tsang AM, Switzer P, Behar J V, Hern SC, Engelmann WH. The National Human Activity Pattern Survey (NHAPS): a resource for assessing exposure to environmental pollutants. *J Expo Anal Environ Epidemiol*. 2001;11(3):231-252.

2. Liu Y, Misztal PK, Xiong J, Tian Y, Arata C, Weber RJ, Nazaroff WW, Goldstein AH. Characterizing sources and emissions of volatile organic compounds in a northern California residence using space-and time-resolved measurements. *Indoor Air*. 2019;29(4):630-644.

3. Jia C, Batterman S, Godwin C. VOCs in industrial, urban and suburban neighborhoods, Part 1: Indoor and outdoor concentrations, variation, and risk drivers. *Atmos Environ*. Published online 2008.

4. Duncan SM, Tomaz S, Morrison G, Webb M, Atkin J, Surratt JD, Turpin BJ. Dynamics of residential water-soluble organic gases: Insights into sources and sinks. *Environ Sci Technol*. 2019;53(4):1812-1821.

5. Goldstein AH, Galbally IE. Known and unexplored organic constituents in the earth's atmosphere. *Environ Sci Technol*. Published online 2007.

6. Schwartz-Narbonne H, Wang C, Zhou S, Abbatt JPD, Faust J. Heterogeneous Chlorination of Squalene and Oleic Acid. *Environ Sci Technol*. Published online 2019.

7. Wong JPS, Carslaw N, Zhao R, Zhou S, Abbatt JPD. Observations and impacts of bleach washing on indoor chlorine chemistry. *Indoor Air*. 2017;27(6):1082-1090.

8. Weschler CJ, Michael B, Petros K. Indoor Ozone and Nitrogen Dioxide: A Potential Pathway to the Generation of Nitrate Radicals, Dinitrogen Pentoxide, and Nitric Acid Indoors. *Environ Sci Technol*. 1992;26(1):179-184.

9. Nazaroff WW, Cass GR. Mathematical Modeling of Chemically Reactive Pollutants in Indoor Air. *Environ Sci Technol*. 1986;20(9):924-934.

10. Weschler CJ. Ozone in indoor environments: Concentration and chemistry. *Indoor Air*. 2000;10(4):269-288.

11. Britigan N, Alshawa A, Nizkorodov SA. Quantification of ozone levels in indoor environments generated by ionization and ozonolysis air purifiers. *J Air Waste Manag Assoc*. Published online 2006.

12. Lee SC, Lam S, Kin Fai H. Characterization of VOCs, ozone, and PM10 emissions from office equipment in an environmental chamber. *Build Environ*. Published online 2001.

13. Nazaroff WW, Goldstein AH. Indoor chemistry: Research opportunities and challenges. *Indoor Air*. 2015;25(4):357-361.

14. Singer BC, Hodgson AT, Hotchi T, Ming KY, Sextro RG, Wood EE, Brown NJ. Sorption of organic gases in residential rooms. *Atmos Environ*. 2007;41(15):3251-3265.

15. Weschler CJ, Shields HC. Production of the hydroxyl radical in indoor air. *Environ Sci Technol*. 1996;30(11):3250-3258.

16. Weschler CJ, Shields HC. Measurements of the hydroxyl radical in a manipulated but realistic indoor environment. *Environ Sci Technol*. 1997;31(12):3719-3722.

17. Carslaw N, Fletcher L, Heard D, Ingham T, Walker H. Significant OH production under surface cleaning and air cleaning conditions: Impact on indoor air quality. *Indoor Air*. 2017;27(6):1091-1100.

18. Gomez Alvarez E, Amedro D, Afif C, Gligorovski S, Schoemaecker C, Fittschen C, Doussin J-F, Wortham H. Unexpectedly high indoor hydroxyl radical concentrations

associated with nitrous acid. *Proc Natl Acad Sci*. 2013;110(33):13294-13299.

19. Blocquet M, Guo F, Mendez M, Ward M, Coudert S, Batut S, Hecquet C, Blond N, Fittschen C, Schoemaecker C. Impact of the spectral and spatial properties of natural light on indoor gas-phase chemistry: Experimental and modeling study. *Indoor Air*. Published online 2018.

20. Young CJ, Zhou S, Siegel JA, Kahan TF. Illuminating the dark side of indoor oxidants. *Environ Sci Process Impacts*. Published online 2019.

21. Lelieveld J, Gromov S, Pozzer A, Taraborrelli D. Global tropospheric hydroxyl distribution, budget and reactivity. *Atmos Chem Phys*. Published online 2016.

22. Zhu J, Newhook R, Marro L, Chan CC. Selected volatile organic compounds in residential air in the city of Ottawa, Canada. *Environ Sci Technol*. Published online 2005.

23. Brown SK, Sim MR, Abramson MJ, Gray CN. Concentrations of Volatile Organic Compounds in Indoor Air – A Review. *Indoor Air*. 1994;4(2):123-134.

24. Bari MA, Kindzierski WB, Wheeler AJ, Héroux MÈ, Wallace LA. Source apportionment of indoor and outdoor volatile organic compounds at homes in Edmonton, Canada. *Build Environ*. Published online 2015.

25. Weschler CJ. Roles of the human occupant in indoor chemistry. *Indoor Air*. 2016;26(1):6-24.

26. Haghighat F, De Bellis L. Material emission rates: literature review, and the impact of indoor air temperature and relative humidity. *Build Environ*. 1998;33(5):261-277.

27. Yu C, Crump D. A review of the emission of VOCs from polymeric materials used in buildings. *Build Environ*. 1998;33(6):357-374.

28. Gunschera J, Mentese S, Salthammer T, Andersen JR. Impact of building materials on indoor formaldehyde levels: Effect of ceiling tiles, mineral fiber insulation and gypsum board. *Build Environ*. 2013;64:138-145.

29. Stönner C, Edtbauer A, Williams J. Real-world volatile organic compound emission rates from seated adults and children for use in indoor air studies. *Indoor Air*. 2018;28(1):164-172.

30. Williams J, Stönner C, Wicker J, Krauter N, Derstroff B, Bourtsoukidis E, Klüpfel T, Kramer S. Cinema audiences reproducibly vary the chemical composition of air during films, by broadcasting scene specific emissions on breath. *Sci Rep*. 2016;6:25464.

31. Liu S, Thompson SL, Stark H, Ziemann PJ, Jimenez JL. Gas-phase carboxylic acids in a university classroom: Abundance, variability, and sources. *Environ Sci Technol*. 2017;51(10):5454-5463.

32. Huangfu Y, Lima NM, O'Keeffe PT, Kirk WM, Lamb BK, Pressley SN, Lin B, Cook DJ, Walden VP, Jobson BT. Diel variation of formaldehyde levels and other VOCs in homes driven by temperature dependent infiltration and emission rates. *Build Environ*. 2019;159:106153.

33. Huangfu Y, Lima NM, O'Keeffe PT, Kirk WM, Lamb BK, Walden VP, Jobson BT. Whole-House Emission Rates and Loss Coefficients of Formaldehyde and Other Volatile Organic Compounds as a Function of the Air Change Rate. *Environ Sci Technol*. 2020;54(4):2143-2151.

34. Zhao J, Zhang R. Proton transfer reaction rate constants between hydronium ion (H3O+) and volatile organic compounds. *Atmos Environ*. 2004;38:2177-2185.

35. Nøjgaard JK. Indoor measurements of the sum of the nitrate radical, NO3, and nitrogen pentoxide, N2O5 in Denmark. *Chemosphere*. 2010;79(8):898-904.

36. Nazaroff WW, Weschler CJ. Cleaning products and air fresheners: Exposure to primary and secondary air pollutants. *Atmos Environ*. 2004;38(18):2841-2865.

37. Liebmann JM, Schuster G, Schuladen JB, Sobanski N, Lelieveld J, Crowley JN. Measurement of ambient NO3 reactivity: Design, characterization and first deployment of a new instrument. *Atmos Meas Tech*. 2017;10(3):1241-1258.

38. Fischer A, Ljungström E, Langer S. Ozone removal by occupants in a classroom. *Atmos Environ*. 2013;81:11-17.

39. Wisthaler A, Tamás G, Wyon DP, Strøm-Tejsen P, Space D, Beauchamp J, Hansel A, Märk TD, Weschler CJ. Products of ozone-initiated chemistry in a simulated aircraft environment. *Environ Sci Technol*. 2005;39(13):4823-4832.

40. Anderson SE, Franko J, Jackson LG, Wells JR, Ham JE, Meade BJ. Irritancy and allergic responses induced by exposure to the indoor air chemical 4-Oxopentanal. *Toxicol Sci*. 2012;127(2):371-381.

41. Wolkoff P, Larsen ST, Hammer M, Kofoed-Sørensen V, Clausen PA, Nielsen GD. Human reference values for acute airway effects of five common ozone-initiated terpene reaction products in indoor air. *Toxicol Lett*. 2013;216(1):54-64.

42. Weschler CJ, Wisthaler A, Cowlin S, Tamás G, Strøm-Tejsen P, Hodgson AT, Destaillats H, Herrington J, Zhang J, Nazaroff WW. Ozone-initiated chemistry in an occupied simulated aircraft cabin. *Environ Sci Technol*. 2007;41(17):6177-6184.

43. Nicolaides N. Skin lipids: Their biochemical uniqueness. *Science*. 1974;186(4158):19-26.

44. Heine N, Houle FA, Wilson KR. Connecting the Elementary Reaction Pathways of Criegee Intermediates to the Chemical Erosion of Squalene Interfaces during Ozonolysis. *Environ Sci Technol*. 2017;51(23):13740-13748.

45. Markowicz P, Larsson L. Influence of relative humidity on VOC concentrations in indoor air. *Environ Sci Pollut Res*. 2015;22(8):5772-5779.

46. Huang S, Xiong J, Cai C, Xu W, Zhang Y. Influence of humidity on the initial emittable concentration of formaldehyde and hexaldehyde in building materials: Experimental observation and correlation. *Sci Rep*. 2016;6(1):23388.

47. Huang H, Haghighat F, Blondeau P. Volatile organic compound (VOC) adsorption on material: Influence of gas phase concentration, relative humidity and VOC type. *Indoor Air*. 2006;16(3):236-247.

48. Coleman BK, Destaillats H, Hodgson AT, Nazaroff WW. Ozone consumption and volatile byproduct formation from surface reactions with aircraft cabin materials and clothing fabrics. *Atmos Environ*. 2008;42(4):642-654.

49. Gall E, Darling E, Siegel JA, Morrison GC, Corsi RL. Evaluation of three common green building materials for ozone removal, and primary and secondary emissions of aldehydes. *Atmos Environ*. 2013;77:910-918.

50. Farmer DK, Vance ME, Abbatt JPD, Abeleira A, Alves MR, Arata C, Boedicker E, Bourne S, Cardoso-Saldaña F, Corsi R. Overview of HOMEChem: House observations of microbial and environmental chemistry. *Environ Sci Process Impacts*. 2019;21(8):1280-1300.

51. Thickett KM, McCoach JS, Gerber JM, Sadhra S, Burge PS. Occupational asthma caused by chloramines in indoor swimming-pool air. *Eur Respir J*. 2002;19(5):827-832.

52. Bernard A, Carbonnelle S, de Burbure C, Michel O, Nickmilder M. Chlorinated pool attendance, atopy, and the risk of asthma during childhood. *Environ Health Perspect*. 2006;114(10):1567-1573.

53. Jacobs JH, Spaan S, Van Rooy G, Meliefste C, Zaat VAC, Rooyackers JM, Heederik D. Exposure to trichloramine and respiratory symptoms in indoor swimming pool workers. *Eur Respir J*. 2007;29(4):690-698.

54. Zwiener C, Richardson SD, De Marini DM, Grummt T, Glauner T, Frimmel FH. Drowning in disinfection byproducts? Assessing swimming pool water. *Environ Sci Technol*. 2007;41(2):363-372.

55. Tang X, Misztal PK, Nazaroff WW, Goldstein AH. Volatile Organic Compound Emissions from Humans Indoors. *Environ Sci Technol*. 2016;50(23):12686-12694.

2. Measurement of NO_3 and N_2O_5 in a residential kitchen

This chapter is adapted from:
Caleb Arata, Kyle J. Zarzana, Pawel K. Misztal, Yingjun Liu, Steven S. Brown, William W Nazaroff, Allen H. Goldstein "Measurement of NO_3 and N_2O_5 in a residential kitchen" *Environmental Science & Technology Letters* **2018**, 5, 10, 595-599.

2.1. Abstract

We present direct indoor measurements of the nitrate radical (NO_3) and dinitrogen pentoxide (N_2O_5) produced from combustion cooking emissions in a residential kitchen. When indoor ozone (O_3) concentration was low (~4 ppbv), nitric oxide (NO) emitted from gas-stove combustion suppressed NO_3 formation. However, at moderate O_3 levels (~40 ppbv), measured NO_3 concentrations reached 3 to 4 pptv, and the indoor NO_3 reactivity loss rate coefficient reached 0.8 s^{-1}. A box model of known chemistry agrees with the reactivity estimate and shows that moderate O_3 levels led to a nitrate radical production rate of 7 ppbv h^{-1}. These indoor NO_3 production rates and reactivities are much higher than is typical outdoors. We conclude that at low O_3 levels indoor combustion suppresses nitrate radical chemistry, but when sufficient O_3 enters residences from outdoors or is emitted directly from indoor sources, gas stove combustion emissions promote indoor NO_3 chemistry.

2.2. Introduction

As humans commonly spend ~ 90% of their lives indoors, the chemical composition of indoor air is important for assessing total human inhalation exposures.[1] Indoor air composition is influenced by air change rates, outdoor air composition, indoor emissions, physical loss processes, and indoor chemical transformation processes. Indoor-relevant atmospheric oxidants include ozone (O_3), hydroxyl radical (OH), and nitrate radical (NO_3). Among these, NO_3 abundance is least well characterized. Ozone is easily measured, has been broadly studied indoors, is transported indoors from outside, and in some cases is emitted directly indoors.[2] Knowledge about indoor OH is emerging.[3,4] Because of its short lifetime, OH introduction from outdoors is insignificant. Production indoors may occur by ozonolysis of unsaturated volatile organic compounds (VOC), or by photolysis, under certain lighting conditions.[5–8]

The nitrate radical could be important for indoor reactions involving unsaturated VOCs, such as monoterpenes.[9,10] Monoterpene concentrations are often high indoors owing to emissions from cleaning products, air fresheners, citrus fruits, and other sources. Their oxidation is of interest because it leads to various byproducts including secondary particulate matter.[11] Nazaroff and Weschler (2004) compared expected reaction rates of indoor VOCs assuming 20 ppbv O_3, 5×10^{-3} pptv OH, and 1 pptv NO_3.[12] At these levels, for many terpenoids, indoor reactions with NO_3 would be more important than with O_3 or OH.

The NO_3 radical is produced from the reaction of O_3 with nitrogen dioxide:

$$NO_2 + O_3 \rightarrow NO_3 + O_2 \quad (1)$$

In outdoor daylight, NO_3 is lost through reaction with NO and by photolysis. Indoors, and at night outdoors, if NO concentration is low enough, NO_3 reacts with NO_2 to form N_2O_5. This formation is balanced by N_2O_5 thermal dissociation:[13]

$$NO_2 + NO_3 + M \rightarrow N_2O_5 + M \quad (2)$$
$$N_2O_5 + M \rightarrow NO_2 + NO_3 + M \quad (3)$$

The main fates of NO_3 are reaction with NO or with unsaturated VOCs, here denoted generically as X:[14]

$$NO + NO_3 \rightarrow 2\ NO_2 \quad (4)$$
$$NO_3 + X \rightarrow \text{products} \quad (5)$$

Ozone also reacts with NO to form NO_2:

$$NO + O_3 \rightarrow NO_2 + O_2 \quad (6)$$

Outdoors during daytime, sunlight rapidly photolyzes NO_2 leading to NO and O_3 regeneration. At night, absent fresh emissions and photolysis, NO is quantitatively converted to NO_2 when O_3 is in excess. Competition between NO and VOC reactions determine the influence of NO_3 as an indoor oxidant.[7] Indoors, in the absence of photolysis and in the presence of O_3, NO is depleted and NO_3 production increases. NO_3 is thought to be potentially important as an indoor oxidant.[9,10]

There have been no direct measurements of NO_3 published for indoor air. Nøjgaard reported measuring the undifferentiated sum of NO_3 and N_2O_5 between 1 and 58 pptv using an indirect technique in an office building.[15]

Unvented combustion from gas-fired stoves and ovens can be the dominant indoor NO_x (NO + NO_2) source in residences. Houses with gas-burning appliances often exceed outdoor air quality standards for NO_2.[16,17] In residences without natural gas service, portable butane stoves are widely used, as in Asia for "hot-pot" cooking.[18]

We undertook this study to determine whether ordinary activity in a residence could lead to appreciable NO_3 production relevant for indoor chemistry. Specifically, we performed experiments in a kitchen with a butane stove that emitted NO_x. In some experiments O_3 was added, mimicking expected O_3 intrusion from outdoors. The results reported here include the first direct measurement of NO_3 indoors.

2.3. Materials and Methods

2.3.1. Site Description and Instrumentation

Experiments were done in January 2017 in the kitchen of a single-family house in Oakland, California as part of a comprehensive residential air chemistry study.[19]

A teakettle containing one liter of fresh tap water was placed on a portable butane stove (Turbo Portable Stove model TS-2500), which was then ignited and operated with a high flame. When the water boiled (after ~6 min) the stove was shut off and the kettle removed from the kitchen. Except for these brief visits by a researcher, all doors were kept closed to isolate the kitchen from the remainder of the house. As a control, the same experiment was carried out using the kitchen's built-in electric stove.

Between experiments the kitchen was ventilated to restore "background" conditions by opening the two interior doors and one exterior door. Experiments were done with and without deliberate O_3 additions. An O_3 generator provided constant indoor emissions for the duration of the addition experiments. It was tuned to provide a stable concentration of 40 ppbv prior to the addition of NO_x from the butane stove.

Concentrations of NO_3 and N_2O_5 were measured by cavity ring-down spectroscopy.[20-22] Background absorption due to NO_2, O_3, and water vapor was measured every 10 minutes via addition of excess NO to the inlet to chemically destroy NO_3 via reaction (4). The background was linearly interpolated between the zero measurement periods. If background conditions change rapidly (and nonlinearly) this correction may be invalid. Consequently, for periods with quickly changing conditions (i.e., until 20 minutes after stove is extinguished), we do not report NO_3 and N_2O_5 concentration measurements. The detection limit for NO_3 was 1.5 ppt (2 sigma, 1 min). Measurements of VOCs were by proton-transfer-reaction time-of-flight mass spectrometry (Ionicon PTR-TOF-MS 8000).[19] Measurements of CO_2, NO and NO_2, and O_3 were by LICOR LI820, Thermo Scientific 42i, and Thermo Scientific 49i instruments, respectively. The decline of CO_2 concentrations after the stove was turned off was used to estimate the kitchen air-change rate during each experiment.

2.4. Results and Discussion

Six experiments were conducted over a two-day period; three used the gas stove without added O_3, two used the gas stove with added O_3, and one control used the electric stove with O_3 added. For the experiments without deliberate O_3 addition, the O_3 concentration prior to stove ignition was 5-10 ppbv and quickly dropped to below 1 ppbv following ignition. For experiments with no O_3 added, NO and NO_2 concentrations remained elevated for the duration of the experiment (at least 1 hour after stove ignition), and no NO_3 or N_2O_5 was detected. For the control in which O_3 was added, none of the measured species (NO, NO_2, NO_3, N_2O_5, CO_2) showed any response to electric stove use.

For the two experiments with added O_3 the starting concentration was 40 ppbv, maximum NO concentrations were 117 and 101 ppbv, respectively, whereas maximum NO_2 concentrations were 208 and 169 ppbv. These values are not solely indicative of the NO_2/NO_x ratio emitted from the stove, as the supplied O_3 converted some emitted NO to NO_2. (For comparison, average peak NO and NO_2 concentrations measured during the three no-ozone added experiments were 130 and 137 ppbv, respectively.) After NO was completely converted, the O_3 concentration began to rise, and N_2O_5 concentrations increased to maxima of 190 pptv in each run. Kitchen air-change rates for these runs were 1.4 and 1.0 h^{-1}.

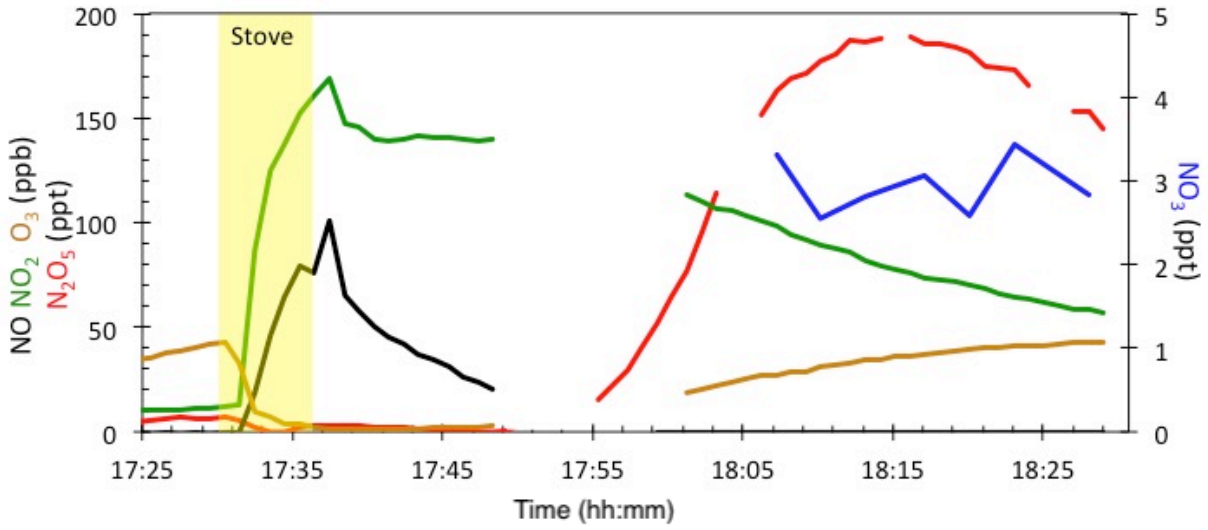

Figure 2.4.1 Concentrations of NO, NO_2, NO_3, N_2O_5, and O_3 during an ozone-added stove experiment. The yellow shaded region indicates when the stove was on.

During the first with-ozone experiment, 4 pptv of NO_3 was observed during the period from 45 min to 1 h after stove ignition. Rapid changes in background concentrations — and a 10-minute period in which NO, NO_2, and O_3 were measured outdoors rather than in the kitchen — limit our NO_3 measurements to this interval. Measurements for this experiment are shown in the Supplementary Information, Figure 2.7.1. For the second experiment, we measured 3 pptv of NO_3 beginning 45 minutes after stove ignition. This experiment had a longer period of uninterrupted measurements allowing for more accurate NO_3 measurements. The results of this experiment are used in later calculations.

Figure 2.4.1 shows the concentration measurements during the second stove experiment with added O_3. The stove was ignited at 17:30 when the O_3 concentration was 40 ppbv. The stove emitted NO and NO_2, which quickly reacted with O_3. Measurements of NO_3 are reported only after 18:05 to avoid changing conditions affecting the background determination; the N_2O_5 measurement suggests that NO_3 levels during and shortly after combustion remained very low. After NO has been almost completely reacted with O_3 to form NO_2, O_3 levels rose and N_2O_5 was observed. By 18:05, when background interferences are constant enough to make a reliable measurement, NO_3 was measured at a relatively stable concentration of 3 pptv over a 20-min duration. N_2O_5 reaches a maximum of 190 pptv at 18:15, about 40 minutes after the stove is turned off.

The delay in peak concentrations of NO_3 and N_2O_5 following cooking with the gas stove has important implications for when NO_3 can be a significant indoor oxidant. Combustion-based cooking produces enough NO to rapidly react with and remove NO_3, which will not rise to measurable concentrations until NO levels are reduced by dilution and oxidation via O_3. In the case of the stove experiments with O_3 added, the NO_3 is not observed at a measurable level until ~15 minutes after the stove is extinguished as signaled by a rising N_2O_5 level.

The presence of NO suppresses the NO_3 mixing ratio in two ways: first, it directly consumes NO_3 via reaction (4), and, second, the reaction between NO and O_3 (reaction (6)) alters the NO_3 production rate, P_{NO3}, in reaction (1). For a given O_3 level, P_{NO3} increases as reaction (6) converts NO into NO_2 until the NO_2 and O_3 mixing ratios are equal. Further consumption of O_3 then reduces P_{NO3} as NO emissions continue.

Because the presence of NO alters NO_3 production and loss, the ratio of NO_2 to NO from combustion sources influences the concentrations of NO_3 that may be attained indoors. Traynor *et al.* reported that 32% (+/- 18%) of NO_x emissions from gas stoves are in the form of NO_2 (n = 522 burners).[23] Our measurements for the portable butane stove during the experiments with no O_3 added fall in the upper portion of this range, with about half of NO_x observed as NO_2. Nitrate radical production has been predicted to occur indoors due to similarity of conditions with the outdoor environment at night (lack of NO_2 photolysis and low NO concentration), but only when O_3 is also available. Combustion increases the concentration of NO, which can directly react with NO_3 and thus suppress its concentration. With sufficient O_3 available, the NO_x emitted by combustion can lead to elevated NO_3 concentrations only after the combustion ceases to supply a fresh source of NO. The dominant source of indoor O_3 is typically transport from outdoors. In well-ventilated spaces, the indoor concentration is commonly reported to be 20-70% of the outdoor concentration.[2] Continuous influx of outdoor O_3 could potentially overcome the NO produced from combustion and lead to elevated NO_3 concentrations. Such conditions might be particularly pronounced in high O_3 areas in urban and suburban areas where many people live. Additionally, NO_3 is always produced when O_3 and NO_2 are present — although NO reacts quickly to destroy NO_3, indoor VOC concentrations could be elevated enough to compete with NO leading to high rates of VOC oxidation despite low NO_3 concentrations.

2.4.1. Indoor NO_3 Reactivity

The concentration of VOCs indoors is always many orders of magnitude greater than the concentration of NO_3 (e.g. in the present study ~10^5 times greater for total VOCs, and ~10^2 or more for monoterpenes alone). Consequently, the rate of reaction (5) can be approximated as

$$\text{Rate} = k'_x\,[\text{NO}_3] \tag{7}$$

where k'_x is the pseudo first-order rate constant for the reaction of NO_3 with VOCs. Examining Figure 2.4.1, one observes from 18:08 to 18:29 a steady NO_3 concentration of 3 pptv, implying that the production and loss rates of NO_3 are balanced during this interval:

$$P_{NO_3} = L_{NO_3} \tag{8}$$

Production of NO_3 occurs by O_3 reacting with NO_2 (reaction (1)). Loss of NO_3 can occur by two pathways: reaction with NO (reaction (4)) and oxidation of VOCs (reaction (5)). Including the equilibrium between NO_3 and N_2O_5, the steady-state balance for for NO_3 can be expressed as:

$$k_1[\text{NO}_2][\text{O}_3] + k_3[\text{N}_2\text{O}_5] = k_4[\text{NO}][\text{NO}_3] + k_2[\text{NO}_2][\text{NO}_3] + k'_x[\text{NO}_3] \tag{9}$$

Equation (9) excludes loss due to dilution or heterogeneous reactions of NO_3 or N_2O_5, which are expected to be slow compared to gas-phase chemistry for these conditions. Under conditions

where reactions (2) and (3) are in balance, equation (9) can be further simplified as:

$$k_1[NO_2][O_3] = k_4[NO][NO_3] + k'_x[NO_3] \quad (10)$$

By examining the ratio $[N_2O_5]/([NO_2][NO_3])$ for the experiment depicted in Figure 2.4.1, we determined that equilibrium was reached at 18:13 and continued until 18:30. The NO concentration was below the detection limit (and therefore assumed to be negligible) during this period. Rearranging equation (10) yields an estimate of the pseudo first-order reaction rate constant of NO_3 with VOCs:

$$k'_x = {k_1[NO_2][O_3]}/{[NO_3]} \quad (11)$$

Using measurements from 18:13 to 18:30, we find an indoor NO_3 reactivity with VOCs of k'_x = 0.8 s^{-1}. This value is an order of magnitude higher than determined for outdoor air in a forested mountain site with urban influence. [24] This large reactivity indicates that even a small concentration of NO_3 could influence indoor chemistry. The inferred reactivity rate would be consistent with 330 pptv terpinolene, or 180 pptv of α-terpinene, monoterpenes commonly found in household cleaning products.[12] Total undifferentiated monoterpene concentrations of 700 pptv were measured in the kitchen by PTR-TOF-MS during the time when NO_3 reactivity with VOCs was calculated.

With indoor O_3 and NO_3 of 40 ppbv and 3 pptv, respectively, the pseudo first-order rate constant for the reaction of terpinolene with NO_3 is about 4× faster than the rate of reaction with O_3 (7.2×10^{-3} s^{-1} compared to 1.9×10^{-3} s^{-1}), making NO_3 the dominant oxidant in this case. Both rates are significantly faster than loss by air change at 1 h^{-1} (= 0.3×10^{-3} s^{-1}).

2.4.2. Box Model

A box model was constructed to match the experimental conditions of the experiment with O_3 added. Model parameters are shown in Table 2.7.1. Initial NO and NO_2 levels were set to match the conditions of the kitchen after the stove was extinguished. The rate of continuous O_3 addition was set so the O_3 concentration 30 min after the stove was extinguished matched the experimental conditions (40 ppbv). Dilution was set to match the decay of the NO_x species over the experiment. A rate constant of 1.5×10^{-3} s^{-1} was applied for heterogeneous loss of N_2O_5 to produce HNO_3. This value was derived from estimated values typical of reactive chemicals in indoor environments: surface area to volume ratio of 3.8 m^{-1} and a deposition velocity of 0.04 cm/s.[25-27]

A constant d-limonene level of 700 pptv was assumed to be present throughout the experiment, yielding 0.2 s^{-1} of NO_3 reactivity. An additional 0.5 s^{-1} of VOC reactivity was needed to reach experimentally observed steady state NO_3 concentration, bringing the total NO_3 reactivity with VOC in the model, 0.7 s^{-1} into agreement with the experimentally derived value, 0.8 s^{-1}. The best model estimate is 0.7 s^{-1} of NO_3 reactivity in the kitchen, but even at the upper bound heterogeneous loss rate for N_2O_5 of 0.0028 s^{-1} we estimate at least 0.6 s^{-1} of reactivity in the

kitchen.[25-27]

Figure 2.4.2 shows the model output for the production rate of NO_3 (P_{NO3}), the fractional NO_3 loss, and the concentration of the products from NO_3 loss. Production of NO_3 begins immediately after the stove is extinguished and rises as O_3 concentrations increase. However, NO reacts effectively with NO_3 produced early in the experiment. Only after sufficient NO has been consumed by O_3 do oxidation sinks for NO_3 compete for its loss, oxidizing and reducing the concentrations of d-limonene and the unspecified VOC. Peak NO_3 production is realized when most of the NO_x is NO_2 rather than NO. The O_3 concentration grows, and it can only react with NO_2 to form NO_3, or with d-limonene to form the 'O_3+MT' oxidation product. The peak NO_3 production rate, 7 ppbv h^{-1}, is high compared to most reports from outdoor environments, where P_{NO3} has been reported in the range 0.01 to 1.2 ppbv h^{-1}.[28] The model illustrates that NO_3 production does not contribute significantly to oxidation of VOCs until NO is removed and VOC reactions compete for the available NO_3.

In the model, ozonolysis of d-limonene occurs at about half the rate of this compound's reaction with NO_3. The dominant source of oxidation products comes from NO_3 reacting with the unspecified VOC. Heterogeneous loss of N_2O_5 to form HNO_3 is significant, at times accounting for 20% of NO_3 loss.

For decades NO_3 has been proposed as an important indoor oxidant. We have presented here the first direct indoor measurements of NO_3 along with evidence of its high reactivity indoors. With moderate O_3 levels, routine combustion emissions of NO_x can lead to significant production and measurable concentrations of NO_3 and N_2O_5. Furthermore, the inferred NO_3 production rates and reactivity are high compared to outdoors, and, when NO_3 is elevated, it may become the dominant indoor oxidant for some VOCs, including certain terpenoids.

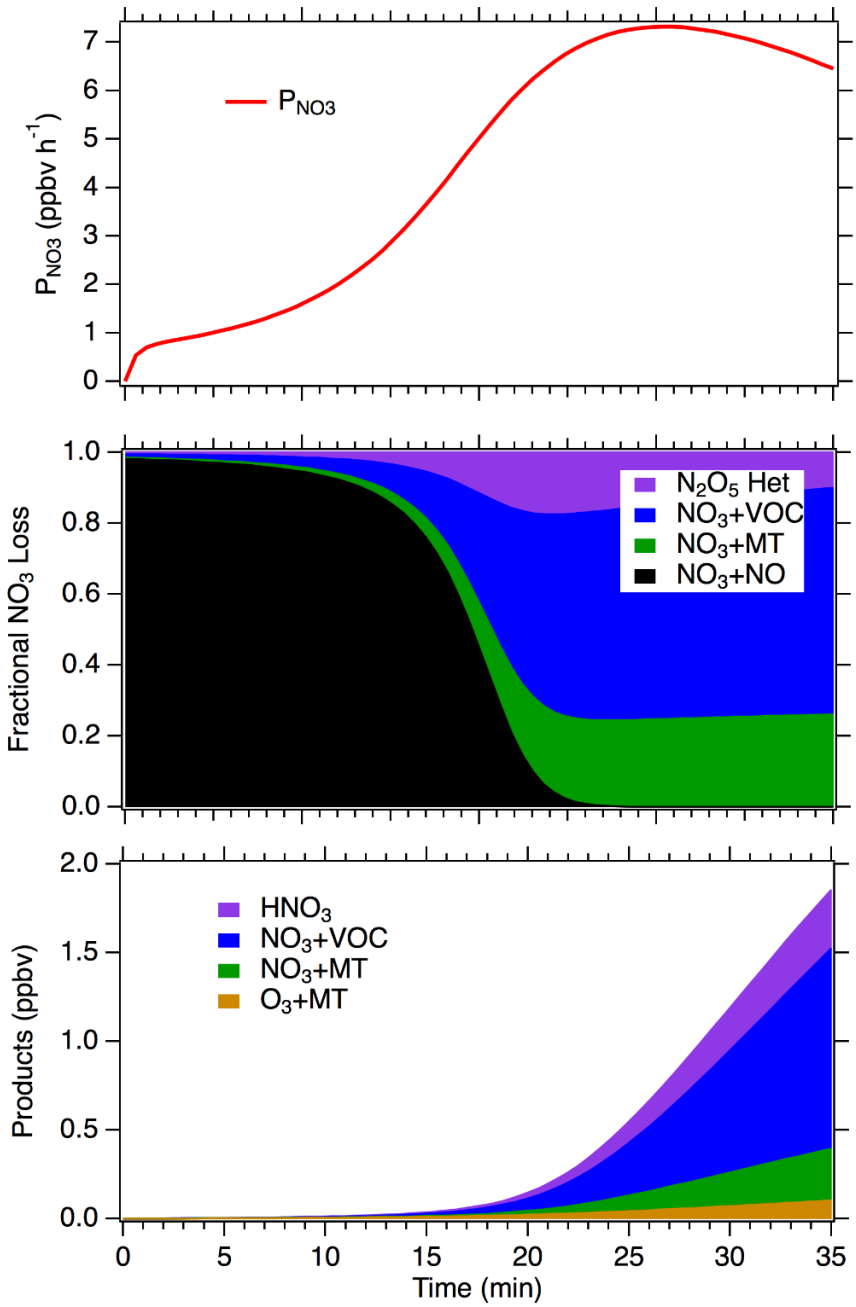

Figure 2.4.2 Box model outputs of NO_3 production rate (top), fractional time dependent losses of NO_3 and N_2O_5 (middle), and mixing ratios of reaction products (bottom). Note that time t=0 corresponds to the extinguishing of the stove. The center plot shows fractional NO_3 losses for 4 reaction pathways: heterogeneous reaction of N_2O_5 to form HNO_3 (N_2O_5 Het), NO_3 oxidation of the 'generic' VOC (NO_3 + VOC), NO_3 oxidation of d-limonene (NO_3 + MT), and NO_3 consumption by NO (NO_3 + NO). The bottom plot shows the concentration of the NO_3 loss products, as well as the concentration of products from ozonolysis of d-limonene (O_3 + MT).

2.5. Acknowledgments

This work was funded by the Alfred P. Sloan Foundation via Grant 2016-7050.

2.6. References

(1) Klepeis, N. E.; Nelson, W. C.; Ott, W. R.; Robinson, J. P.; Tsang, A. M.; Switzer, P.; Behar, J. V.; Hern, S. C.; Engelmann, W. H. The National Human Activity Pattern Survey (NHAPS): A resource for assessing exposure to environmental pollutants. *J. Expos. Anal. Environ. Epidemiol.* **2001**, *11*, 231–252.

(2) Weschler, C. J. Ozone in indoor environments: Concentration and chemistry. *Indoor Air* **2000**, *10*, 269–288.

(3) Carslaw, N.; Fletcher, L.; Heard, D.; Ingham, T.; Walker, H. Significant OH production under surface cleaning and air cleaning conditions: Impact on indoor air quality. *Indoor Air* **2017**, *27*, 1091–1100.

(4) Emmerson, K. M.; Carslaw, N.; Carslaw, D. C.; Lee, J. D.; McFiggans, G.; Bloss, W. J.; Gravestock, T.; Heard, D. E.; Hopkins, J.; Ingham, T.; Pilling, M. J.; Smith, S. C.; Jacob, M.; Monks, P. S. Free radical modelling studies during the UK TORCH campaign in summer 2003. *Atmos. Chem. Phys.* **2007**, *7*, 167–181.

(5) Sarwar, G.; Corsi, R.; Kimura, Y.; Allen, D.; Weschler, C. J. Hydroxyl radicals in indoor environments. *Atmos. Environ.* **2002**, *36*, 3973–3988.

(6) Weschler, C. J.; Shields, H. C. Production of the hydroxyl radical in indoor air. *Environ. Sci. Technol.* **1996**, *30*, 3250– 3258.

(7) Gómez Alvarez, E.; Amedro, D.; Afif, C.; Gligorovski, S.; Schoemaecker, C.; Fittschen, C.; Doussin, J.-F.; Wortham, H. Unexpectedly high indoor hydroxyl radical concentrations associated with nitrous acid. *P. Natl. Acad. Sci. USA* **2013**, *110*, 13294–13299.

(8) Forester, C. D.; Wells, J. R. Hydroxyl radical yields from reactions of terpene mixtures with ozone. *Indoor Air* **2011**, *21*, 400–409.

(9) Weschler, C. J.; Shields, H. C. Potential reactions among indoor pollutants. *Atmos. Environ.* **1997**, *31*, 3487–3495.

(10) Weschler, C. J.; Brauer, M.; Koutrakis, P. Indoor ozone and nitrogen dioxide: A potential pathway to the generation of nitrate radicals, dinitrogen pentaoxide, and nitric acid indoors. *Environ. Sci. Technol.* **1992**, *26*, 179–184.

(11) McDonald, B. C.; de Gouw, J. A.; Gilman, J. B.; Jathar, S. H.; Akherati, A.; Cappa, C. D.; Jimenez, J. L.; Lee-Taylor, J.; Hayes, P. L.; McKeen, S. A.; Cui, Y. Y.; Kim, S.-W.; Gentner, D. R.; Isaacman-VanWertz, G.; Goldstein, A. H.; Harley, R. A.; Frost, G. J.; Roberts, J. M.; Ryerson, T. B.; Trainer, M. Volatile chemical products emerging as largest

petrochemical source of urban organic emissions. *Science* **2018**, *359***,** 760–764.

(12) Nazaroff, W. W.; Weschler, C. J. Cleaning products and air fresheners: Exposure to primary and secondary air pollutants. *Atmos. Environ.* **2004**, *38*, 2841–2865.

(13) Brown, S. S.; Stark, H.; Ravishankara, A. R. Applicability of the steady state approximation to the interpretation of atmospheric observations of NO_3 and N_2O_5. *J. Geophys. Res.* **2003**, *108*, 4539.

(14) Atkinson, R.; Winer, A. M.; Pitts Jr., J. N. Estimation of night-time N_2O_5 concentrations from ambient NO_2 and NO_3 radical concentrations and the role of N_2O_5 in night-time chemistry. *Atmos. Environ.* **1986**, *20*, 331–339.

(15) Nøjgaard, J. K. Indoor measurements of the sum of the nitrate radical, NO_3, and nitrogen pentoxide, N_2O_5 in Denmark. *Chemosphere* **2010**, *79*, 898–904.

(16) Mullen, N. A.; Li, J.; Russell, M. L.; Spears, M.; Less, B. D.; Singer, B. C. Results of the California Healthy Homes Indoor Air Quality Study of 2011-2013: Impact of natural gas appliances on air pollutant concentrations. *Indoor Air* **2016**, *26*, 231–245.

(17) Garrett, M. H.; Hooper, M. A.; Hooper, B. M. Nitrogen dioxide in Australian homes: Levels and sources. *J. Air Waste Manage. Assoc.* **1999**, *49*, 76–81.

(18) Choke, A.; Chong, S. J.; Tan, B. K. Hot pot burns and the dangers of portable gas stove. *Burns* **2016**, *42*, 238–239.

(19) Liu, Y.; Misztal, P. K.; Xiong, J.; Tian, Y.; Arata, C.; Nazaroff, W. W.; Goldstein, A. H. Detailed investigation of ventilation and airflow patterns in a northern California residence. *Indoor Air* **2018**, *28*, 572–584.

(20) Dubé, W. P.; Brown, S. S.; Osthoff, H. D.; Nunley, M. R.; Ciciora, S. J.; Paris, M. W.; McLaughlin, R. J.; Ravishankara, A. R. Aircraft instrument for simultaneous, in situ measurement of NO_3 and N_2O_5 via pulsed cavity ring-down spectroscopy. *Rev. Sci. Instr.* **2006**, *77*, 034101.

(21) Fuchs, H.; Dubé, W. P.; Ciciora, S. J.; Brown, S. S. Determination of inlet transmission and conversion efficiencies for in situ measurements of the nocturnal nitrogen oxides, NO_3, N_2O_5 and NO_2, via pulsed cavity ring-down spectroscopy. *Anal. Chem*. **2008**, *80*, 6010–6017.

(22) Wagner, N. L.; Dubé, W. P.; Washenfelder, R. A.; Young, C. J.; Pollack, I. B.; Ryerson, T. B.; Brown, S. S. Diode laser-based cavity ring-down instrument for NO_3, N_2O_5, NO, NO_2 and O_3 from aircraft. *Atmos. Meas. Tech*. **2011**, *4*, 1227–1240.

(23) Traynor, G. W.; Apte, M. G.; Chang, G. M. Pollutant emission factors from residential natural gas appliances: A literature review. *Report LBNL- 38123*, **1996**, Berkeley, CA, Lawrence Berkeley National Laboratory.

(24) Liebmann, J. M.; Schuster, G.; Schuladen, J. B.; Sobanski, N.; Lelieveld, J.; Crowley, J. N. Measurement of ambient NO_3 reactivity: Design, characterization and first deployment of a new instrument. *Atmos. Meas. Tech.* **2017**, *10*, 1241–1258.

(25) Singer, B. C.; Hodgson, A. T.; Hotchi, T.; Ming, K. Y.; Sextro, R. G.; Wood, E. E.; Brown, N. J. Sorption of organic gases in residential rooms. *Atmos. Environ.* **2007**, *41*, 3251–3265.

(26) Morrison, G.C. (1999) ‘‘Ozone-surface interactions: investigation of mechanisms, kinetics, mass transport, and implications for indoor air quality’’, Ph.D. Dissertation, Engineering – Civil and Environmental Engineering, University of California, Berkeley, California, USA.

(27) Nazaroff, W., Gadgil, A., & Weschler, C. (1993). Critique of the Use of Deposition Velocity in Modeling Indoor Air Quality. *Modeling of Indoor Air Quality and Exposure*, ASTM STP1205-EB **1993,** 81-104

(28) Edwards, P. M.; Aikin, K. C.; Dube, W. P.; Fry, J. L.; Gilman, J. B.; de Gouw, J. A.; Graus, M. G.; Hanisco, T. F.; Holloway, J.; Hübler, G.; Kaiser, J.; Keutsch, F. N.; Lerner, B. M.; Neuman, J. A.; Parrish, D. D.; Peischl, J.; Pollack, I. B.; Ravishankara, A. R.; Roberts, J. M.; Ryerson, T. B.; Trainer, M.; Veres, P. R.; Wolfe, G. M.; Warneke, C.; Brown, S. S. Transition from high- to low-NO_x control of night-time oxidation in the southeastern US. *Nature Geoscience* **2017**, *10*, 490–495.

2.7. Supporting Information

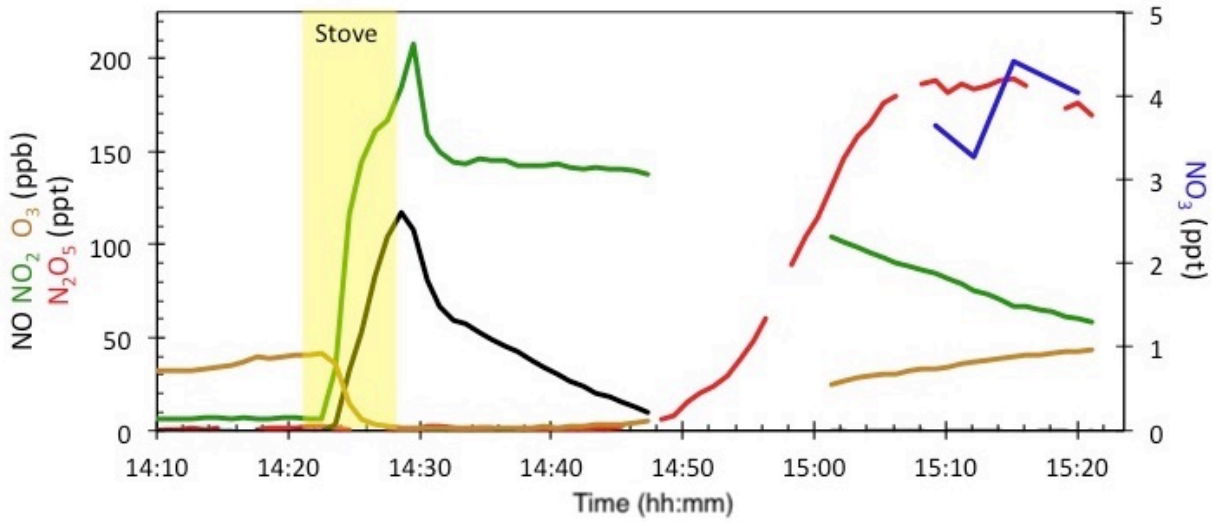

Figure 2.7.1 Concentrations of NO, NO_2, NO_3, N_2O_5, and O_3 during the first ozone-added stove experiment. The yellow shaded region indicates when the stove was on. Due to the short duration of NO_3 measurements, this experiment was not used to calculate NO_3 reactivity.

Table 2.7.1 Model parameters. Dilution, not shown, was at a rate of 0.0007 s-1. Rate coefficients are for 293 K, the temperature at which the model was run.

reaction	**rate coefficient**
$NO + O_3 \rightarrow NO_2 + O_2$	1.74×10^{-14} cm^3 molecule^{-1} s^{-1} [a]
$NO_2 + O_3 \rightarrow NO_3 + O_2$	3.06×10^{-17} cm^3 molecule^{-1} s^{-1} [a]
$NO_2 + NO_3 \rightarrow N_2O_5$	1.25×10^{-12} cm^3 molecule^{-1} s^{-1} [a]
$N_2O_5 \rightarrow NO_2 + NO_3$	0.0238 s^{-1} [a]
$NO + NO_3 \rightarrow 2\ NO_2$	2.62×10^{-11} cm^3 molecule^{-1} s^{-1} [a]
$NO_3 + MT \rightarrow PNO_3MT + MT$	1.20×10^{-11} cm^3 molecule^{-1} s^{-1} [a b]
$N_2O_5 (+ H_2O) \rightarrow 2HNO_3$	0.0015 s^{-1} [c]
$O_3 + MT \rightarrow PO_3MT + MT$	2.10×10^{-16} cm^3 molecule^{-1} s^{-1} [a b]
$NO_3 \rightarrow LNO_3$	0.4 s^{-1} [d]

[a]Coefficients from R. Atkinson, D. L. Baulch, R. A. Cox, J. N. Crowley, R. F. Hampson, R. G. Hynes, M. E. Jenkin, M. J. Rossi, and J. Troe, Atmos. Chem. Phys., 4, 1461-1738 (2004); IUPAC Task Group on Atmospheric Chemical Kinetic Data Evaluation, http://iupac.pole-ether.fr.
[b]Rates used for the 'generic monoterpene', MT, are for reaction with d-limonene.
[c]Estimated using ref [25] - [27s].
[d]NO_3 reactivity was adjusted to match experimental results.

3. Heterogeneous Ozonolysis of Squalene: Gas-Phase Products Depend on Water Vapor Concentration

This chapter is adapted from:
Caleb Arata, Nadja Heine, Nijing Wang, Pawel K. Misztal, Pawel Wargocki, Gabriel Bekö, Jonathan Williams, William W Nazaroff, Kevin R. Wilson, Allen H. Goldstein "Heterogeneous Ozonolysis of Squalene: Gas-Phase Products Depend on Water Vapor Concentration" *Environmental Science and Technology* **2019**, 53, 24, 14441-14448.

3.1. Abstract

Previous work examining the condensed-phase products of pure squalene particle ozonolysis in a flow tube reactor found that an increase in water vapor concentration led to lower concentrations of secondary ozonides, increased concentrations of carbonyls, and smaller particle diameter, suggesting that water changes the fate of the Criegee intermediate. To determine if this loss of volume corresponds to an increase in gas-phase products, we measured gas-phase volatile organic compound (VOC) concentrations via proton-transfer-reaction time-of-flight mass spectrometry. Studies were conducted in a flow-tube reactor at atmospherically relevant ozone (O_3) exposure levels (5-30 ppb h) with pure squalene particles. An increase in water vapor concentration led to strong enhancement of gas-phase oxidation products at all tested O_3 exposures. An increase in water vapor from 0% to 70% relative humidity (RH) at high O_3 exposure increased the total mass concentration of gas-phase VOCs by a factor of three. The observed fraction of carbon in the gas phase correlated well with the fraction of particle volume lost. Experiments involving O_3 oxidation of shirts soiled with skin oil confirms that the RH dependence of gas-phase reaction product generation occurs similarly on surfaces containing skin oil under realistic indoor conditions. Relative humidity changes the fate of the Criegee intermediates and the volatility of the oxidation products, resulting in a RH of the product distribution and amount of gas-phase VOCs emitted from ozonolysis of unsaturated carbon bonds in skin oil. Similar behavior is expected for O_3 reactions with surface bound organics containing unsaturated carbon bonds.

3.2. Introduction

People spend 90% of their lives indoors[1]. Each day, adult humans inhale 12-15 kg of air, compared with ingesting 1-3 kg of food and water, making indoor air a primary route of exposure to many chemicals, including volatile organic compounds (VOCs). People can be the dominant indoor VOC emission source in highly occupied spaces, and, in the presence of ozone (O_3), the oxidation of skin lipids adds ketones and aldehydes to the composition of indoor air[2–8].

Indoor O_3 concentrations are commonly 20-70% of outdoor concentrations, with the ratio depending on building air change rates (ACR), types of ventilation systems used, and the nature of indoor surfaces[9]. Indoor O_3 is estimated to account for 25-60% of an individual's daily O_3 exposure.[10] In densely occupied spaces, occupants may be the dominant indoor sinks for O_3, mainly due to reactions with lipids on their skin, hair, and clothing.[11]

Squalene ($C_{30}H_{50}$) constitutes 10% of the mass of human skin lipids, and contributes 50% of the unsaturated carbon bonds.[12] When exposed to O_3, squalene is quickly oxidized to products that span a wide range of volatility; some products remain in the condensed phase while others become gaseous.[5]

Researchers have investigated effects of human occupancy on aircraft cabin air, considering the sometimes elevated concentration of O_3 found on airplanes.[13] Weschler *et al.* conducted experiments in a simulated aircraft cabin section and found that more than half of the observed oxidation products in the gas phase came from O_3 reacting with human skin lipids.[4] Further work studied O_3 deposition on materials common to aircraft cabin interiors, finding that soiled clothing exposed to O_3 emits 6-methyl-5-hepten-2-one (6-MHO).[14] Surface bound squalene was found to have a very high reaction probability with O_3, 5×10^{-4} - 1×10^{-3}.[15,16] Both 4-oxopentanal (4-OPA) and 6-MHO are known respiratory irritants.[17,18] Both acetone and 6-MHO are among the most prominent VOCs emitted from human skin.[19] While acetone is known to originate from a wide variety of sources including breath, 6-MHO is thought to be specific to squalene oxidation. The high emission rate suggests that squalene oxidation contributes significantly to human skin VOC emission.

Heine *et al.* investigated the influence of RH on squalene ozonolysis using pure squalene particles in a flow-tube reactor.[20] They showed that water vapor concentration does not affect the rate of squalene ozonolysis, but does substantially change the product composition. Under dry conditions, as O_3 consumes squalene, secondary ozonide concentrations increase in the condensed phase and initial particle volume is reduced by 15%. At 60% RH, condensed-phase ozonolysis products shift from secondary ozonides to carbonyls, and particle volume is reduced by as much as 50%. This loss of volume should correspond to an increase in gas-phase oxidation products.

We designed experiments specifically to observe the mass lost to the gas phase and the products formed by O_3-squalene reactions as a function of RH, and to understand the implications for the fate of the Criegee intermediate on squalene particle surfaces and skin oil coated clothing. In this work we investigate the gas-phase products from squalene particle ozonolysis in a flow tube reactor, and on skin-oil soiled shirts in a climate chamber. From the flow-tube experiments, we show that the RH dependent loss of particle diameter corresponds to an increase in gas-phase reaction products, consistent with the mechanism of water molecules promoting carbonyl formation from the Criegee intermediate under real world conditions. We discuss implications for product yields from skin oil ozonolysis indoors under varying RH conditions.

3.3. Experimental Methods

Squalene ozonolysis is carried out in a flow-tube reactor, as described in Heine *et al*.[20,21] Liquid squalene in a tube furnace is heated to 145 ºC, generating polydisperse particles by means of homogeneous nucleation with a mean surface-weighted diameter of 250 +/- 40 nm. A continuous flow of 300 standard cm^3 min^{-1} dry nitrogen (N_2) carries the particles from the furnace through a charcoal denuder to remove any gas-phase contamination. This flow is then combined with flows of oxygen (O_2), O_3, dry N_2, and humidified N_2 for a total flow of 1 L min^{-1}. Levels of O_2 are held at a constant 10%, while the flows of dry and humidified N_2 are varied to give a range of 0% (< 3%) to 100% RH. This combined flow enters the flow tube reactor (130 cm long, 2.5 cm inner

diameter) with a residence time of 37 s.[22] Ozone is produced by a corona discharge generator, and the concentration of O_3 ranges from 0-4 ppm, giving O_3 exposures of 0-44 ppb h. The initial particle loading in the flow reactor is 1000 μg m^{-3}.

Upon leaving the flow-tube reactor, the outflow is measured by proton-transfer-reaction time-of-flight mass spectrometry (Ionicon PTR-TOF-MS 8000), an electrostatic classifier (TSI model 3080L) with a butanol-based condensation particle counter (TSI model 3772), and a custom-built vacuum ultraviolet aerosol mass spectrometer (VUV-AMS). The particle size and composition measurements are described in Heine *et al.*[20]; the PTR-TOF-MS was used to measure speciated gas-phase VOC concentrations.

PTR-TOF-MS uses a chemical ionization technique with minimal fragmentation using H_3O^+ as the primary reagent ion. PTR-TOF-MS has been previously used to detect gas-phase products of squalene ozonolysis.[2,4,5] The instrument was calibrated with a multicomponent VOC gas standard to ensure stability throughout the campaign. Of the compounds reported here, only acetone is directly calibrated. All other compound concentrations were calculated using a default proton transfer reaction rate constant of 2.5×10^{-9} cm^3 s^{-1} for both the primary ion, H_3O^+, and the first water cluster, $H_3O^+(H_2O)$. Calibration accuracies are estimated to be +/- 10%, while concentrations accuracies derived from the default rate constant are typically +/- 50%.[23] Increases in RH can cause increases in instrument sensitivities for certain compounds. However, these changes are typically a few percent, much lower than differences in concentration reported in this work.[24,25]

Measurements of VOCs at each specified RH and O_3 exposure were made by allowing concentrations in the reactor to stabilize. Once stable, the particle flow was quickly replaced with a flow of N_2. After 2 min, 95% of the particles are removed from the reactor, and a background concentration is taken. To account for both compounds being desorbed from the flow-tube walls as well as compounds being produced by heterogeneous oxidation of the walls, O_3 flow is maintained during the background sampling procedure. The difference between the stable concentration and the background concentration is taken as the gas-phase concentration attributable to squalene-particle ozonolysis. Table 3.7.1 through Table 3.7.5 show the concentrations for each species as measured from the flow tube, as well as the measured background.

An experiment to analyze emissions from skin oil soiled clothing under varying conditions of RH and O_3 was performed as part of the Indoor Chemical Human Emissions and Reactivity (ICHEAR) project. Four identical T-shirts (100% cotton) were washed with fragrance-free detergent and tumble dried, before being worn by four people overnight (over 8 h). The skin oil soiled T-shirts were then placed inside a stainless steel climate chamber with a volume of 26.8 m^3 and ventilated with an air exchange rate at 3.2 h^{-1}. Outdoor air was used for ventilation. It was filtered using particle and activated carbon filters to avoid interference from outdoor VOCs, and conditioned to reach the required temperature and RH. Ozone was generated in the HVAC system downstream of the activated carbon filter using an O_3 generator (Jelight Model 600 UV) and continuously introduced into the chamber at levels between 95-100 ppb. The temperature inside the chamber was maintained between 27.4 – 28.3°C during the experiment and the O_3 levels monitored throughout. Four RH levels were established. The lowest RH levels (at the beginning and end of the experiment) were not controlled (humidifier off, no dehumidifying

present), while the two higher RH levels were achieved by operating a steam humidifier in the HVAC system. Each level was maintained for 1.5-2 hours to allow steady state conditions to be reached. The resulting average RH levels during the four periods were 26%, 41%, 56% and 33%; the last RH condition was a decay from 50% to 28% with the humidifier off.

A PTR-TOF-MS (8000, Ionicon Analytik GmbH Innsbruck, Austria) was deployed in ICHEAR to monitor VOCs produced from skin oil O_3 oxidation. The operational conditions of the PTR-TOF-MS are similar to that mentioned before, namely drift tube pressure 2.2 mbar, temperature 60°C and 137 Td (E/N). The 1/8 " Teflon inlet of the instrument was attached to the main exhaust duct of the chamber, approximately 1 m from the terminal through which the air was exhausted from the chamber and set to draw 100 mL min^{-1} (via a main high flow inlet 7 L min^{-1}) continuously into the mass spectrometer. Data reported for the aforementioned skin-oil T-shirt experiment are at 20 s resolution. Before putting T-shirts inside the chamber, a background level of the empty chamber was established and maintained for 10 minutes. The measured background VOC levels were subsequently subtracted from the VOC levels measured while the T-shirts were in the chamber.

3.4. Results and Discussion

Figure 3.4.1 shows the chemical structures of squalene and selected gas-phase ozonolysis products. The first-generation gas-phase products are acetone, 6-methyl-5-hepten-2-one (6-MHO), and geranylacetone. Terminal oxidation products found in the gas phase, i.e. products that are minimally reactive with O_3 because of their lack of carbon-carbon double bonds, are acetone, 4-oxopentanal (4-OPA), and 1,4-butanedial (succinaldehyde). Figure 3.4.2 shows a simplified mechanism for alkenes reacting with O_3. In **R1**, O_3 adds across the double bond, forming a primary ozonide (not shown), which quickly decomposes to one of two combinations of carbonyl and Criegee intermediate. This reaction is fast and does not include water, so water vapor concentration has no effect on the rate of alkene loss. The Criegee intermediate produced by **R1** is reactive, and can proceed through **R2** or **R3**, as well as through rearrangement. **R2** shows the Criegee intermediate reacting with water to form the α-hydroxyhydroperoxide, which decomposes to a carbonyl and to hydrogen peroxide. **R3** shows the Criegee intermediate reacting with another carbonyl to form a secondary ozonide. The carbonyl products are more volatile than their respective secondary ozonides; in the presence of water, **R2** occurs faster than **R3**, leading to greater release of reaction products to the gas phase and a concomitant shrinking of the particle.

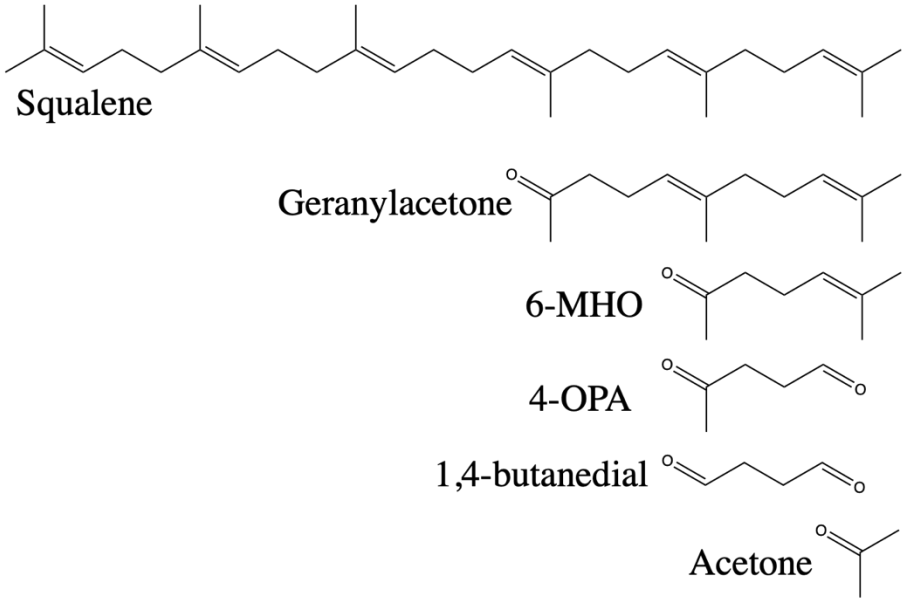

Figure 3.4.1 Chemical structure of squalene and selected squalene ozonolysis products.

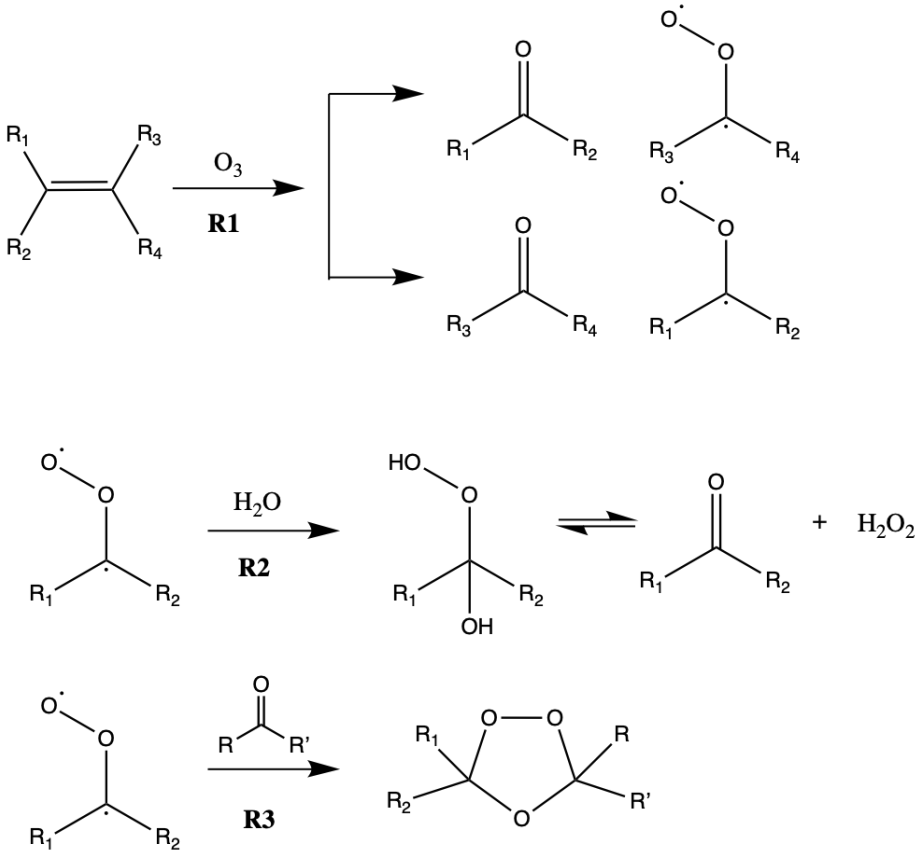

Figure 3.4.2 Simplified reaction mechanism for ozonolysis of alkenes.

Figure 3.4.3 shows the gas-phase concentration of geranylacetone and 6-MHO exiting the flow-tube reactor as a function of O_3 exposure and RH. Both compounds are primary products of squalene oxidation, and both have carbon-carbon double bonds that can further react with O_3. At

all RH levels, geranylacetone production peaks at an O_3 exposure of 10 ppb h. Dry conditions yield 5 μg m^{-3} of geranylacetone, whereas more humid conditions (70% RH) enhance the concentration to 19 μg m^{-3}, an increase by almost 4×. RHs, specifically 30% and 50%, also show an increase in geranylacetone concentration compared to dry conditions. At exposures of 20 ppb h, the geranylacetone is fully consumed by ozonolysis, and is not detected. Compared to other products measured, concentrations of geranylacetone are small. As a 13-carbon ketone, with a vapor pressure of 3.5 Pa at 298 K, most of the compound is expected to remain in the condensed phase.[6] Furthermore, there are fewer possible reaction pathways to produce geranylacetone than the other, shorter chain products. The low concentration measured in this study is consistent with a classroom study by Tang *et al*., where both 6-MHO and 4-OPA were found at significantly higher concentrations than geranylacetone.[2]

The production of 6-MHO shows strong RH dependence. At all levels of O_3 exposure, an increase in RH leads to an increase in 6-MHO concentration. As 6-MHO is a primary product that can also be consumed, peak concentrations are found at the lower levels of O_3 exposure. At 70% RH and 12 ppb h of O_3 exposure, the concentration detected is 170 μg m^{-3}, 3 times the amount of 6-MHO detected at the same O_3 exposure but under dry conditions. Unlike geranylacetone, 6-MHO is detected at even the highest levels of O_3 exposure tested, 30 ppb h. The 6-MHO species is used as a primary tracer compound for squalene oxidation, along with 4-OPA as a secondary tracer. The fact that 6-MHO is consumed at higher O_3 exposures, while 4-OPA is not, suggests that 6-MHO concentrations could be used as a proxy indicator for the age of oxidation products: at longer timescales, 6-MHO becomes depleted while 4-OPA does not.

Figure 3.4.4A-C shows the gas-phase concentrations as a function of O_3 exposure and RH of the three terminal products: acetone, 4-OPA, and 1,4-butanedial. At most levels of O_3 exposure, increasing RH yields increasing concentrations of acetone, again showing strong humidity dependence. At very low O_3 exposure (5-6 ppb h), 30% RH produces 32 μg m^{-3} of acetone, whereas 70% RH conditions give 77 μg m^{-3}, an increase by more than 2×. Under dry conditions, acetone increases to 100 μg m^{-3} at 12 ppb h exposure, and then does not increase with increasing O_3 exposure. As acetone does not have carbon-carbon double bonds, it does not react significantly with O_3 and so increasing exposure is not expected to consume acetone. Under higher RH conditions, the same leveling off is seen, but at higher concentrations. At 70% RH, acetone concentrations begin to plateau at 20 ppb h exposure, at a concentration of 280 μg m^{-3}. At O_3 exposures greater than 10 ppb h, increasing RH from 0% to 70% increases acetone concentrations by a factor of 2.5 to 3.

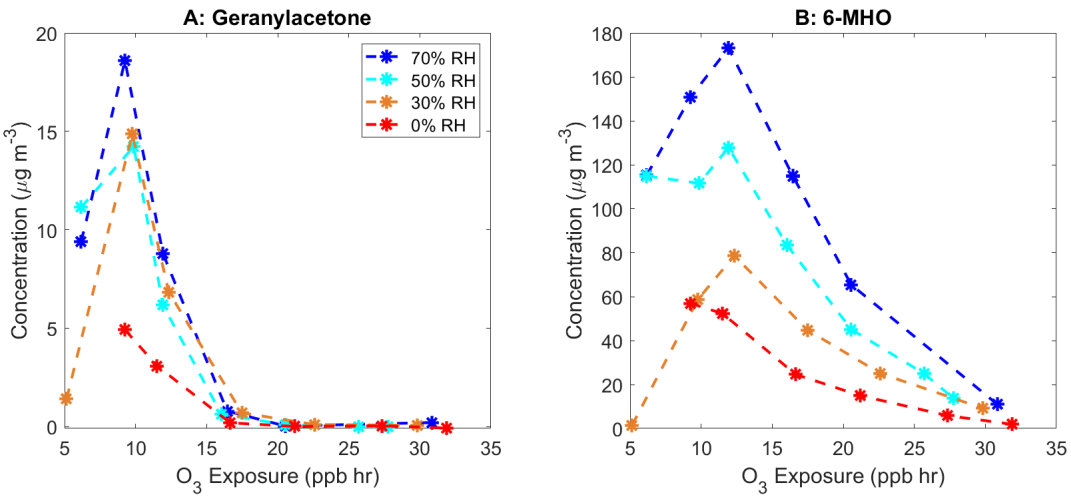

Figure 3.4.3 Primary unsaturated products from squalene ozonolysis as a function of humidity and O3 exposure.

Figure 3.4.4B shows the RH dependence of 4-OPA from the ozonolysis of squalene. A minimum of two reactions involving O_3 are required to produce 4-OPA from squalene, so concentrations are observed to increase later than primary products, such as acetone and 6-MHO. Despite being a terminal product, 4-OPA does not show the same leveling off behavior as acetone. Under dry conditions, production stops increasing at 20 ppb h O_3 exposure, but under high RH conditions no leveling off is seen; production of 4-OPA may increase past 30 ppb h exposure. At O_3 exposures less than 12 ppb h no RH dependence is seen but production is also small. At higher O_3 exposures 4-OPA shows strong RH dependence, with a factor of 6 increase in concentration between dry and humid conditions at 30 ppb h O_3 exposure. In both mixing ratio and mass concentration, 4-OPA is the most abundant gas-phase product, with a peak concentration of 600 μg m^{-3}. If each double bond in squalene proceeds through reaction R2, one molecule of squalene would produce a single 1,4-butanedial molecule, two acetone molecules, and four 4-OPA molecules. While the observed mixing ratios of terminal products do not follow these stoichiometric ratios, the relatively large number of 4-OPA molecules that can be made from a squalene molecule help to explain why it is the most abundant gas-phase product.

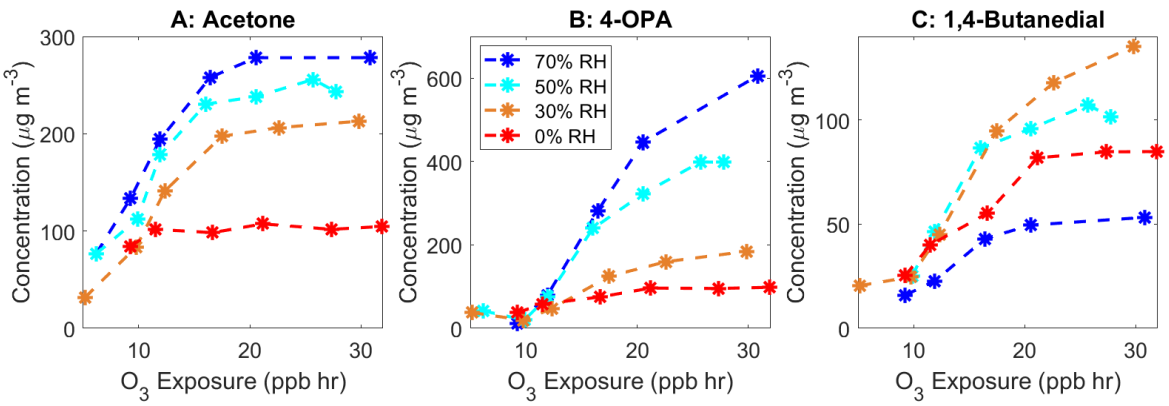

Figure 3.4.4 Terminal products from squalene ozonolysis as a function of humidity and O3 exposure.

Figure 3.4.4C shows the concentration of 1,4-butanedial as a function of RH and O_3 exposure. As a terminal product, abundance of this species increases with O_3 exposure, and, for some RH conditions, eventually levels off. As with 4-OPA, production of 1,4-butanedial requires a minimum of two ozonolysis reactions, so concentrations substantially increase at greater O_3 exposure. Production of 1,4-butanedial shows a more complicated relation to RH than other species. The lowest levels of production, across all O_3 exposures, are under the most humid conditions. The next lowest levels of production are under the driest conditions. Although it does not follow the pattern of the other species measured, 1,4-butanedial levels do show strong variability with RH. At 30 ppb h O_3 exposure, switching from 70% RH to 30% RH increases the concentration of 1,4-butanedial from 52 μg m^{-3} to 140 μg m^{-3}. This ~3× increase in production is in line with the 3×-6× changes in production observed at different RH for other compounds. The fact that 1,4-butanedial production peaks at intermediate RH, and declines at low and high RH, suggests that water plays a more complicated role than depicted in Figure 3.4.2. Specifically, reaction **R2** increases 1,4-butanedial production up to a point, and then facilitates other reactions that suppress production.

Wisthaler and Weschler (2010) observed 12 prominent VOCs from squalene ozonolysis, including the five compounds already discussed.[5] When glass wool soiled with human skin oil was exposed to O_3 (0-75 ppb h), three species — 4-methyl-8-oxo-4-nonenal (4-MON), 4-methyl-4-octene-1,8-dial (4-MOD), and 1-hydroxy-6-methyl-5-hepten-2-one (OH-6MHO) — showed mixing ratios similar to the observed mixing ratios of 4-OPA and 1,4-butanedial. These species were also observed during ozonolysis of a pure squalene film; however, the mixing ratios for that experiment were not reported. In our work, all three compounds are detected (4-MON, 4-MOD, and OH-6MHO), but at very low concentrations, 2 μg m^{-3} or less. Possibly due to the low concentration of these species, a RH dependence isn't discernible.

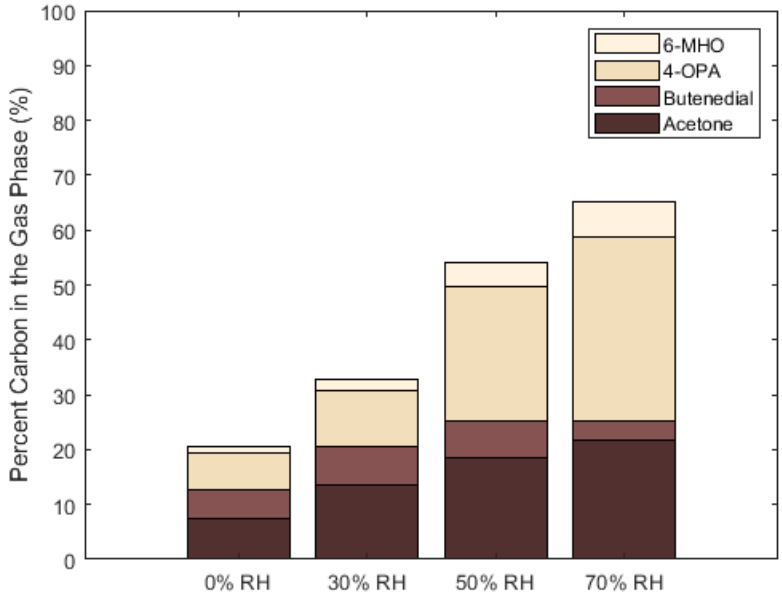

Figure 3.4.5 Percent of carbon in the gas phase at 20 ppb h O_3 exposure as a function of RH. Converting the measurements in Figure 3.4.3 and Figure 3.4.4 from μg m^{-3} to μg C m^{-3} and normalizing to the initial concentration of carbon entering the flow tube gives the percent carbon in the gas phase.

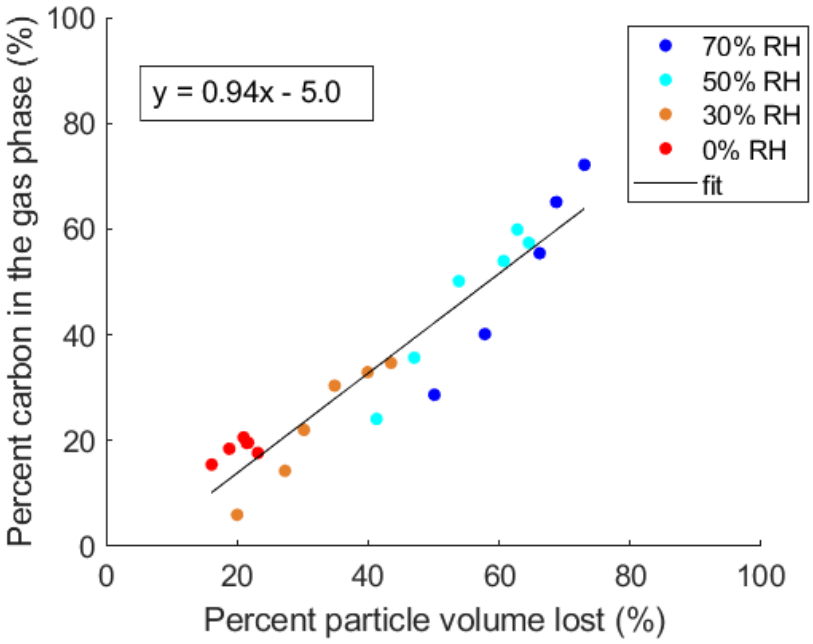

Figure 3.4.6 Percent carbon in the gas phase compared to the percent of particle volume lost for all RH and O_3 exposures.

Four other compounds identified by Wisthaler and Weschler (2010) — 1-hydroxypropan-2-one (hydroxyacetone), 4-oxobutanoic acid, and the isobaric compounds 5-hydroxy-4-oxopentanal and 4-oxopentanoic acid (levulinic acid) — are found in the present work at peak concentrations much lower than 6-MHO, acetone, 4-OPA, and 1,4-butanedial (5-15 μg m^{-3} versus 140-600 μg m^{-3}). All four compounds are terminal products; concentrations either increase or level off with increasing O_3 exposure, and none of the products show increasing production with increasing RH. Hydroxyacetone shows a muted response to changes in RH, as seen in Figure 3.7.1. Production is similar at 30% RH, 50% RH, and 70% RH, but increased by ~50-100% under dry conditions. Concentrations are modest, peaking at 15 μg m^{-3} under dry conditions and 30 ppb h O_3 exposure. Levulinic acid or 5-hydroxy-4-oxopentanal (or a combination of the two) only shows a RH effect at the highest O_3 exposure. At 30 ppb h, 70% RH yields 7 μg m^{-3} while 30% RH produces 15 μg m^{-3}, as seen in Figure 3.7.2. Figure 3.7.3 shows 4-oxobutanoic acid production *decreasing* with increased RH. At 70% RH and 30 ppb h O_3 exposure, we observe 1 μg m^{-3}, whereas under dry conditions we measure 5 μg m^{-3}.

One fragmentation ion was produced in quantities comparable to those of the dominant products, *m/z* 43.018 Da, $C_2H_3O^+$. This fragment is common to acetic acid and acetate esters, but ions consistent with these parent masses were only found in low concentrations, so it is unassigned.[26] The fragment was found at mixing ratios comparable to 1,4-butanedial, and shows similar responses to RH.

To explore whether our gas-phase measurements agree with the amount of material lost from the particle phase, we summed the amount of carbon detected in the gas-phase products at different levels of RH. We used a carbon-balance approach to test whether the loss of material from the particle phase could be accounted for by generation of gas-phase products. The concentration of squalene entering the flow tube reactor is 1000 μg m^{-3}, corresponding to 880 μg m^{-3} of carbon. Converting the measurements in Figure 3.4.3 and Figure 3.4.4 from μg m^{-3} to μg C m^{-3}, and normalizing to the initial concentration of carbon entering the flow tube, gives the percent carbon in the gas phase. Figure 3.4.5 shows the percent carbon in the gas phase at 20 ppb h O_3 exposure. Note that only the dominant products are shown. Switching from 0% RH to 70% RH increases the proportion of carbon entering the gas phase from 21% to 65%, with increases in all dominant products except 1,4-butanedial. Even a moderate change from dry conditions to 30% RH, increases the proportion of carbon entering the gas phase by 60%. The largest increases are seen in 4-OPA production.

Because the VUV-AMS only measures relative concentrations of species, there is no direct measurement of the amount of carbon present in the condensed phase. However, measurements in the change in particle volume can be used as a quantitative indicator for mass loss from the particle. Note that this approach ignores the mass gained by the addition of oxygen to condensed phase products of ozonolysis, as well as any difference in densities between squalene and condensed-phase reaction products. Despite these limitations, using this approach, there is a clear and strong correlation between the carbon detected in the gas phase and the volume lost from the particle, as shown in Figure 3.4.6. Under dry conditions, at all levels of O_3 exposure, ~20% of the particle volume is lost, and ~20% of the carbon from squalene is found in the gas phase. At higher RHs, both the particle volume lost and the amount of carbon entering the gas phase are more sensitive to O_3 exposure, shown by the larger spread for these humidified conditions. The highest RH level (70%) gives both the greatest particle volume loss and the largest percent of

carbon in the gas phase. Notwithstanding experimental uncertainties, the evidence displayed in Figure 3.4.6 is consistent with expectations for the quantitative loss of particle-phase carbon being balanced with increased abundances of gaseous carbon species.

Figure 3.4.7 and S9 show the measurements in chamber air of several pertinent VOCs with O_3 and RH. Four T-shirts were placed inside the measurement chamber at 10:25 with RH maintained at ~26% for 1.5 h. Thereafter the RH was increased in a series of steps. The previously identified squalene oxidation products (4-OPA, 1,4-butanedial, acetone, 6-MHO, and geranylacetone) were observed to vary under the changing RH levels. Owing to the working principle of the humidifier, the RH in the chamber fluctuated regularly within a 10% range with a cycle of 38 minutes. In the data shown, primary unsaturated products and terminal products all faithfully follow the RH variation, confirming the dependence of gas-phase squalene ozonolysis products on RH, consistent with the flow-tube experiments. In accordance with previous studies, 4-OPA was the most abundant product (especially at higher RH levels); geranylacetone concentration was consistently the lowest among the quantified species.

In contrast with the flow tube experiment in which squalene particles were continuously supplied, the skin-oil soiled T-shirts contained a limited amount of squalene that was progressively consumed by the O_3 supplied. Therefore, at any given RH, most of the compounds showed a decreasing trend as the available squalene was depleted, except the first level where the lagging terminal products still increase towards steady state. In particular, acetone, the product of squalene ozonolysis at the terminal double bond, clearly followed the RH modulation while steadily decreasing as the experiment progressed. To better quantify the relative yields of the VOCs as a function of RH, two pairs of RH levels were selected, corresponding to points labeled 1-4 in Figure 3.4.7. As shown in Table 3.4.1**Error! Reference source not found.**, the concentration of 4-OPA increased by 5.9 μg m^{-3} as the RH increased from 26% (point 1) to 44% (point 2). A similar increase of 5.1 μg m^{-3} was seen in a second cycle as the RH changed from 46% (point 3) to 59% (point 4). The other terminal products (1,4-butanedial, hydroxy acetone, 4-oxobutanoic acid and 5-hydroxy-4-oxopentanal/levulinic acid) also showed slightly higher yields during the first RH increase (point 1 to point 2). Although the level of the first-generation products (acetone, 6-MHO and geranylacetone) tended to decrease with time overall, an increase was still observed in the second step (points 3 and 4) when the RH increased from 46% to 59%. However, unlike 4-OPA, the concentrations were much lower than during the first RH increase (points 1 and 2), as shown in Table 3.4.1. For 6-MHO and geranylacetone, enhanced oxidation by O_3 could also be a contributing factor. Ozone removal was 3.4 ppb greater in the second RH step (46% to 59%), indicating that more 6-MHO and geranylacetone were produced and subsequently oxidized by O_3 at this stage. Significantly elevated 4-OPA concentrations after the second increase of RH further supports this explanation.

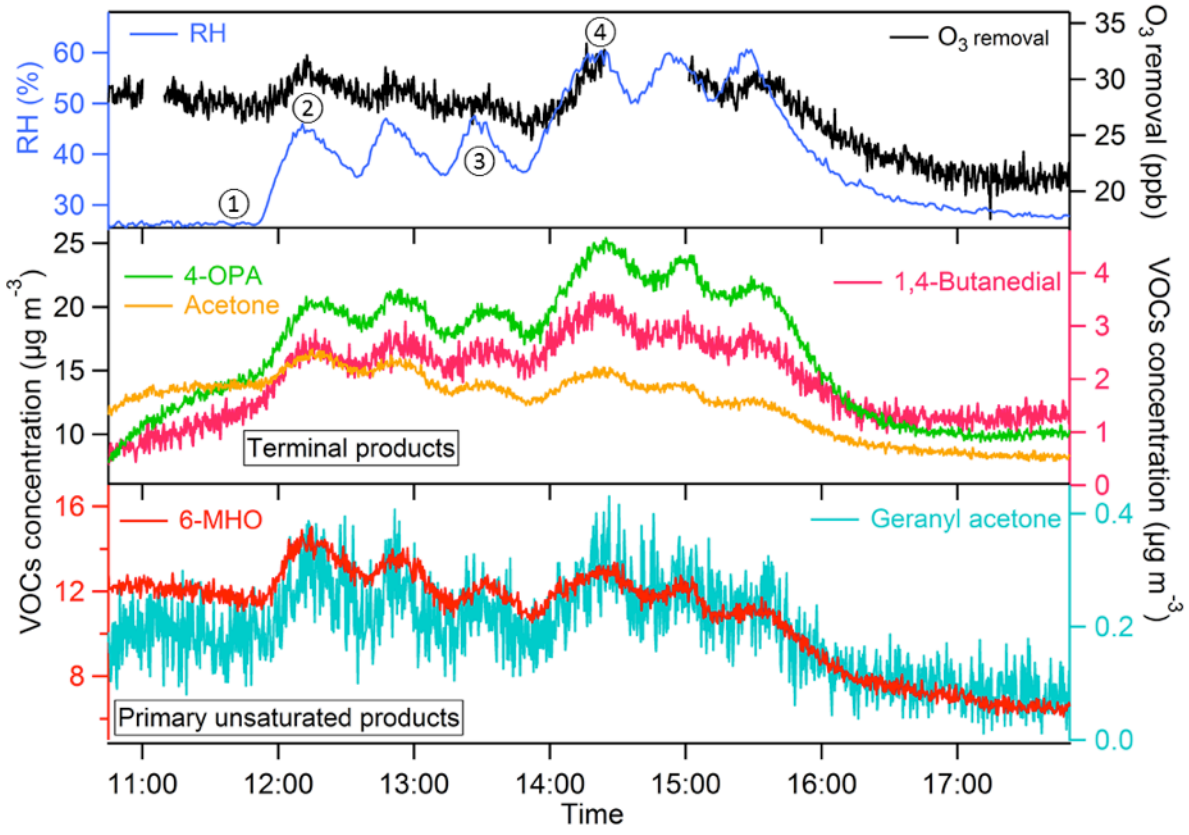

Figure 3.4.7 Time series of primary unsaturated products (lower panel) and terminal products (middle panel) with relative humidity and O_3 removal (upper panel) for clothing experiment (O_3 removal was obtained by subtracting measured O_3 level from the level of O_3 in supply air; the gap in the O_3 removal curve is due to the measurement of the O_3 concentration in the supply air.)

Table 3.4.1 Concentration change of squalene oxidation products (ΔVOCs, μg m^{-3}) due to relative humidity (RH) increase. Circled numbers refer to points in Figure 3.4.7.

			Δ VOCs (μg m^{-3})							
RH(%)		Δ O_3 (ppb)	acetone	4-OPA	6-MHO	geranyl acetone	1,4-butanedial	hydroxy acetone	4-oxobutanoic acid	5-hydroxy-4-oxopentanal
① 26	② 44	2.90	2.17	5.91	2.54	0.117	1.14	1.28	0.340	0.339
③ 46	④ 59	3.37	0.96	5.09	0.652	0.084	0.812	0.881	0.327	0.284

Effects of RH on squalene ozonolysis have been observed in prior studies. Petrick and Dubowski studied the condensed phase of squalene film oxidation while varying RH, finding that increased RH led to more ketone production.[27] They also note that RH did not influence reaction kinetics, a

finding also reported by Fu *et al*.[28] Wang and Waring examined secondary organic aerosol formation from the ozonolysis of surface-film squalene at 21% RH and 51% RH.[29] At high O_3 exposures, they found that the higher RH increased the aerosol mass fraction (AMF) from squalene. This increase suggests that higher RH leads to more oxidation products entering the gas phase, where they then can condense onto airborne particles. Zhou *et al*. examined the RH dependence of squalene film oxidation on the condensed phase products, finding that increasing the RH increased the yield of lower molecular weight products and decreased the yield of higher molecular weight products.[30] Although not quantitatively comparable, these previous studies qualitatively agree that an increase in RH leads to an increase in volatile products from squalene ozonolysis.

Humidity is already known to be an important factor that can influence VOC emissions from materials, compete with VOCs for sorptive uptake, and influence how indoor air is perceived.[31–40] Humidity is also known to change the deposition velocity of O_3 on indoor surfaces, a relationship that appears to depend on the material.[41] Few studies have assessed how RH changes ozonolysis products and emission rates. Coleman *et al*. (2008) found that increasing RH from 10% to 50% doubled the emissions of most ozonolysis byproducts from a cotton surface, with nonanal and decanal emissions increasing by about 5×.[14] Gall *et al*. (2013) studied primary and secondary ozonolysis emissions from building materials, finding RH to have mixed effects.[42] Secondary emissions increased with RH for painted drywall, while emissions from carpet and ceiling tile did not. The present work contributes new knowledge, showing that RH can directly influence the products of squalene ozonolysis, providing an alternate route by which water vapor can increase VOC concentrations. At realistic indoor O_3 exposures, a change from 0% RH to 70% RH results in ~3 times the amount of carbon entering the gas phase. Squalene, with six carbon-carbon double bonds, is a model molecule to show this effect. Other unsaturated compounds, especially those with double bonds separating small moieties, may show similar behavior. The reactions shown in Figure 3.4.2 are not specific to squalene, and so long as the carbonyls formed by reaction R2 have sufficient volatility, increased production of gas-phase products are generally expected from increases in RH.

The effects seen in this study suggest that RH can significantly alter the gas-phase composition of indoor air. In high occupancy settings, skin oil oxidation can be the dominant source of VOCs, and we show changes in RH can alter the strength of this source by a factor of 3. In the flow-tube reactor, at the highest level of O_3 exposure and RH, the sum of the concentrations of dominant products was 940 μg m^{-3}, comparable to the 1000 μg m^{-3} of squalene entering the reactor. It should be noted that RH does not change the rate of squalene ozonolysis; at low RH oxidized products are still being formed, but remain in the condensed phase. If that condensed phase is the skin surface, then the products might be taken up dermally, where they could influence health.[17,43] The large effect of RH on ozonolysis products from squalene, and the potential for the underlying mechanism to act on other alkenes, warrants further research on how humidity may modulate the consequences of indoor reactive chemistry.

3.5. Acknowledgements

The UC Berkeley team was funded by the Alfred P. Sloan Foundation via Grant 2016-7050. Kevin R. Wilson and Nadja Heine were supported by the Department of Energy, Office of

Science, Office of Basic Energy Sciences, Chemical Sciences, Geosciences, and Biosciences Division, in the Gas Phase Chemical Physics Program under Contract DE-AC02- 05CH11231. This research used resources of the Advanced Light Source, which is a DOE Office of Science User Facility under contract DE-AC02-05CH11231. The ICHEAR team (MPI and DTU) were funded by the Alfred P. Sloan Foundation via Grant G-2018-11233. Allen H. Goldstein gratefully acknowledges a Humboldt Research Award from the Alexander von Humboldt Foundation. The authors gratefully acknowledge members of the ICHEAR team including Nora Zannoni, Mengze Li, and Lisa Ernle for their contributions in performing the T-shirt experiments.

3.6. References

(1) Klepeis, N. E.; Nelson, W. C.; Ott, W. R.; Robinson, J. P.; Tsang, A. M.; Switzer, P.; Behar, J. V; Hern, S. C.; Engelmann, W. H. The National Human Activity Pattern Survey (NHAPS): a resource for assessing exposure to environmental pollutants. *J. Exposure Anal. Environ. Epidemiol*. **2001**, *11*, 231–252.

(2) Tang, X.; Misztal, P. K.; Nazaroff, W. W.; Goldstein, A. H. Volatile Organic Compound Emissions from Humans Indoors. *Environ. Sci. Technol.* **2016**, *50*, 12686–12694.

(3) Weschler, C. J. Roles of the human occupant in indoor chemistry. *Indoor Air* **2016**, *26*, 6–24.

(4) Weschler, C. J.; Wisthaler, A.; Cowlin, S.; Tamás, G.; Strøm-Tejsen, P.; Hodgson, A. T.; Destaillats, H.; Herrington, J.; Zhang, J.; Nazaroff, W. W. Ozone-Initiated Chemistry in an Occupied Simulated Aircraft Cabin. *Environ. Sci. Technol*. **2007**, *41*, 6177–6184.

(5) Wisthaler, A.; Weschler, C. J. Reactions of ozone with human skin lipids: Sources of carbonyls, dicarbonyls, and hydroxycarbonyls in indoor air. *Proc. Natl. Acad. Sci. U. S. A.* **2010**, *107*, 6568–6575.

(6) Lakey, P. S. J.; Wisthaler, A.; Berkemeier, T.; Mikoviny, T.; Pöschl, U.; Shiraiwa, M. Chemical kinetics of multiphase reactions between ozone and human skin lipids: Implications for indoor air quality and health effects. *Indoor Air* **2017**, *27*, 816–828.

(7) Lakey, P. S. J.; Morrison, G. C.; Won, Y.; Parry, K. M.; von Domaros, M.; Tobias, D. J.; Rim, D.; Shiraiwa, M. The impact of clothing on ozone and squalene ozonolysis products in indoor environments. *Commun. Chem*. **2019**, *2*, 56.

(8) Kruza, M.; Carslaw, N. How Do Breath and Skin Emissions Impact Indoor Air Chemistry? *Indoor Air* **2019**, *29*, 369–379.

(9) Weschler, C. J. Ozone in Indoor Environments: Concentration and Chemistry. *Indoor Air* **2000**, *10*, 269–288.

(10) Weschler, C. J. Ozone's Impact on Public Health: Contributions from Indoor Exposures to Ozone and Products of Ozone-Initiated Chemistry. *Environ. Health Perspect.* **2006**, *114*, 1489–1496.

(11) Fischer, A.; Ljungström, E.; Langer, S. Ozone removal by occupants in a classroom. *Atmos. Environ.* **2013**, *81*, 11–17.

(12) Nicolaides, N. Skin Lipids: Their Biochemical Uniqueness. *Science* **1974**, *186*, 19–26.

(13) Bhangar, S.; Cowlin, S. C.; Singer, B. C.; Sextro, R. G.; Nazaroff, W. W. Ozone Levels in Passenger Cabins of Commercial Aircraft on North American and Transoceanic Routes. *Environ. Sci. Technol.* **2008**, *42*, 3938–3943.

(14) Coleman, B. K.; Destaillats, H.; Hodgson, A. T.; Nazaroff, W. W. Ozone consumption and volatile byproduct formation from surface reactions with aircraft cabin materials and clothing fabrics. *Atmos. Environ.* **2008**, *42*, 642–654.

(15) Wells, J. R.; Morrison, G. C.; Coleman, B. K. Kinetics and Reaction Products of Ozone and Surface-Bound Squalene. *J. ASTM Int.* **2008**, *5*, JAI101629.

(16) Jacobs, M. I.; Xu, B.; Kostko, O.; Heine, N.; Ahmed, M.; Wilson, K. R. Probing the Heterogeneous Ozonolysis of Squalene Nanoparticles by Photoemission. *J. Phys. Chem. A* **2016**, *120*, 8645–8656.

(17) Anderson, S. E.; Franko, J.; Jackson, L. G.; Wells, J. R.; Ham, J. E.; Meade, B. J. Irritancy and Allergic Responses Induced by Exposure to the Indoor Air Chemical 4-Oxopentanal. *Toxicol. Sci.* **2012**, *127*, 371–381.

(18) Wolkoff, P.; Larsen, S. T.; Hammer, M.; Kofoed-Sørensen, V.; Clausen, P. A.; Nielsen, G. D. Human reference values for acute airway effects of five common ozone-initiated terpene reaction products in indoor air. *Toxicol. Lett.* **2013**, *216*, 54–64.

(19) Mochalski, P.; King, J.; Unterkofler, K.; Hinterhuber, H.; Amann, A. Emission rates of selected volatile organic compounds from skin of healthy volunteers. *J. Chromatogr. B* **2014**, *959*, 62–70.

(20) Heine, N.; Houle, F. A.; Wilson, K. R. Connecting the Elementary Reaction Pathways of Criegee Intermediates to the Chemical Erosion of Squalene Interfaces during Ozonolysis. *Environ. Sci. Technol.* **2017**, *51*, 13740–13748.

(21) Heine, N.; Arata, C.; Goldstein, A. H.; Houle, F. A.; Wilson, K. R. Multiphase Mechanism for the Production of Sulfuric Acid from SO_2 by Criegee Intermediates Formed During the Heterogeneous Reaction of Ozone with Squalene. *J. Phys. Chem. Lett.* **2018**, *9*, 3504–3510.

(22) Smith, J. D.; Kroll, J. H.; Cappa, C. D.; Che, D. L.; Liu, C. L.; Ahmed, M.; Leone, S. R.; Worsnop, D. R.; Wilson, K. R. The heterogeneous reaction of hydroxyl radicals with sub-

micron squalane particles: a model system for understanding the oxidative aging of ambient aerosols. *Atmos. Chem. Phys.* **2009**, *9*, 3209–3222.

(23) Zhao, J.; Zhang, R. Proton transfer reaction rate constants between hydronium ion (H_3O^+) and volatile organic compounds. *Atmos. Environ.* **2004**, *38*, 2177–2185.

(24) Kari, E.; Miettinen, P.; Yli-Pirilä, P.; Virtanen, A.; Faiola, C. L. PTR-ToF-MS product ion distributions and humidity-dependence of biogenic volatile organic compounds. *Int. J. Mass Spectrom.* **2018**, *430*, 87–97.

(25) Vlasenko, A.; Macdonald, A. M.; Sjostedt, S. J.; Abbatt, J. P. D. Formaldehyde measurements by Proton transfer reaction – Mass Spectrometry (PTR-MS): correction for humidity effects. *Atmos. Meas. Tech.* **2010**, *3*, 1055–1062.

(26) Pagonis, D.; Sekimoto, K.; de Gouw, J. A Library of Proton-Transfer Reactions of H 3 O + Ions Used for Trace Gas Detection. *J. Am. Soc. Mass Spectrom.* **2019**, *30*, 1330–1335.

(27) Petrick, L.; Dubowski, Y. Heterogeneous oxidation of squalene film by ozone under various indoor conditions. *Indoor Air* **2009**, *19*, 381–391.

(28) Fu, D.; Leng, C.; Kelley, J.; Zeng, G.; Zhang, Y.; Liu, Y. ATR-IR Study of Ozone Initiated Heterogeneous Oxidation of Squalene in an Indoor Environment. *Environ. Sci. Technol.* **2013**, *47*, 10611–10618.

(29) Wang, C.; Waring, M. S. Secondary organic aerosol formation initiated from reactions between ozone and surface-sorbed squalene. *Atmos. Environ.* **2014**, *84*, 222–229.

(30) Zhou, S.; Forbes, M. W.; Abbatt, J. P. D. Kinetics and Products from Heterogeneous Oxidation of Squalene with Ozone. *Environ. Sci. Technol.* **2016**, *50*, 11688–11697.

(31) Markowicz, P.; Larsson, L. Influence of relative humidity on VOC concentrations in indoor air. *Environ. Sci. Pollut. Res.* **2015**, *22*, 5772–5779.

(32) Andersen, I.; Lundqvist, G. R.; Mølhave, L. Indoor Air Pollution Due to Chipboard Used as a Construction Material. *Atmos. Environ.* **1975**, *9*, 1121–1127.

(33) Fang, L.; Clausen, G.; Fanger, P. O. Impact of Temperature and Humidity on Chemical and Sensory Emissions from Building Materials. *Indoor Air* **1999**, *9*, 193–201.

(34) Huang, H.; Haghighat, F.; Blondeau, P. Volatile organic compound (VOC) adsorption on material: influence of gas phase concentration, relative humidity and VOC type. *Indoor Air* **2006**, *16*, 236–247.

(35) Huang, S.; Xiong, J.; Cai, C.; Xu, W.; Zhang, Y. Influence of humidity on the initial emittable concentration of formaldehyde and hexaldehyde in building materials: experimental observation and correlation. *Sci. Rep.* **2016**, *6*, 23388.

(36) Liang, W.; Yang, S.; Yang, X. Long-Term Formaldehyde Emissions from Medium-Density Fiberboard in a Full-Scale Experimental Room: Emission Characteristics and the Effects of Temperature and Humidity. *Environ. Sci. Technol.* **2015**, *49*, 10349–10356.

(37) Parthasarathy, S.; Maddalena, R. L.; Russell, M. L.; Apte, M. G. Effect of Temperature and Humidity on Formaldehyde Emissions in Temporary Housing Units. *J. Air Waste Manage. Assoc.* **2011**, *61*, 689–695.

(38) Sidheswaran, M.; Chen, W.; Chang, A.; Miller, R.; Cohn, S.; Sullivan, D.; Fisk, W. J.; Kumagai, K.; Destaillats, H. Formaldehyde Emissions from Ventilation Filters under Different Relative Humidity Conditions. *Environ. Sci. Technol.* **2013**, *47*, 5336–5343.

(39) Xu, J.; Zhang, J. S. An experimental study of relative humidity effect on VOCs' effective diffusion coefficient and partition coefficient in a porous medium. *Build. Environ.* **2011**, *46*, 1785–1796.

(40) Won, D.; Corsi, R. L.; Rynes, M. Sorptive Interactions between VOCs and Indoor Materials. *Indoor Air* **2001**, *11*, 246–256.

(41) Shen, J.; Gao, Z. Ozone removal on building material surface: A literature review. *Build. Environ.* **2018**, *134*, 205–217.

(42) Gall, E.; Darling, E.; Siegel, J. A.; Morrison, G. C.; Corsi, R. L. Evaluation of three common green building materials for ozone removal, and primary and secondary emissions of aldehydes. *Atmos. Environ.* **2013**, *77*, 910–918.

(43) Anderson SE, Franko J, Jackson LG, Wells J, Ham JE, Meade B. Irritancy and allergic responses induced by exposure to the indoor air chemical 4-oxopentanal. Toxicol Sci. **2012**, 127, 371–381.

3.7. Supporting Information

Table 3.7.1 Geranyl acetone concentration data used to calculate production from ozonolysis. Once concentrations were stable in the flow tube reactor, a 'Raw' measurement was taken. Shortly after, the particle flow was replaced with a flow of N_2, and squalene particles were removed from the flow tube reactor, allowing for a background measurement. Background measurements were taken 2 min after the particle flow was removed, when 95% of particles are removed from the flow tube.

RH (%)	O_3 Exposure (ppb h)	Background (μg m^{-3})	Raw (μg m^{-3})	Difference (μg m^{-3})
0	9	9	14	5
0	12	1	4	3
0	17	0	0	0
0	21	0	0	0
0	27	0	0	0
0	32	0	0	0
30	5	69	70	1
30	10	22	37	15
30	12	3	10	7
30	17	0	1	1
30	23	0	0	0
30	30	0	0	0
50	6	149	160	11
50	10	20	34	14
50	12	3	9	6
50	16	0	1	1
50	21	0	0	0
50	26	0	0	0
50	28	0	0	0
70	6	118	127	9
70	9	24	43	19
70	12	3	12	9
70	16	0	1	1
70	21	0	0	0
70	31	0	0	0

Table 3.7.2 6-MHO concentration data used to calculate production from ozonolysis. Once concentrations were stable in the flow tube reactor, a 'Raw' measurement was taken. Shortly after, the particle flow was replaced with a flow of N_2, and squalene particles were removed from the flow tube reactor, allowing for a background measurement. Background measurements were taken 2 min after the particle flow was removed, when 95% of particles are removed from the flow tube.

RH (%)	O_3 Exposure (ppb h)	Background (μg m^{-3})	Raw (μg m^{-3})	Difference (μg m^{-3})
0	9	36	94	57
0	12	15	69	52
0	17	7	31	25
0	21	2	18	15
0	27	1	7	6
0	32	1	3	2
30	5	151	152	1
30	10	112	172	59
30	12	51	132	79
30	17	12	58	45
30	23	6	31	25
30	30	3	13	9
50	6	290	401	115
50	10	105	218	112
50	12	41	169	128
50	16	6	90	83
50	21	2	47	45
50	26	1	27	25
50	28	1	15	14
70	6	240	355	115
70	9	109	260	151
70	12	42	216	173
70	16	6	121	115
70	21	2	68	65
70	31	2	12	11

Table 3.7.3 4-OPA concentration data used to calculate production from ozonolysis. Once concentrations were stable in the flow tube reactor, a 'Raw' measurement was taken. Shortly after, the particle flow was replaced with a flow of N_2, and squalene particles were removed from the flow tube reactor, allowing for a background measurement. Background measurements were taken 2 min after the particle flow was removed, when 95% of particles are removed from the flow tube.

RH (%)	O_3 Exposure (ppb h)	Background (μg m^{-3})	Raw (μg m^{-3})	Difference (μg m^{-3})
0	9	148	185	38
0	12	147	205	58
0	17	134	209	75
0	21	105	202	96
0	27	96	192	95
0	32	101	199	98
30	5	191	229	38
30	10	335	353	19
30	12	378	425	47
30	17	368	492	125
30	23	344	502	160
30	30	337	522	184
50	6	848	887	42
50	10	579	601	20
50	12	712	785	75
50	16	676	917	240
50	21	626	950	323
50	26	618	1020	399
50	28	640	1038	398
70	9	857	871	11
70	12	1083	1165	79
70	16	1233	1516	282
70	21	1179	1630	447
70	31	1136	1734	606

Table 3.7.4 1,4-butanedial concentration data used to calculate production from ozonolysis. Once concentrations were stable in the flow tube reactor, a 'Raw' measurement was taken. Shortly after, the particle flow was replaced with a flow of N_2, and squalene particles were removed from the flow tube reactor, allowing for a background measurement. Background measurements were taken 2 min after the particle flow was removed, when 95% of particles are removed from the flow tube.

RH (%)	O_3 Exposure (ppb h)	Background (μg m^{-3})	Raw (μg m^{-3})	Difference (μg m^{-3})
0	9	81	106	25
0	12	87	126	40
0	17	88	143	55
0	21	67	150	82
0	27	57	142	85
0	32	57	143	85
30	5	66	87	20
30	10	112	135	25
30	12	122	166	45
30	17	110	205	95
30	23	100	218	118
30	30	92	229	135
50	10	153	178	25
50	12	161	207	46
50	16	152	238	86
50	21	146	242	96
50	26	149	257	107
50	28	159	260	101
70	9	189	206	16
70	12	223	246	23
70	16	254	297	43
70	21	239	289	50
70	31	257	309	53

Table 3.7.5 Acetone concentration data used to calculate production from ozonolysis. Once concentrations were stable in the flow tube reactor, a 'Raw' measurement was taken. Shortly after, the particle flow was replaced with a flow of N_2, and squalene particles were removed from the flow tube reactor, allowing for a background measurement. Background measurements were taken 2 min after the particle flow was removed, when 95% of particles are removed from the flow tube.

RH (%)	O_3 Exposure (ppb h)	Background (μg m^{-3})	Raw (μg m^{-3})	Difference (μg m^{-3})
0	9	81	167	84
0	12	71	173	102
0	17	71	169	98
0	21	57	165	107
0	27	52	154	102
0	32	52	158	105
30	5	105	137	32
30	10	142	227	84
30	12	123	267	141
30	17	92	293	197
30	23	81	289	206
30	30	75	288	213
50	6	163	240	77
50	10	135	249	112
50	12	110	289	178
50	16	71	301	230
50	21	62	302	238
50	26	60	319	256
50	28	62	307	243
70	6	137	216	77
70	9	158	293	133
70	12	142	337	194
70	16	122	381	258
70	21	149	428	278
70	31	184	459	278

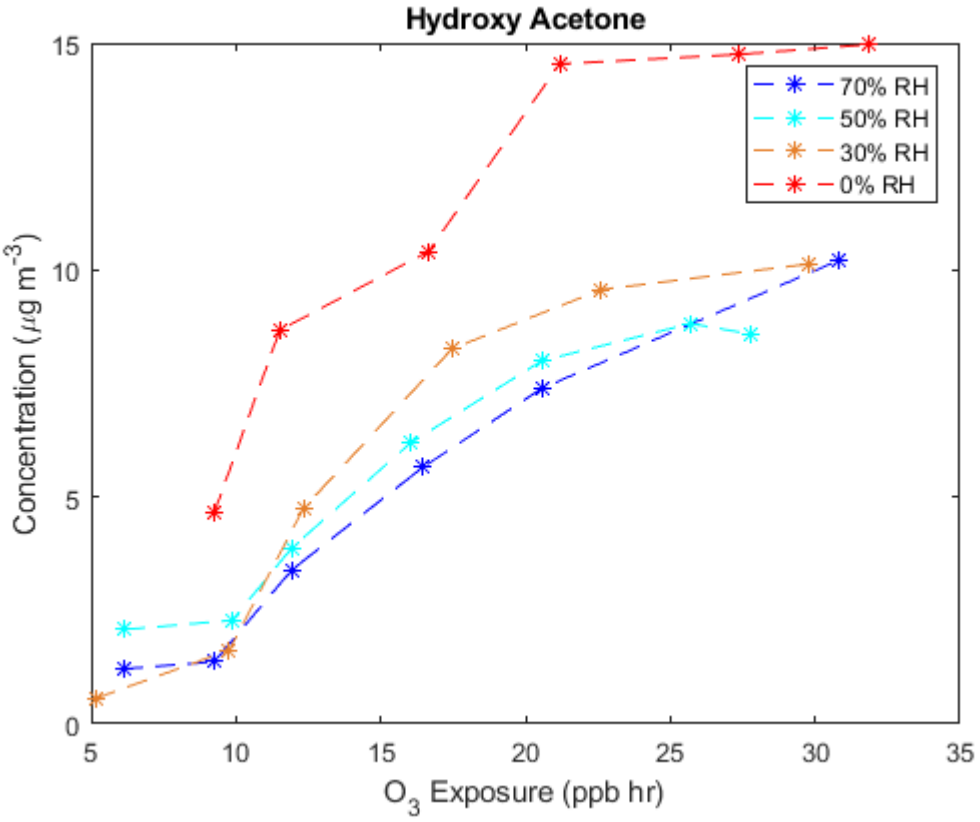

Figure 3.7.1 Hydroxy acetone concentration as a function of humidity and O_3 exposure.

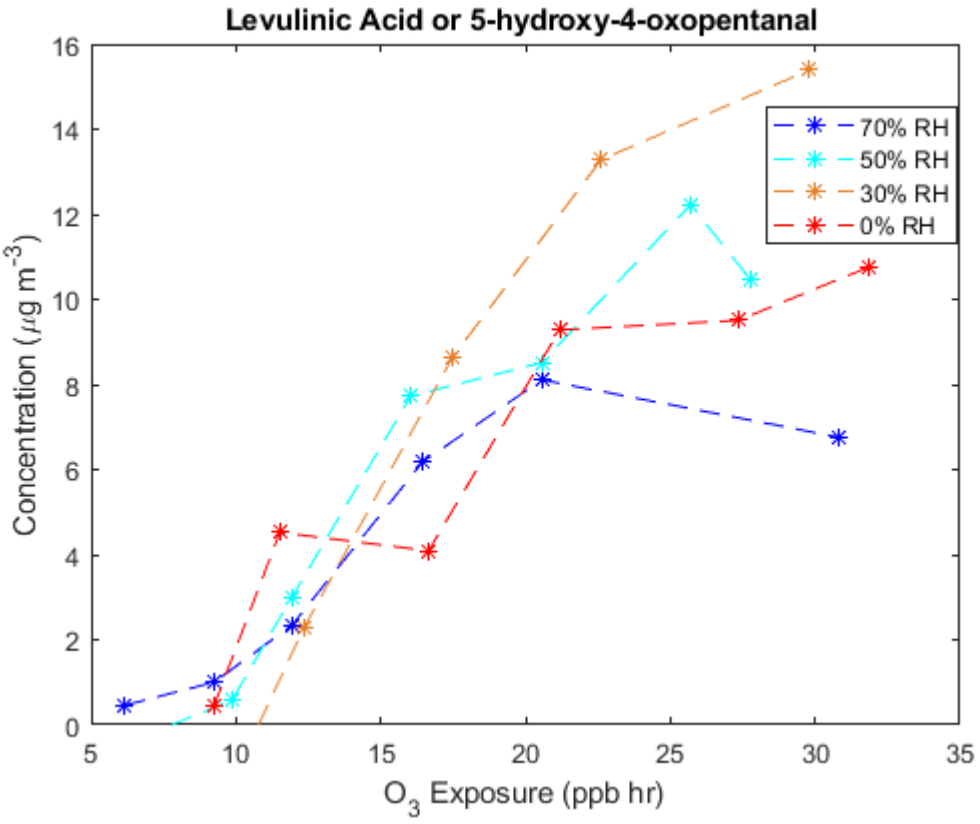

Figure 3.7.2 Levulinic acid and 5-hydroxy-4-oxopentanal concentration as a function of humidity and O_3 exposure.

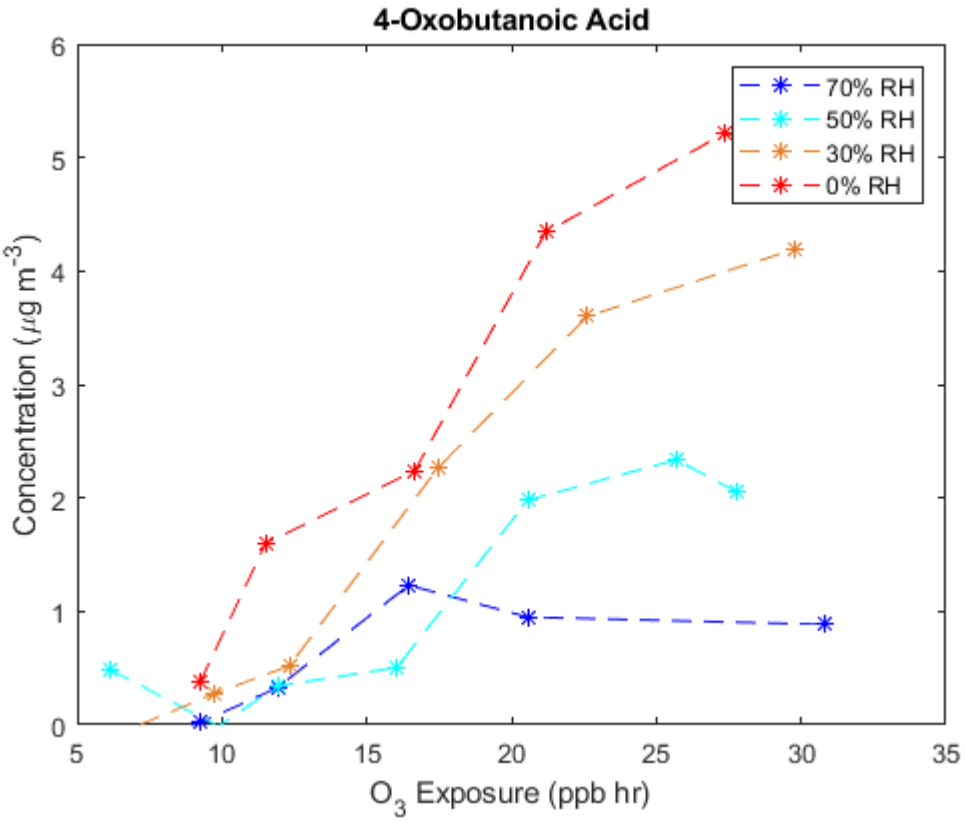

Figure 3.7.3 4-oxobutanoic acid concentration as a function of humidity and O_3 exposure.

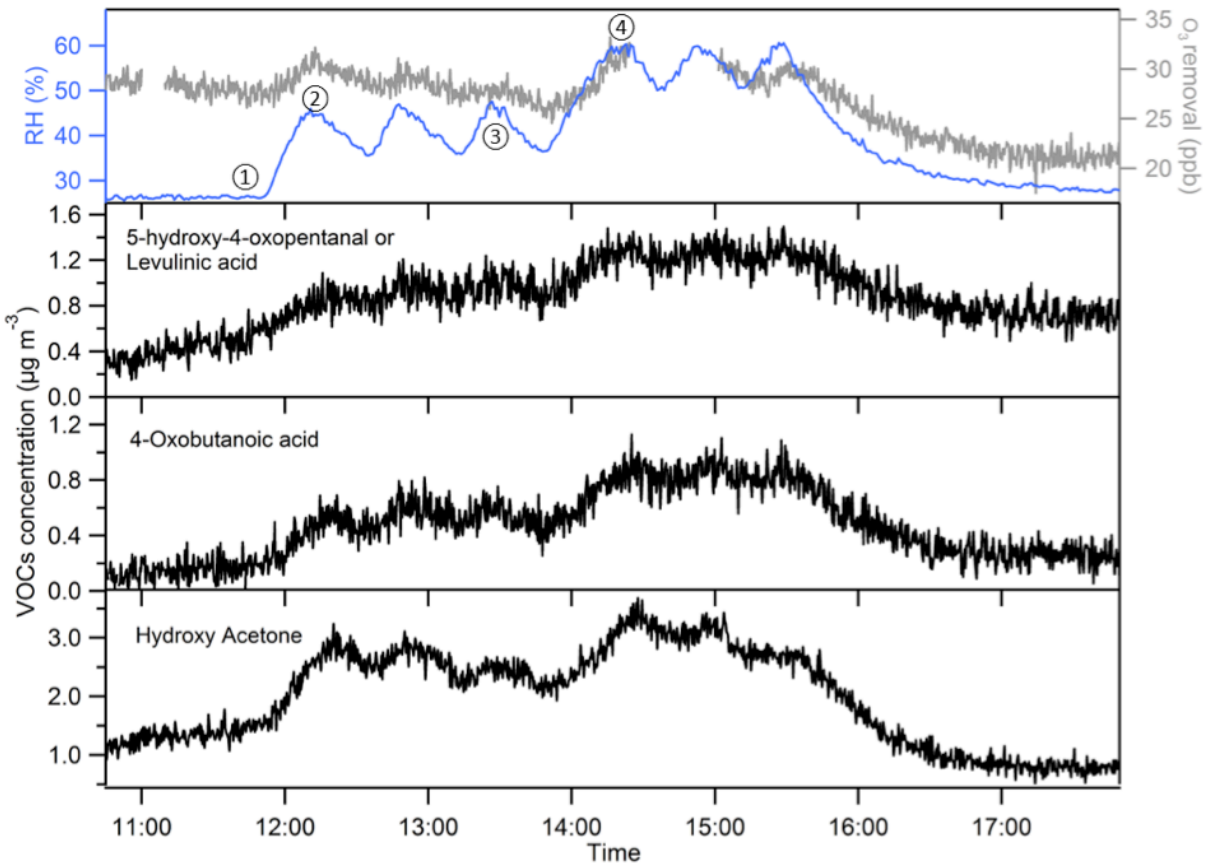

Figure 3.7.4 Time series of other squalene oxidation products with relative humidity and O_3 removal (upper panel) for the clothing experiment (O_3 removal is the difference between O_3 measured in supply air and the chamber; the data gap is due to the supply air measurement).

4. Volatile Organic Compound Emissions During HOMEChem

4.1. Abstract

Quantifying speciated VOC concentrations and emissions is critical to understanding and modeling the processes that control indoor dynamics, human exposure, and the chemistry of indoor air. Much of the previous building-scale research on indoor VOCs has utilized broad surveys with low time resolution concentration measurements for specific target compounds. Such studies cannot reveal the influence of short-term dynamic processes that control temporal variability in concentrations. Few field studies have been able to quantify emission rates associated with various activities and processes. Here, we present source strength profiles from the HOMEChem study, quantifying the VOC emissions from the building and its contents, and from scripted experiments (with multiple replicates) of cooking, cleaning, and human occupancy. Measurements of VOCs were performed with a proton transfer reaction time of flight mass spectrometer (PTR-ToF-MS), which continuously measured the time-resolved mass spectrum of indoor and outdoor air. Continuous tracer releases enabled determination of air change rates enabling mass-balance based calculations of speciated, time resolved VOC source strengths. The building and its contents were the dominant emission source into the house, with large emissions of acetic acid, methanol, and formic acid. Cooking emissions were greater than cleaning emissions, and were dominated by ethanol. Bleach cleaning generated high emissions of reactive chlorinated compounds, whereas cleaning with a natural product emitted predominantly monoterpenes and terpenoids. Emissions from occupancy experiments showed large enhancements of siloxanes from personal-care products in the morning; these emissions were strongly diminished in the afternoon. We use our results to construct VOC emissions for a hypothetical 24 h, and show that emissions from the house and its contents make up nearly half of the total indoor VOC emissions.

4.2. Introduction

Indoor VOC concentrations in residences are generally higher than outdoors.[1–4] People spend approximately 70% of their time at home.[5] Thus, it is expected that an important route of human exposure to volatile organic compounds (VOCs) is from the indoor air of a residence. While much is known about outdoor VOCs, outdoor air plays a small role in the concentrations of VOCs found indoors. Rather it is emissions from the residence, occupants, or occupant activities that lead to elevated indoor VOC concentrations.

Due to analytical constraints of sampling and typical chromatographic methods, many prior VOC emission studies of buildings, building materials, and furnishings have focused on a target set of compounds, such as formaldehyde or BTEX.[6–8] Recent advances in chemical ionization mass spectrometry allow for real-time, speciated measurements of tens to hundreds of indoor VOCs.[1,9–14] Huangfu *et al.* (2019) use the high time resolution of proton transfer reaction mass

spectrometry (PTR-MS) to show a temperature and air change rate (ACR) dependence of VOC mixing ratios in multiple unoccupied homes.[13] Liu *et al*. (2019) determine building VOC emissions of an occupied home by filtering for compounds that have steady rates of emission, rather than episodic emissions characteristic of occupancy and activities.[1] They find that most VOC emissions are dominated by continuous emissions from the building and its contents.

Among residential occupant activities, cooking is typically the dominant indoor VOC emission source.[1,15] While cooking styles and techniques vary, a common factor in cooking emissions is carbonyl compounds from the heating of oils and fats. A study of 15 commercial kitchens in Hong Kong showed large emissions of carbonyl compounds, especially formaldehyde, acrolein, and longer chain aldehydes.[16]. A laboratory study of the emissions from charbroiled hamburgers found 36% of the VOC emissions were C_1-C_{10} aldehydes.[17] Klein *et al*. (2016) investigated cooking VOC emissions with PTR-MS and found a wide array of aldehydes emitted from hot cooking oil.[18] In a study of European households, Klein *et al*. (2019) identify these aldehydes as the dominant VOC emission from residential cooking.[15] Other VOCs identified from cooking include terpenes from herbs and spices, methanol from the boiling of vegetables, and dimethyl sulfide from cruciferous vegetables.[18,19]

Cleaning products often contain VOCs, either as fragrance, solvent, or as an active ingredient of the cleaning agent itself.[20] It is estimated that American adults spend an average of 20-30 minutes per day house cleaning.[21] "Natural" cleaning products do not have a strict definition, but broadly speaking are cleaners that claim to be environmentally friendly and contain plant derived ingredients often including terpenoid compounds (e.g., d-limonene from orange-oil or alpha-pinene from pine-oil based cleaners). Common household cleaning products such as bleach contain strong oxidants. Bleach sold for household use is typically an aqueous solution of ~5% sodium hypochlorite (NaOCl) mixed with a strong base to establish a pH of 12. Its cleaning power comes from the oxidative potential of the chlorine atom: in hypochlorite the Cl oxidation state is +I while in the more common chloride form the oxidation state is -I.[22] Bleach cleaning has been found to generate large (>100 ppb) gas phase concentrations of hypochlorous acid (HOCl), a strong oxidant.[23,24]

PTR-MS does not measure HOCl mixing ratios, but does measure many products of bleach cleaning. Wang *et al*. (2019) used PTR-MS to study the reaction products of HOCl and limonene.[24] They found reaction products consistent with the addition of O or Cl to the terpene, as well as many products of lower molecular mass than the terpene, either directly produced or from larger molecules that fragmented during measurement. Matilla *et al*. 2020 report elevated concentrations of inorganic species, especially chloramines (NH_2Cl, $NHCl_2$, NCl_3), during bleach cleaning from the same HOMEChem study we analyze here. [25]

Occupants can be an important source of VOCs indoors.[26] Occupancy emissions come from both naturally produced VOCs on the skin or in breath, oxidation products of skin oil, as well as the volatilization of chemicals in personal care products (PCPs). Isoprene and acetone are the most prominent breath VOCs.[27] Oxidation of skin oil leads to many volatiles, the most studied of which are 6-methyl-5-hepten-2-one (6-MHO) and 4-oxopentanal (4-OPA), arising from the ozonolysis of squalene.[28] A study of VOC emissions inside a movie theater showed large emissions of isoprene and acetone, as well as methanol (suspected to be produced

endogenously), and siloxanes and monoterpenes from PCPs.[9] Other VOCs were shown to correlate with on-screen activity, such as comedic moments or depictions of injury.[10]

With respect to PCPs, hundreds or thousands of different volatile species may be in wide usage. However, Yeoman *et al*. (2020) find the dominant products to be 2-propanol, benzyl alcohol, octamethylcyclotetrasiloxane (D4), decamethylcyclopentasiloxane (D5), ethanol, limonene, and methanol.[29] Grouped together, the siloxanes were the largest emission source observed in the classroom study by Tang *et al*. (2015), which is likely indicative of many highly populated indoor environments.[26,30]

Here we report baseline VOC emissions from the building and its contents, and from scripted replicated activities including cleaning, cooking, and occupancy, during the House Observations of Microbial and Environmental Chemistry (HOMEChem) study.

4.3. Methods

Measurements were performed at The University of Texas at Austin's test house (UTest House) in June 2018. An overview of the HOMEChem study, including descriptions of the scripted experiments and test house facilities can be found in Farmer *et al*. (2019).[31]

Cleaning experiments were done with either bleach (120 ml Clorox in 3.8 L of tap water) or a natural cleaner (60 ml Mrs. Meyer's Clean Day in 3.8 L of tap water). One person entered the house, prepared the solution, and mopped the kitchen and living room areas of the house (40 m^2). The cleaning activity typically took 25 minutes, then the person would immediately leave the house. Measurements continued with the house unoccupied, giving a total sampling time of 1 hour. Experiments with each cleaner were performed 7 times.

Cooking experiments consisted of making rice and a vegetable stir fry for 3 people. Volunteers enter the house and set water (480 ml) to boil for rice (240 ml uncooked). Cooking oil (30-45 ml) was added to a wok or cast-iron pan and heated until shimmering or smoking. Frozen vegetables (~1-1.5 L) were then added, followed by sauces (30 ml sriracha, 60-180 ml stir fry sauce, and a small amount of soy sauce). The food was eaten and dishes cleaned in a dishwasher with detergent, while pots and pans were cleaned with soap and water by hand. Each experiment lasted 2 hours. A total of 7 cooking experiments were performed.

Occupancy experiments were conducted in 15-minute intervals, sequentially increasing to a maximum occupancy, then leaving in the reverse order that people entered (first in, last out). Due to the mixing rate of the house (20 min) being on the order of the time between occupancy changes, we chose to integrate emissions over the entire two-hour experiment, and normalize the emissions by the person-hours of occupation. Occupancy experiments were conducted with cumulative occupancy of 15 person-hours (except for one experiment, "Regular PCP", which had a cumulative occupancy of 12.5 person-hours). Emissions are only reported if, prior to normalizing to occupancy, the total emission above baseline for the experiment period was greater than 0.001 mg.

Volunteers varied their personal care product usage for the occupancy experiments. In two experiments, volunteers wore minimal PCPs, or chose "naturally" branded products. In one

experiment occupants were instructed to apply their regularly used amounts of PCPs. In two other experiments, occupants were instructed to heavily apply PCPs. These experiments are referred to as "Low PCP", "Regular PCP", and "High PCP" occupancy experiments. Duplicate experiments were carried out on the same day, with one experiment in the morning and one in the afternoon. During the Regular PCP experiment the ACR could not be calculated from the tracer-gas data so a default value of 0.5 h^{-1} was used.

Baseline emission rates are attributable to the building materials, finishing materials, and stationary furnishings. We assessed baseline emission rates during a period with no indoor occupancy or activities, by leaving the house at rest for 24 hours. The air conditioner and associated ventilation fans were left on. The day used for baseline analysis occurred halfway through the month-long campaign so as to capture the house in a used but unoccupied state. Due to overnight calibrations we do not measure a full 24 hours; instead we calculate emissions from 6:30 am to 2:30 am the following day.

Measurements of VOCs were made by proton transfer reaction time-of-flight mass spectrometry (PTR-TOF-MS, PTR-TOF-8000, IONICON Analytik GmbH, Austria), a chemical ionization technique with minimal fragmentation that uses H_3O^+ as the reagent ion. PTR-TOF-MS provides mixing ratio measurements of VOCs that possess a proton affinity greater than that of water, namely alkenes and oxygenated VOCs as well as some halogenated species. It is not sensitive to most alkanes because of their low proton affinity. Measurements were collected at 1 Hz resolution, processed with the PTRwid software package, and later averaged to 1-minute time series.[32]

Multipoint calibrations were run each night, alternating between two multicomponent mixtures. A total of 18 compounds were directly calibrated. Uncertainty in reported mixing ratios for directly calibrated compounds is +/- 10%. All other compound mixing ratios were calculated using a default proton transfer reaction rate constant of 2.5×10^{-9} cm^3 s^{-1} for both the primary ion as well as the for first water cluster, $H_3O^+(H_2O)$. Mixing ratios calculated from the default reaction rate constant are typically accurate to +/- 50%; uncertainties could be higher for inorganic species such as chloramines.[33]

Sample air was continuously drawn from two sample inlets through tubes (PFA; OD 0.635 cm; length 8.4 m; flow rate 1.5 L/min). One inlet was located in the kitchen of the test house, the other was outdoors. The sample flows were subsampled at 150 ml/min through a 6-way valve (NResearch, 648T091; PTFE inner contact surfaces) and PEEK tubing (length 2m) into the PTR-TOF-MS. Indoor air was measured for 25 minutes then outdoor air was measured for 5 minutes during each 30-minute period throughout the experiment. To avoid carryover effects, only the last minute of outdoor sampling is used for to calculate the outdoor concentrations, allowing 4 minutes for compounds to equilibrate in the valve, PEEK tubing, and instrument. Similarly, after switching back to indoor sampling the first 5 minutes of data are discarded, to allow for sample-line equilibration. In summary, under this sampling scheme, for every 30 minutes, the analysis utilizes 20 minutes of indoor measurements and 1 minute of outdoor measurement.

Air-change rates (ACR) were determined by the continuous release of a tracer compound (butene D3, Cambridge Isotopes, Inc.) as in Liu *et al*. (2018).[34] Throughout the experiments the test house was mechanically ventilated at a target ACR of 0.5 h^{-1}. ACR during the activity and

occupancy had a mean value of 0.6 h^{-1} and an interquartile range of 0.5-0.7 h^{-1} (n = 25). For occupancy and activity experiments ACR is calculated at the time resolution of the experiment, 1 h for cleaning experiments, 2 h for cooking and occupancy experiments. ACR is calculated with 1 h time resolution during the unoccupied experiment. A separate recirculation system contained the air conditioner (AC). Although the cooling function of AC unit was thermostatically controlled, the recirculation fans were left on continuously. With a recirculation turnover time of ~7 min, the house is expected to become well-mixed within 20 min after a localized emission event.

Total emissions into the house, M_{total} (mg), over a time interval, Δt, are the sum of the mass of the compound that remains in the house and the mass that is removed by ventilation. Mathematically this works out to:

$$M_{total} = \rho V\left(C_{final} - C_{initial}\right) + \rho VA\Delta t(C_{avg} - C_{outdoors}) \quad (1)$$

Where $C_{initial}$ and C_{final} are the indoor mixing ratios (ppb) at the beginning and end of the interval Δt (h), A is the ACR (h^{-1}), C_{avg} is the average indoor mixing ratio (ppb) over Δt, and $C_{outdoors}$ is the average outdoor mixing ratio over Δt. To convert mixing ratios to mass emitted each term is multiplied by V, the mixed volume of the house (235,000 L), and ρ (mg mm^{-3}), the gas density at 20 °C of the species emitted, as calculated from the molar mass of the compound and the ideal gas law. The first term of equation 1 is the mass of a given compound that remains in the house after being emitted over the interval Δt, while the second term is the mass of emitted compound that has been lost to ventilation over Δt.

For the reported emissions M (mg) from occupancy and activities, continuous emissions from the house and its contents are subtracted from M_{total}:

$$M = M_{total} - M_{baseline} = \rho V\left(C_{final} - C_{initial}\right) + \rho VA\Delta t(C_{avg} - C_{initial}) \quad (2)$$

This assumes baseline emissions, $M_{baseline}$ (mg), and corresponding baseline mixing ratios are constant over the integration period. The baseline subtraction is susceptible to two types of errors: changes in baseline emission rates or ACR over the course of the experiment, and $C_{initial}$ not being a steady state concentration. The first case is likely to be small. For cleaning experiments Δt is 1 h; for cooking and occupancy experiments Δt is 2 h. Temperatures in the test house remain stable over this timeframe, so changes in baseline emissions due to changes in surface temperatures are expected to be low. Additionally, emissions *caused* by changes in temperature due to the activity (i.e. kitchen surface temperatures increasing during cooking) should be included as emissions due to the activity. ACR is calculated over the same time interval as the experiments, giving a representative rate of ventilation over the entire integration time.

Causes of unstable initial mixing ratios could be declining concentrations from an earlier emission, increasing concentrations after the house has been flushed with outside air, and concentration fluctuations of compounds due to the cycling of the AC system. The first two errors are minimized by allowing the house VOC concentrations to equilibrate before beginning the experiment. In experiments preceded by flushing the house with outside air, ~80 min is given for indoor concentrations to approach steady state after the house is re-sealed. In a study of VOC

and SVOC rebound rates at the test house, Wang *et al*. (2020) find compound rebound time constants of ~1000 s (17 min), with the slowest compounds showing a time constant of 2600 s (43 min), indicating that after 80 min signals should be approaching steady state concentrations.[35] In experiments not preceded with a flushing, the house was allowed to rest for 3 hours. At an ACR of 0.6 h^{-1} at least 80% of the elevated concentrations from the previous experiments would be removed. Only one type of experiment is performed on a given day preventing a "cross contamination" of emitted species. Changes in concentration due to AC cycling are minimized by averaging over the 15 minutes prior to the beginning of the experiment for the $C_{initial}$ term. Mixing ratio terms C_{final}, $C_{initial}$, and C_{avg} are all derived from 1 min averages of mixing ratios measured indoors. During periods where outdoor measurements were being made, indoor mixing ratios are linearly interpolated.

Errors are also minimized by conducting replicates. For each activity experiment 7 replicates are performed. Emissions are calculated for each replicate. For each ion signal the mean emission is calculated, as well as the 95% confidance interval (CI , 6 DOF, 2-sided). If the mean is both greater the 0.001 mg and greater than the CI it is reported as an emission.

Note that Equation 1 will give a *net* emission over Δt, where any loss process other than ventilation will be reported as a negative emission: it is the total emission minus any chemical or physical loss over the integration period. Values of M given by equation 2 are similar despite background subtractions and should be taken as the net emission over the integration time Δt due to the activity or occupancy.

In addition to emissions, M, we report emission rates, E (mg h^{-1}) , from the unoccupied house. Emission rates are calculated by dividing Equation 1 by Δt, giving the same equation used by Liu *et al*. (2019):[1]

$$E = \frac{M_{total}}{\Delta t} = \rho V(\frac{C_{final} - C_{initial}}{\Delta t} + A(C_{avg} - C_{out}) \quad (3)$$

E is calculated with a 1 min time step (Δt = 0.017 h) by linearly interpolating mixing ratios and ACR. For events with emission spikes this is too short of a time step, slower than the 7 min turnover time of the ventilation system. However emissions during the unoccupied day are continuous and changes in emissions driven by the AC system are evenly distributed throughout the house as they occur in the ventilation system. Performing the analysis with a 1 h timestep did not change the results. Emissions rates during the unoccupied period are reported as the mean emission rate over the 20 h measurement period.

4.4. Results and Discussion

4.4.1. Baseline Emissions from the Building and its Contents

Over the entire 30-day measurement campaign, 250 VOC signals were detected indoors above a minimum threshold average of 5 ppt and limit of detection (LOD), whichever was greater. While the house was unoccupied, 222 VOC signals were detected above this threshold. More than 95% of these VOCs (216) were measured at elevated concentrations in the house when it was unoccupied for 24 hours, indicative of persistent VOC emissions indoors. Median mixing ratios,

ratios of median indoor to median outdoor concentrations (I/O), and mean baseline emission rates for the 15 highest emitted compounds are found in Table 4.4.1, while a complete list is found in Table 4.8.1.

Table 4.4.1 Top 15 emitted compounds from the unoccupied house. Median mixing ratios (C_{avg}), median-indoor to median-outdoor concentration ratios (I/O), and mean indoor emission rates (E_{avg}) over the unoccupied day.

m/z	Ion Formula	Compound Assignment	C_{avg} (ppb)	I/O	E_{avg} (mg h^{-1})
61.0275	$C_2H_5O_2^+$	acetic acid	55.9	>10	17
33.0333	CH_5O^+	methanol	39.8	>10	6.3
47.0124	$CH_3O_2^+$	formic acid	11.9	>10	2.8
47.0485	$C_2H_7O^+$	ethanol	12.6	2-10	2.8
143.142	$C_9H_{19}O^+$	C9 saturated carbonyl	2.2	2-10	1.5
371.091	$C_{10}H_{31}O_5Si_5^+$	siloxane D5	0.743	>10	1.5
43.0537	$C_3H_7^+$	propanol fragment + propene	5.6	>10	1.2
45.033	$C_2H_5O^+$	acetaldehyde	5.23	>10	1.1
59.0484	$C_3H_7O^+$	acetone + propanal	3.6	2-10	0.92
83.0847	$C_6H_{11}^+$	alkyl fragment	1.78	>10	0.75
97.0277	$C_5H_5O_2^+$	furfural	1.44	Outdoor < LOD	0.75
137.132	$C_{10}H_{17}^+$	monoterpenes	1.35	2-10	0.61
117.09	$C_6H_{13}O_2^+$	hexanoic acid	0.873	2-10	0.49
71.0847	$C_5H_{11}^+$	pentanol fragment + pentene	1.4	2-10	0.46
41.0382	$C_3H_5^+$	alkyl fragment	2.22	>10	0.45

For the vast majority of VOC signals, I/O ratios are above 1, indicating indoor sources. Median outdoor concentrations are below the limit of detection for 82 (37%) of the VOC signals found indoors, thus we infer these VOCs originated exclusively indoors. Another 20 signals (9%) are an order of magnitude (I/O > 10) more abundant indoors than outdoors, while 107 (48%) have I/O ratios between 2 and 10. In total, based on the I/O ratio, 94% of VOC detected are more than twice as high indoors indicating the dominance of indoor sources across a broad suite of VOCs even without including the effects of occupancy and occupant activities. A further 10 VOC signals (5%) are found with I/O ratios between 1 and 2, whereas only 3 (1%) were lower indoors than outdoors.

Only 4 signals show net negative emissions, indicating loss either indoors or at the building envelope. Only two of the VOCs show appreciable removal, acetonitrile and $C_5H_5O^+$, lost at rates of 0.09 mg h^{-1} and 0.12 h^{-1}, respectively. Time series of the indoor and outdoor mixing ratios (Figure 4.8.1) show elevated morning outdoor concentrations of acetonitrile which does not appear indoors. By the afternoon concentrations between the two sites are equal. For $C_5H_5O^+$ it is the opposite pattern, elevated outdoor concentrations leading to loss in the afternoon. The total VOC signal loss rate is 0.22 mg h^{-1}, or roughly 200 times smaller than VOC emissions indoors.

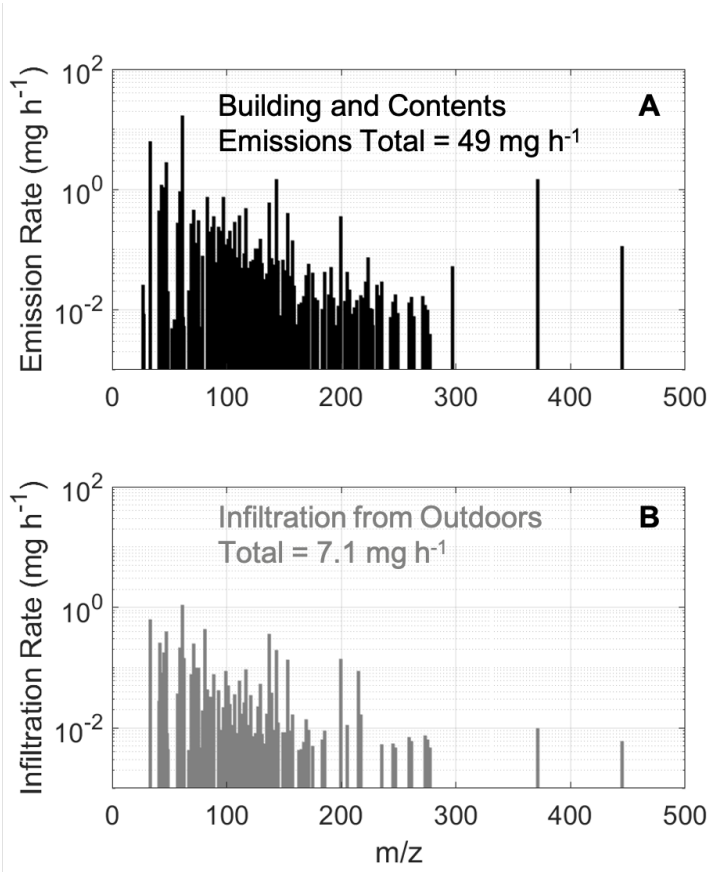

Figure 4.4.1 Mass spectra of (A) the VOC emissions rate from the building and its contents (top, mg h^{-1}), and (B) the VOC infiltration rate from outdoors (bottom, mg h^{-1}). Emissions from the building and its contents are 7 times greater than transport from the outdoors, with the two figures showing the different chemical fingerprint of each source.

The total VOC emission rate in the unoccupied house over the 20 h sampling period from the building and its static contents was 49 mg h^{-1}, whereas the total VOC infiltration rate from outdoors was a factor of 7 smaller at 7.1 mg h^{-1} (Figure 4.4.1). The most emitted VOC indoors for baseline conditions was acetic acid at 17 mg h^{-1}, accounting for one third of the detected VOC emissions from the building and its contents. The second and third most emitted VOCs were methanol (6.3 mg h^{-1}, 13%) and formic acid (2.8 mg h^{-1}, 6%) respectively. Liu *et al*. (2019) identified the same three compounds as the top emissions from a normally occupied residence in California, independent of occupant activity.[1] In their study these three compounds comprise ~75% of the total "baseline" emissions, whereas we find a more diverse spectrum of emissions, with these three compounds accounting for 50% of total quantified emissions from the building and its contents. The Liu *et al*. analysis of baseline emissions specifically excluded VOCs that also had significant occupant activity sources (e.g. ethanol from cooking). Doing so systematically biases the comparison of their baseline emissions low versus the way we have calculated emissions here, including all observed VOC during the unoccupied period. In their study Liu *et al*. (2019) report the average baseline total VOC emission rate of 37.3 mg h^{-1} had a strong temperature dependence, doubling as temperatures increased from the minimum observed 16 °C to the maximum observed 23 °C. The mean air temperature of the HOMEChem test house on the unoccupied day was 25.1 °C (interquartile range of 24.7-25.5 °C), and the larger total

VOC emission rate reported here is at least qualitatively consistent with the Liu *et al*. results when accounting for temperature dependence of baseline emissions.

The AC system caused air temperature swings of 2 °C on ~30 min cycles, and 1 hour averaging reveals that the afternoon sees warming of 0.4 °C, smaller than the swings caused by AC (Figure 4.8.2). Surfaces see a smaller temperature effect from AC. Kitchen floor temperatures fluctuate 1 °C with the AC. At 5:30 AM the 1 hour mean temperature of the kitchen floor was 25.2 °C, and increased steadily to 25.9 °C at 4:30 PM. By 2:30 AM the following day the 1 hour mean temperature returned to 25.2 °C. As with the air temperature, surface temperature swings caused by AC are larger than the general trend in warming over the day. Figure 4.8.3 shows the hourly mean total VOC emission rate as well as the surface floor temperature during the unoccupied day. There is no apparent trend between the temperature and emissions, perhaps due to the AC temperature signal being larger than the warming over the day and the noise introduced into the emissions signal by the AC cycling.

During the unoccupied period 32 VOC signals were found to vary in concentration with the air conditioner supply temperature, which oscillated as the compressor cycled on and off. Duncan *et al*. (2019) reported similar behavior for water soluble organic gases, such as organic acids.[11] Consistent with their work, we find that acetic acid and formic acid were the most abundant compounds exhibiting this cycling. The time-resolved analysis results suggest that these two compounds experience negative indoor emissions with the air conditioner active, implying that the compounds are condensing in the HVAC system, likely on the cooling coils, which drain to the outdoors. Figure 4.4.2A shows the mixing ratio of acetic acid, as well as the temperature of the air leaving the AC system over 5 air conditioning cycles. Soon after the AC turns off, as indicated by a rise in temperature, the concentration of acetic acid increases. Once the temperature setpoint is reached, causing the AC to resume operation, the temperature drops, and fluxes become negative as acetic acid is (apparently) lost to cold, water coated parts of the ventilation system. The oscillation of acetic acid accounts for more than half of the total VOC signal oscillation that is associated with AC operation.

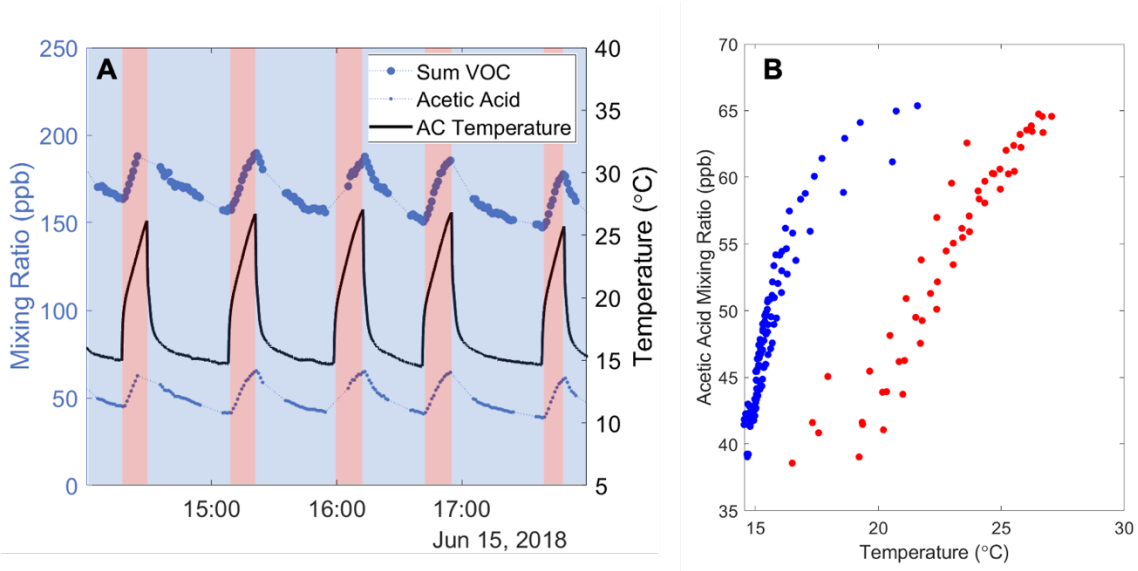

Figure 4.4.2 Acetic acid mixing ratios cycle with the AC outlet temperature (A, left), the oscillation of which is clearly seen in the total VOC signal of the unoccupied house. Red shading indicates AC is off and temperature is increasing, blue shading indicates AC is on and cooling. Note that the AC outlet temperature is not the ambient temperature of the house, rather a proxy measurement of the temperature of the AC cooling coils. Figure B (right) shows the acetic acid mixing ratio as a function of AC outlet temperature. Red indicates warming and blue indicates cooling. The cycle is asymmetric, moving counterclockwise around the plot.

On a time-resolved basis, acetic acid emissions range between positive 150 mg h^{-1} and negative 120 mg h^{-1}, while formic acid emission rates range between 27 mg h^{-1} and -24 mg h^{-1}. Figure 4.4.2B shows acetic acid mixing ratio as a function of AC outlet temperature. Red markers indicate warming and blue indicate cooling. The cooling cycle is asymmetric, moving counterclockwise around the figure. At the bottom left the temperature and concentration are both at their lowest. The AC cycles off, and the temperature rises before concentration. After a few degrees of warming, the concentration then rises with temperature until the AC cycles on, at the top right corner of the plot. Again, there is a lag between the change in temperature and change in mixing ratio. It is unclear how efficient is the net removal of these acids because of the air conditioner. For example, it is possible that much of the acetic acid deposited in the HVAC system is reemitted when the cooling cycle ends and warmer air flows through the system.

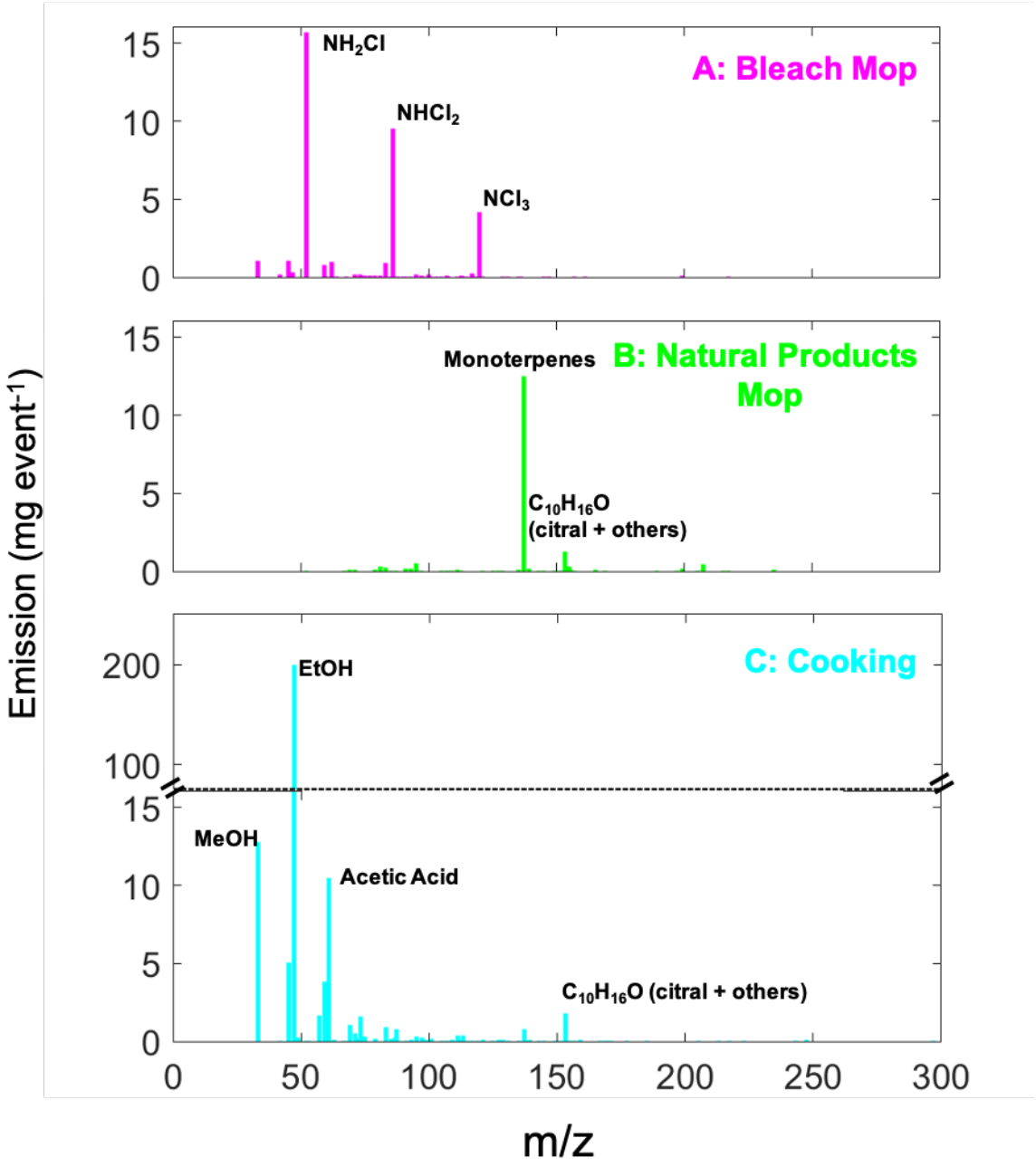

Figure 4.4.3 Emissions from bleach cleaning (A), natural product mopping (B), and cooking (C). Bleach mopping is dominated by chlorine compounds, specifically monochloramine, dichloramine, and trichloramine. Natural product mopping has the least diverse emissions of the activities, with monoterpenes comprising 60% of the emissions. Cooking emissions are large due to the 200 mg of ethanol emitted per event, as well as the many compounds released in the mg range.

4.4.2. Emissions from Cleaning

Cleaning emissions depend substantially on the types of cleaning solutions used. Emissions from mopping with bleach produced twice as much observed VOC emissions per mopping event as mopping with natural products, and the chemical composition of emissions from these events are completely different (see Figure 4.4.3).

Total gas phase emissions from bleach mopping are 38 ± 6 mg per mopping event including 32 ± 6 mg of chlorinated species. Table 4.4.2 lists the top 10 emitted ion signals, while Table 4.8.2 lists the complete emissions and relative 95% CI for all ion signals during bleach mopping. The top three emissions are chloramine, dichloramine, and trichloramine, comprising 82% of total emissions. These species are not VOCs, as they are inorganic. Mattila *et al*. 2020 showed that these compounds are removed significantly faster than the air-change rate, implying that they are either lost through additional physical or chemical processes.[25](and Mattila in prep) These species, especially trichloramine, are known respiratory irritants with links to asthma, and much research on exposure has focused on emissions from swimming pools.[36–39] In addition to chloramines, chlorinated VOCs are emitted, although in smaller quantities. Of particular note is cyanogen chloride (NCCl), a toxic compound that has been used as a military poison gas.[40] The highest concentrations of NCCl observed during this study were 1-2 ppb during bleach mopping, corresponding to an emission of 1 ± 0.2 mg per mopping event. Possibly a fragment of a larger chlorinated species, the ion $CHCl_2^+$ is among the top 10 emitted VOC ions. Chloroform, previously identified in bleach, is also found.[41]

In total we detect 97 distinct ions emitted from bleach cleaning, the vast majority in small quantities. These trace organics, many of which are highly oxidized, may come from the oxidation and fragmentation of organic surface films due to the oxidizing nature of bleach. It is also possible that their emission stems from a physical rather than chemical process: mopping with a bleach solution could liberate these oxygenated species from the organic surface film through changing the water content and/or pH of the surface. Regardless, both the major and minor emissions from bleach cleaning can be thought of as "secondary": they do not originate from the cleaner, but rather chemical or physical processes that are a result of cleaning.

Natural product mopping produces large emissions of terpenoids. The 10 highest emissions from natural product mopping is listed in Table 4.4.3, while the complete list of emissions as well as 95% CI are listed in Table 4.8.3. Of the total 19 ± 3 mg of VOC emitted per mopping event, 12 ± 3 mg are monoterpenes, and the top 10 highest emitted VOCs include ions consistent with citral, monoterpene alcohols, and $C_{14}H_{23}O^+$, an ion formula suggestive of a class of fragrance compounds called ionones. Overall, we report 79 emitted VOCs, fewer than reported from bleach cleaning, possibly due to lesser oxidative activity associated with the cleaning solution. Also, these VOC ions appear to be emitted directly from the cleaner, rather than chemically produced or physically liberated from surfaces.

Natural product mopping releases large amounts of reactive terpenes. During the HOMEChem experiments, indoor ozone concentrations were low, ~8 ppb on average. However, in a more polluted urban environment, the large release of terpenes indoors could lead to the formation of secondary organic aerosol (SOA). Additionally, we find that the loss rate of monoterpenes from

indoor air during cleaning activities is consistent with the ventilation rate suggesting they are transported outdoors much faster than they can react indoors. Once outdoors, these compounds are precursors to photochemical smog chemistry, in particular, the formation of secondary organic aerosol.

Table 4.4.2 Top 10 emissions from bleach cleaning (mg per mop). Compound assignments with double asterisk are tentative (**).

Ion Formula	Compound Assignment	Emission (mg per mop)
NH3Cl+	chloramine	16
H2Cl2N+	dichloramine	9.5
HCl3N+	trichloramine	4.2
CH5O+	methanol	1.1
C2H5O+	acetaldehyde	1
CHClN+	cyanogen chloride	1
CHCl2+	-	0.91
C3H7O+	acetone + propanal	0.78
CH3O2+	formic acid	0.35
CCl3+	chloroform**	0.23

Table 4.4.3 Top 10 emissions from natural product cleaning (mg per mop).

Ion Formula	Compound Assignment	Emission (mg per mop)
C10H17+	monoterpenes	12
C10H17O+	citral + others	1.2
C7H11+	-	0.53
C14H23O+	-	0.44
C10H19O+	monoterpene alcohols	0.35
C5H5O+	furanoid fragment	0.32
C6H11+	alkyl fragment	0.26
C8H9O2+	4-anisaldehyde + others	0.22
C7H9+	toluene	0.18
C7H7+		0.18

Table 4.4.4 Top 10 emissions from stir fry cooking (mg per event).

Ion Formula	Compound Assignment	Emission (mg per event)
C2H7O+	ethanol	200
CH5O+	methanol	13
C2H5O2+	acetic acid	10
C2H5O+	acetaldehyde	5.1
C3H7O+	acetone + propanal	3.8
C10H17O+	citral + others	1.8
C3H5O+	acrolein + propionic acid fragment	1.7
C4H9O+	butanal + methyl ethyl ketone	1.6
C5H9+	isoprene	1.1
C6H11+	alkyl fragment	0.89

4.4.3. Emissions from Cooking

The top 10 emissions from stir-fry cooking are listed in Table 4.4.4. Table 4.8.4 lists the complete emissions from stir fry cooking. Total emissions are 250 ± 50 mg per cooking event, with 80% of the emitted mass accounted for as ethanol (200 ± 40 mg per event). This high emission of ethanol originates from the addition of stir-fry sauce to a hot pan, which quickly volatilizes the compound. Figure 4.4.4 shows a time series of selected compound mixing ratios for a cooking event. Ethanol is not commonly discussed in literature we found regarding cooking VOC emissions. More emphasized are saturated alkanes (from the gas fuel used for combustion) and carbonyl compounds.[18,42] However, Liu *et al*. (2019) identified ethanol as the most abundant VOC in the living space of a normally occupied residence, and noted large spikes in emissions during a wide variety of cooking events.[1] At HOMEChem, the next highest emitted VOCs are methanol and acetic acid, with emissions of 13 and 10 mg per event, respectively. Acetic acid has many potential sources but we suspect that it originates in the stir fry sauce as well. Klein *et al*. (2016) identified boiling vegetables as a source of methanol; the frozen vegetables added to the hot pan may be the source at HOMEChem.[18] VOC ions consistent with short chain aldehydes (acetaldehyde, acrolein, butanal, pentanal, and methacrolein) contribute 10 mg per event to total emissions. These compounds are expected to arise from high temperature degradation of cooking oil, and some are deleterious to human health.[18,43]

Cooking emissions are more chemically complex than emissions from mopping with either bleach or natural products (Figure 4.4.3). In total we report emissions for 164 VOC ions, compared to the 79 from natural product cleaning and 97 from bleach cleaning. Furthermore, it is clear that cooking emissions depend substantially on the method of cooking as well as the types of food, thus our experiments are specific to the chosen experimental conditions, rather than broadly representative.

Figure 4.4.5 compares the baseline emissions from the building and its contents with bleach mopping, natural products mopping, and cooking. Each pie chart shows the top 10 emitted VOCs as well as one slice representing the sum remainder of emissions. Activity emissions are dominated by 1-3 VOC ions, while baseline emissions show a more diverse distribution.

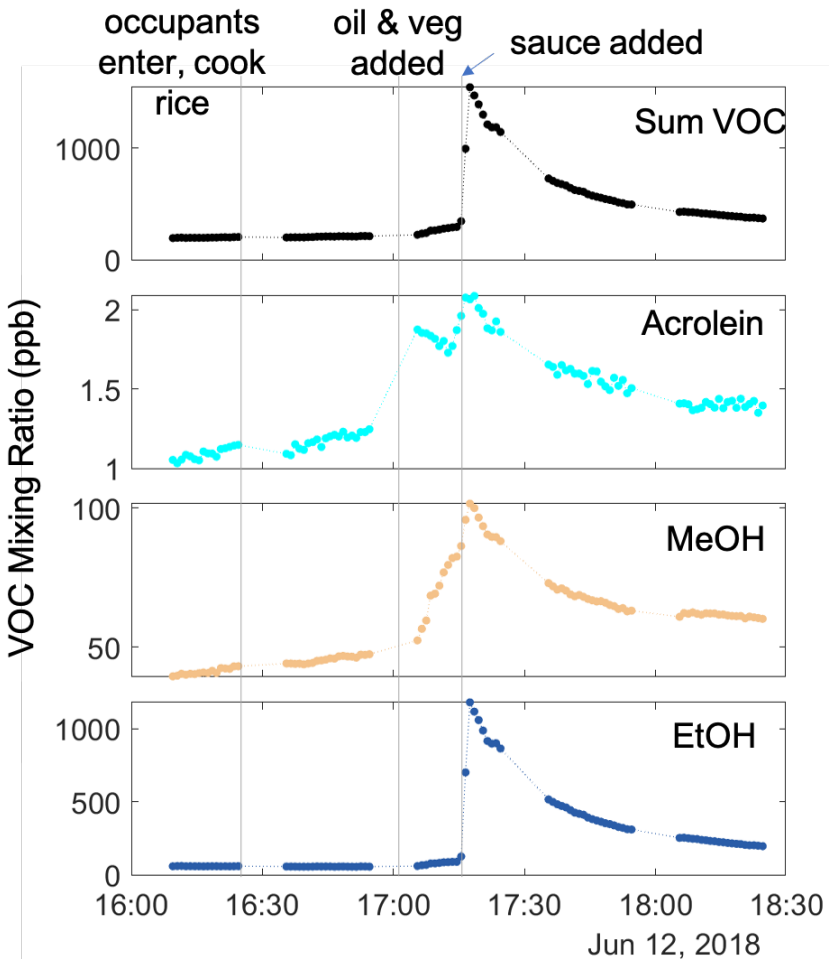

Figure 4.4.4 Time series of meal cooking. Points indicate 1 minute averaged measurements, while the thin dotted lines indicate periods with no indoor data due to outdoor sampling. The addition of sauce to the hot pan results in rapidly evaporation of large amounts of ethanol, as seen in the bottom plot, as well as the sum VOC in the top plot. Both acrolein and methanol increase in concentration before the addition of sauce, most likely from heated oil and heated vegetables, respectively.

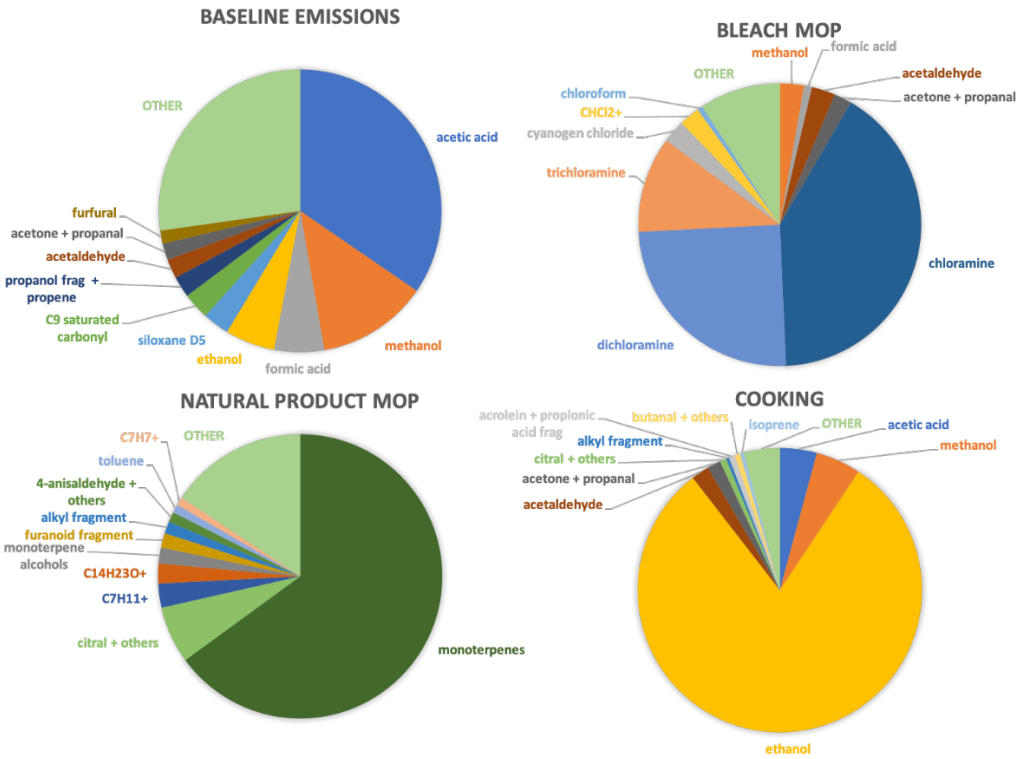

Figure 4.4.5 Relative speciation of emissions from activities and the building itself. Each chart shows the 10 most emitted compounds, as well as one slice for the remaining compounds. Emissions from the building and its contents are the most diverse.

4.4.4. Emissions from Occupancy

A total of 238 VOC ions were emitted in at least one occupancy experiment. Only 71 of these were detected across all five occupancy experiments. Per capita emission rates of select VOC signals and CO_2 are presented in Table 4.4.5. We compare our results to reported emission rates from Tang *et al*. (2016) and Stönner *et al*. (2018).[9,26] A complete list of occupancy emission rates are found in Table 4.8.5. Average CO_2 emissions were 27 g person^{-1} h^{-1}, in general agreement with the 21 g person^{-1} h^{-1} reported by Tang and 30 g person^{-1} h^{-1} reported by Stönner. Here, we separate emissions into three broad categories: metabolic emissions, emission of skin oil oxidation products, and personal-care product emissions.

Emissions of acetone ranged from 380 µg person^{-1} h^{-1} to 550 µg person^{-1} h^{-1} with no clear pattern related to PCP usage. The average emission rate, 460 µg person^{-1} h^{-1}, agrees well with Stönner *et al*., but is less than half the reported acetone emission rate from Tang *et al*. Isoprene emissions show similar variability unrelated to PCP usage. The average emission across all experiments is 72 µg person^{-1} h^{-1}, less than half of the ~160 µg person^{-1} h^{-1} reported by both Tang *et al*.and Stönner *et al*. This variability has precedence: in a review of human breath VOCs, Fenske and Paulson report that exhaled mixing ratios spanned ranges of 12-580 ppb for isoprene and 1.2-1880 ppb for acetone.[44] Interestingly, the variability of the two breath volatiles does not correlate: for instance the experiment with the largest per person emission of isoprene, "High PCP Morning," has the second lowest per person emission of acetone. Emissions of C_4H_6O, an

unsaturated carbonyl, remain consistent across all five experiments, in the range 14-20 μg person^{-1} h^{-1}. The ubiquity and stability of this emission suggests it may be a human produced VOC. Tang *et al*. do not report emissions for this compound; however, Stönner *et al*. report an emission rate of 8 μg person^{-1} h^{-1}.

Emissions of ethanol could originate either from PCP or from breath. For both "Low PCP" experiments (conducted on the same day), ethanol emissions are in line with reported results from both Tang *et al*. and Stönner *et al*. For the other three experiments, ethanol emissions were an order of magnitude higher, 1500-5300 μg person^{-1} h^{-1}. Alcoholic beverages were not consumed during these experiments; however, consumption from the night before could conceivably have led to elevated breath emissions the following day. Additionally, ethanol is used as a solvent for perfumes and colognes, as well as in hair spray.

Despite the low ozone concentration during the HOMEChem experiments, emissions were detected and quantifiable for reaction products of skin oil ozonoylsis. The intermediate product 6-MHO was detected across all five occupancy experiments, while 4-OPA was only found during three experiments and at lower levels than 6-MHO. These observations are consistent with the production mechanism for both products: 6-MHO can be produced from a single ozonolysis of squalene, whereas 4-OPA requires a minimum of two ozone-initiated reactions. Low ozone concentration will favor more production of 6-MHO over 4-OPA.[28] An ion consistent with decanal, $C_{10}H_{21}O^+$, was emitted during all five experiments at an average emission of 16 μg person^{-1} h^{-1}. Decanal can be formed from the ozonolysis of unsaturated fatty acids; it was a major product when Wisthaler and Weschler (2010) exposed skin oil soiled glass wool to ozone.[28] While acetone can be produced from skin oil oxidation, the large quantities we observe suggest that skin oil oxidation would be responsible for only a small fraction of overall indoor acetone emissions.

The most striking effect of varying PCP usage is seen in terpene and siloxane emissions. The highest emission of monoterpenes is seen in the "High PCP Morning" experiment, 300 μg person^{-1} h^{-1}, compared to the "Regular" and "Low PCP" experiments with monoterpene emissions in the range 33-84 μg person^{-1} h^{-1}. However, the "High PCP Afternoon" experiment has monoterpene emissions of 47 μg person^{-1} h^{-1}, well in line with the "Low" and "Regular PCP" experiments. We attribute this outcome to the product being applied in the morning and volatilizing away over the course of the day.

The effect of PCP depletion during the day is evident in D5 siloxane emissions: for both Low and High PCP experiments, the compound showed high emissions in the morning and low emissions in the afternoon. This is especially remarkable for the High PCP usage case: in the morning, the emission rate was 16 mg person^{-1} h^{-1}, but in the afternoon experiment emissions of D5 siloxane were not detected. The High PCP morning emission rate was 6 times greater than in the Regular PCP experiment, and almost 50 times greater than the Low PCP Morning experiment. This declining per person emission rate of siloxanes was also observed in the classroom study of Tang *et al*. (2015).[30] With respect to modeling indoor VOC emissions, time-dependent emissions introduce an added challenge: occupancy alone is not sufficient to accurately capture siloxane emissions. Also important for this purpose would be the time since application of PCP.

Total emissions from the two Low PCP experiments are 1.5 and 1.9 mg person^{-1} h^{-1}. For "regular" application of PCPs, total emissions increase to 6.6 mg person^{-1} h^{-1}; this increase is mainly attributable to higher emission rates of ethanol and D5 siloxane. The "High PCP Morning" experiment yields a total VOC emission rate of 20 mg person^{-1} h^{-1} of which 80% is D5 siloxane. By the afternoon, D5 emissions are not detected, and total occupancy-associated VOC emissions drop to 7.0 mg person^{-1} h^{-1}.

Table 4.4.5 Per-capita occupant emissions for select compounds (μg person^{-1} h^{-1}) from this study as well as Tang *et al*. (2016) and Stönner *et al*. (2018).[9,26]

		Emissions per occupant (μg person^{-1} h^{-1})							
		Low PCP		Regular PCP	High PCP		This study avg	Tang *et al*.	Stönner *et al*.
Ion Formula	Formula Assignment	Morning	Afternoon	Morning	Morning	Afternoon			
CO_2	carbon dioxide	2.2E+07	2.7E+07	2.6E+07	2.8E+07	3.3E+07	2.7E+07	2.1E+07	3.0E+07
CH_5O+	methanol	46	310	-	-	170	180	156	650
C_2H_7O+	ethanol	170	200	2600	1500	5400	2000	94.9	216
C_3H_7O+	acetone	450	550	380	390	510	460	1060	419
C_5H_9+	isoprene	76	75	60	83	66	72	162	166
C_4H_7O+	unsaturated carbonyl (e.g., methyl vinyl ketone)	15	19	13	22	18	17	-	8
$C_8H_{13}+$ & $C_8H_{14}O+$	6-MHO	25	37	13	15	21	22	99.3	3
$C_5H_9O_2+$	4-OPA	0.25	7.2	-	-	3	3	37.9	-
$C_{10}H_{21}O+$	C10 saturated carbonyl	15	20	14	15	17	16	31.2	4
$C_{10}H_{17}+$	monoterpenes	84	51	33	300	47	100	187	201
$C_{15}H_{25}+$	sesquiterpenes	3.6	5.8	3.7	22	4.6	8	8.1	12
$C_8H_{25}O_4Si_4+$	siloxane D4	2.3	0.97	3.4	160	2.5	34	90.2	-
$C_{10}H_{31}O_5Si_5+$	siloxane D5	340	8.2	2900	16000	-	4800	3400	112
$C_{12}H_{37}O_6Si_6+$	siloxane D6	5.1	5.5	130	270	19	86	102	-

4.5. Conclusion

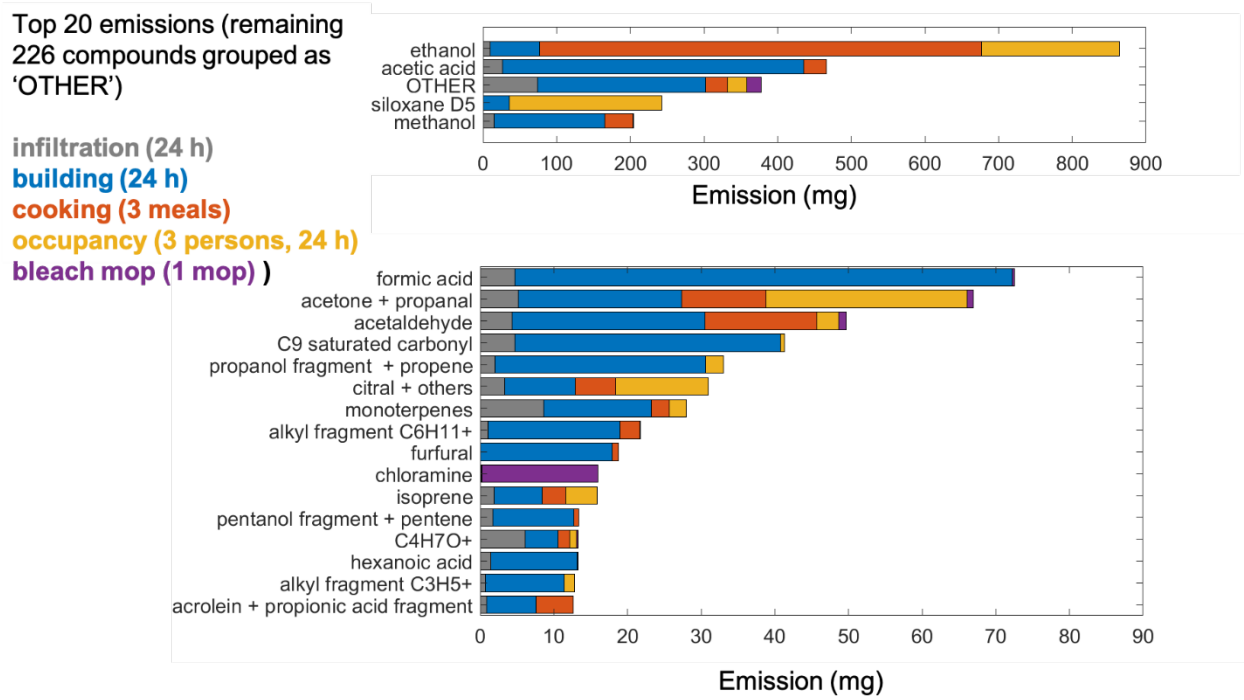

Figure 4.5.1 Speciated emissions for a hypothetical day consisting of 3 meals cooked, 1 bleach mop, 3 occupants with regular PCP usage, and 24 hours of both VOC infiltration and emission from the building and its contents.

During a typical day at HOMEChem, we observed 1200 mg of VOC signal emitted directly from the house and its contents, while only 170 mg of VOC are transported to indoors from outdoors. If the occupants cook 3 meals and also mop once with bleach, these activities will emit another 790 mg of VOC. Assuming 3 occupants with regular PCP usage, another 470 mg of VOC will be added to the house from the occupants themselves, and a total of 246 VOC signals will be emitted. For this hypothetical day, total VOC emissions into the house would be 2600 mg, with 45% coming from baseline emissions, 28% from cooking, 18% from occupancy, 7% from the outdoors, and 1% from bleach cleaning. Clearly, ranked only on the total mass of emissions, the house and its furnishings are the largest source of VOCs. Figure 4.5.1 shows the top 20 emitted ions for this hypothetical day, speciated by emission source. Emissions from the building are the dominant source for 80% of the emitted ions. That is, of the 246 VOC signals emitted, 196 are emitted mostly from the house and its contents. One day of emissions from the house and its contents will generate more monoterpenes (15 mg) than one natural product mopping event (12 mg), more acetaldehyde (26 mg) than three stir fry cooking events (15 mg), and more isoprene (7 mg) than three occupants continuously present (4 mg).

However, from the standpoint of health impacts or indoor chemistry, more than total VOC mass must be taken into account. For instance, while bleach mopping contributes relatively small emissions by mass, the injection of reactive chlorine compounds into the air may have greater health impacts than do the chemicals released from baseline emissions. And while acetic acid is the largest single baseline emission, it may not play much of a role in indoor chemistry. For this

reason, we have provided speciated emissions for hundreds of compounds, most of which are emitted at quite low levels, yet may prove to be important for indoor chemistry, outdoor chemistry, and human exposure.

4.6. Acknowledgements

This work was funded by the Alfred P. Sloan Foundation via Grant 2016-7050 and 2019-11412.

4.7. References

1. Liu Y, Misztal PK, Xiong J, et al. Characterizing sources and emissions of volatile organic compounds in a northern California residence using space-and time-resolved measurements. *Indoor Air*. 2019;29:630-644.

2. Zhu J, Newhook R, Marro L, Chan CC. Selected volatile organic compounds in residential air in the city of Ottawa, Canada. *Environ Sci Technol*. Published online 2005.

3. Brown SK, Sim MR, Abramson MJ, Gray CN. Concentrations of Volatile Organic Compounds in Indoor Air – A Review. *Indoor Air*. Published online 1994.

4. Bari MA, Kindzierski WB, Wheeler AJ, Héroux MÈ, Wallace LA. Source apportionment of indoor and outdoor volatile organic compounds at homes in Edmonton, Canada. *Build Environ*. Published online 2015.

5. Klepeis NE, Nelson WC, Ott WR, et al. The National Human Activity Pattern Survey (NHAPS): a resource for assessing exposure to environmental pollutants. *J Expo Anal Environ Epidemiol*. 2001;11:231-252.

6. Haghighat F, De Bellis L. Material emission rates: literature review, and the impact of indoor air temperature and relative humidity. *Build Environ*. 1998;33:261-277.

7. Yu C, Crump D. A review of the emission of VOCs from polymeric materials used in buildings. *Build Environ*. 1998;33:357-374.

8. Gunschera J, Mentese S, Salthammer T, Andersen JR. Impact of building materials on indoor formaldehyde levels: Effect of ceiling tiles, mineral fiber insulation and gypsum board. *Build Environ*. 2013;64:138-145.

9. Stönner C, Edtbauer A, Williams J. Real-world volatile organic compound emission rates from seated adults and children for use in indoor air studies. *Indoor Air*. 2018;28:164-172.

10. Williams J, Stönner C, Wicker J, et al. Cinema audiences reproducibly vary the chemical composition of air during films, by broadcasting scene specific emissions on breath. *Sci Rep*. 2016;6:25464.

11. Duncan SM, Tomaz S, Morrison G, et al. Dynamics of residential water-soluble organic gases: Insights into sources and sinks. *Environ Sci Technol*. 2019;53:1812-1821.

12. Liu S, Thompson SL, Stark H, Ziemann PJ, Jimenez JL. Gas-phase carboxylic acids in a university classroom: Abundance, variability, and sources. *Environ Sci Technol*. 2017;51:5454-5463.

13. Huangfu Y, Lima NM, O'Keeffe PT, et al. Diel variation of formaldehyde levels and other VOCs in homes driven by temperature dependent infiltration and emission rates. *Build Environ*. 2019;159:106153.

14. Huangfu Y, Lima NM, O'Keeffe PT, et al. Whole-House Emission Rates and Loss Coefficients of Formaldehyde and Other Volatile Organic Compounds as a Function of the Air Change Rate. *Environ Sci Technol*. 2020;54:2143-2151.

15. Klein F, Baltensperger U, Prévôt ASH, El Haddad I. Quantification of the impact of cooking processes on indoor concentrations of volatile organic species and primary and secondary organic aerosols. *Indoor Air*. 2019;29:926-942.

16. Ho SSH, Yu JZ, Chu KW, Yeung LL. Carbonyl emissions from commercial cooking sources in Hong Kong. *J Air Waste Manage Assoc*. 2006;56:1091-1098.

17. Schauer JJ, Kleeman MJ, Cass GR, Simoneit BRT. Measurement of emissions from air pollution sources. 1. C1 through C29 organic compounds from meat charbroiling. *Environ Sci Technol*. 1999;33:1566-1577.

18. Klein F, Platt SM, Farren NJ, et al. Characterization of gas-phase organics using proton transfer reaction time-of-flight mass spectrometry: cooking emissions. *Environ Sci Technol*. 2016;50:1243-1250.

19. Klein F, Farren NJ, Bozzetti C, et al. Indoor terpene emissions from cooking with herbs and pepper and their secondary organic aerosol production potential. *Sci Rep*. 2016;6:36623.

20. Wolkoff P, Schneider T, Kildesø J, Degerth R, Jaroszewski M, Schunk H. Risk in cleaning: chemical and physical exposure. *Sci Total Environ*. 1998;215:135-156.

21. Wiley JA, Robinson JP, Piazza T, et al. *Activity Patterns of California Residents*. California Environmental Protection Agency, Air Resources Board, Research …; 1991.

22. Nazaroff WW, Weschler CJ. Indoor acids and bases. Published online 2020.

23. Wong JPS, Carslaw N, Zhao R, Zhou S, Abbatt JPD. Observations and impacts of bleach washing on indoor chlorine chemistry. *Indoor Air*. 2017;27:1082-1090.

24. Wang C, Collins DB, Abbatt JPD. Indoor illumination of terpenes and bleach emissions leads to particle formation and growth. *Environ Sci Technol*. 2019;53:11792-11800.

25. Mattila JM, Lakey PSJ, Shiraiwa M, et al. Multiphase Chemistry Controls Inorganic Chlorinated and Nitrogenated Compounds in Indoor Air during Bleach Cleaning. *Environ Sci Technol*. 2020;54:1730-1739.

26. Tang X, Misztal PK, Nazaroff WW, Goldstein AH. Volatile Organic Compound Emissions from Humans Indoors. *Environ Sci Technol*. 2016;50:12686-12694.

27. de Lacy Costello B, Amann A, Al-Kateb H, et al. A review of the volatiles from the healthy human body. *J Breath Res*. 2014;8:14001.

28. Wisthaler A, Weschler CJ. Reactions of ozone with human skin lipids: Sources of carbonyls, dicarbonyls, and hydroxycarbonyls in indoor air. *Proc Natl Acad Sci*. 2010;107:6568-6575.

29. Yeoman AM, Shaw M, Carslaw N, Murrells T, Passant N, Lewis AC. Simplified speciation and atmospheric volatile organic compound emission rates from non-aerosol personal care products. *Indoor Air*. 2020;30:459-472.

30. Tang X, Misztal PK, Nazaroff WW, Goldstein AH. Siloxanes are the most abundant volatile organic compound emitted from engineering students in a classroom. *Environ Sci Technol Lett*. 2015;2:303-307.

31. Farmer DK, Vance ME, Abbatt JPD, et al. Overview of HOMEChem: House observations of microbial and environmental chemistry. *Environ Sci Process Impacts*. 2019;21:1280-1300.

32. Holzinger R. PTRwid: A new widget tool for processing PTR-TOF-MS data. *Atmos Meas Tech*. 2015;8:3903-3922.

33. Zhao J, Zhang R. Proton transfer reaction rate constants between hydronium ion (H3O+) and volatile organic compounds. *Atmos Environ*. 2004;38:2177-2185.

34. Liu Y, Misztal PK, Xiong J, et al. Detailed investigation of ventilation rates and airflow patterns in a northern California residence. *Indoor Air*. 2018;28:572-584.

35. Wang C, Collins DB, Arata C, et al. Surface reservoirs dominate dynamic gas-surface partitioning of many indoor air constituents. *Sci Adv*. Published online 2020.

36. Thickett KM, McCoach JS, Gerber JM, Sadhra S, Burge PS. Occupational asthma caused by chloramines in indoor swimming-pool air. *Eur Respir J*. 2002;19:827-832.

37. Bernard A, Carbonnelle S, de Burbure C, Michel O, Nickmilder M. Chlorinated pool attendance, atopy, and the risk of asthma during childhood. *Environ Health Perspect*. 2006;114:1567-1573.

38. Jacobs JH, Spaan S, Van Rooy G, et al. Exposure to trichloramine and respiratory symptoms in indoor swimming pool workers. *Eur Respir J*. 2007;29:690-698.

39. Zwiener C, Richardson SD, De Marini DM, Grummt T, Glauner T, Frimmel FH. Drowning in disinfection byproducts? Assessing swimming pool water. *Environ Sci Technol*. 2007;41:363-372.

40. Aldridge WN, Evans CL. THE PHYSIOLOGICAL EFFECTS AND FATE OF CYANOGEN CHLORIDE. *Q J Exp Physiol Cogn Med Sci*. Published online 1946.

41. Odabasi M, Elbir T, Dumanoglu Y, Sofuoglu SC. Halogenated volatile organic compounds in chlorine-bleach-containing household products and implications for their use. *Atmos Environ*. 2014;92:376-383.

42. Wang L, Xiang Z, Stevanovic S, et al. Role of Chinese cooking emissions on ambient air quality and human health. *Sci Total Environ*. 2017;589:173-181.

43. O'Brien P, Siraki A, Shangari N. Aldehyde sources, metabolism, molecular toxicity mechanisms, and possible effects on human health. *Crit Rev Toxicol*. 2005;35:609-662.

44. Fenske JD, Paulson SE. Human breath emissions of VOCs. *J Air Waste Manag Assoc*. 1999;49:594-598.

4.8. Supporting Information

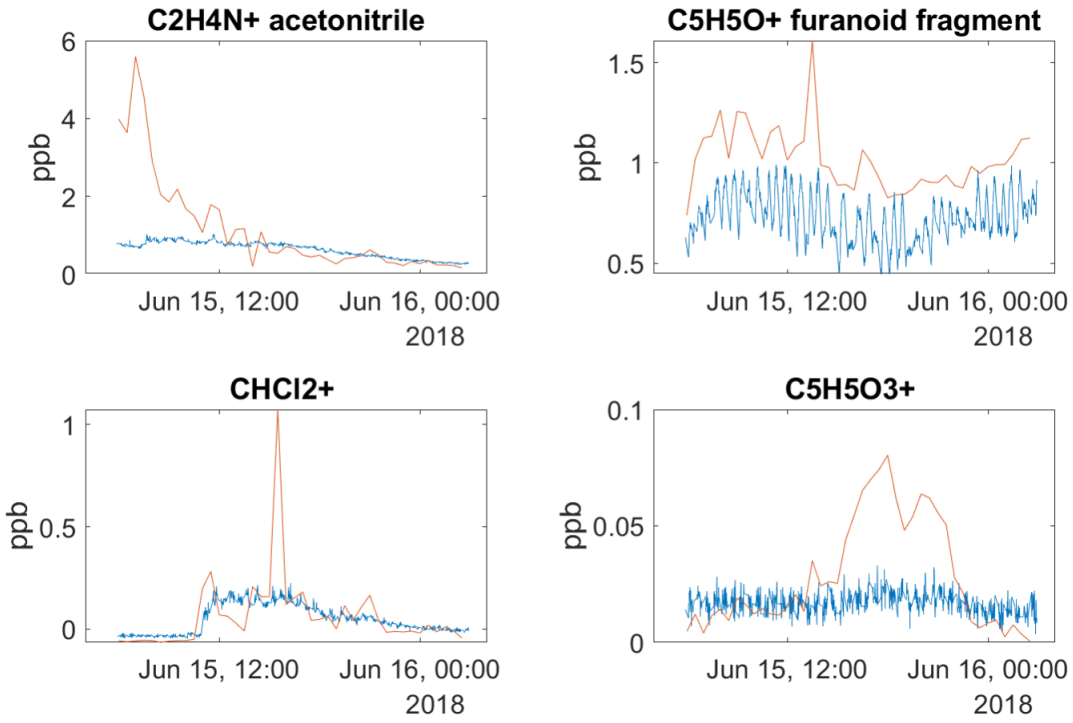

Figure 4.8.1 Indoor (blue) and outdoor (orange) mixing ratios for the 4 compounds that showed net negative emissions on the unoccupied day.

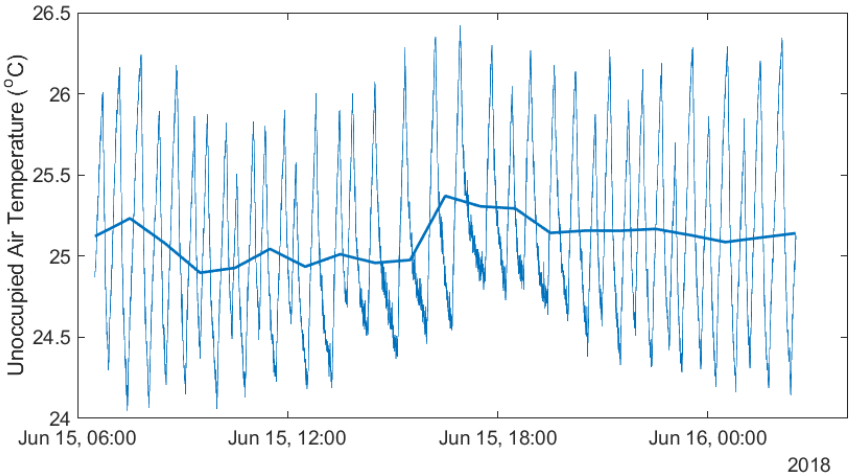

Figure 4.8.2 Indoor air temperature during the unoccupied day. Thick line depicts 1 h average.

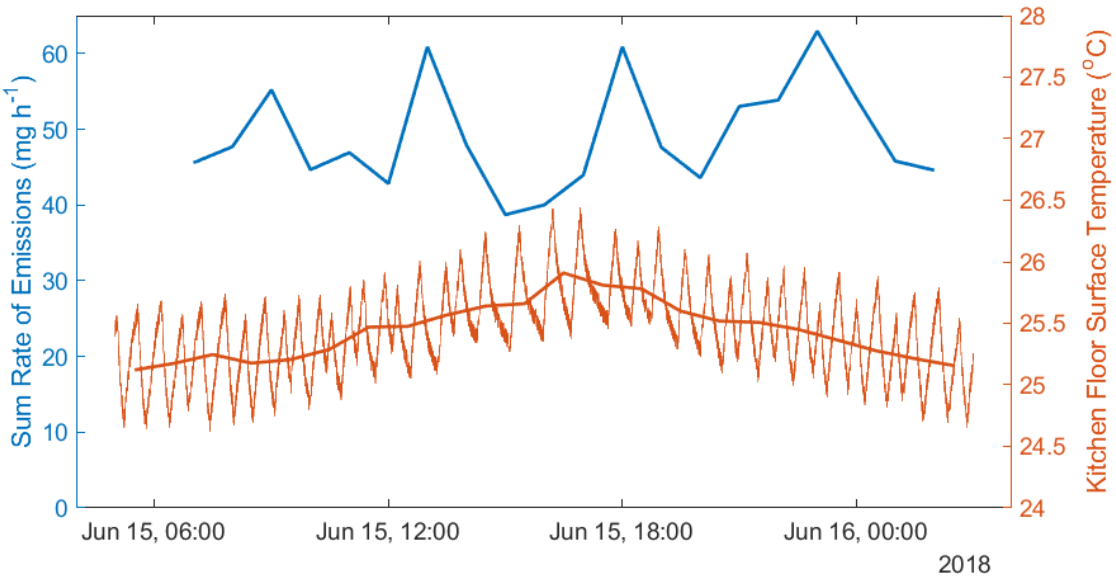

Figure 4.8.3 Rate of total emission into the house, averaged to 1 h (blue). Orange lines show the temperature of the kitchen floor, with the thicker line depicting 1 h averages.

Table 4.8.1 Average mixing ratios, median-indoor to median-outdoor concentration ratio, and indoor emissions for the unoccupied day. Compound assignments are meant to denote the suspected primary compound measured at that signal. Compound assignments with double asterisk are tentative (**).

m/z	Ion Formula	Compound Assignment	C avg (ppb)	I/O	E avg (mg h^{-1})
27.0238	C2H3+	alkyl fragment	0.197	Outdoor < LOD	0.026
28.0182	CH2N+	hydrogen cyanide	0.04	Outdoor < LOD	0.008
28.0304	C2H4+	alkyl fragment	0.038	Outdoor < LOD	0.005
33.0333	CH5O+	methanol	39.8	>10	6.3
41.0382	C3H5+	alkyl fragment	2.22	>10	0.45
42.0336	C2H4N+	acetonitrile	0.707	1-2	-0.09
43.0537	C3H7+	propanol fragment + propene	5.6	>10	1.2
45.033	C2H5O+	acetaldehyde	5.23	>10	1.1
47.0124	CH3O2+	formic acid	11.9	>10	2.8
47.0485	C2H7O+	ethanol	12.6	2-10	2.8
48.0086	H2O2N+	nitrous acid	0.088	2-10	0.015
49.0162	CH5S+	methanethiol	0.083	2-10	0.019
49.0275	CH5O2+	methane diol	0.096	2-10	0.021
51.9947	NH3Cl+	chloramine	0.017	Outdoor < LOD	0.005
53.0389	C4H5+	alkyl fragment	0.013	Outdoor < LOD	0.002
54.0333	C3H4N+	acrylonitrile**	0.029	Outdoor < LOD	0.007
57.0328	C3H5O+	acrolein + propionic acid fragment	1.05	>10	0.28
59.0484	C3H7O+	acetone + propanal	3.6	2-10	0.92
60.0456	C2H6NO+	acetamide	0.694	2-10	0.15
61.0275	C2H5O2+	acetic acid	55.9	>10	17
61.9788	CHClN+	cyanogen chloride	0.052	1-2	0.008
63.0069	CH3O3+		0.454	1-2	0.005
67.0537	C5H7+	alkyl fragment	0.072	2-10	0.021
68.0503	C4H6N+	pyrrole	0.029	Outdoor < LOD	0.009
69.033	C4H5O+	furan	0.172	2-10	0.053
69.0691	C5H9+	isoprene	0.977	2-10	0.27
71.0485	C4H7O+	unsaturiated carbonyl (e.g., methyl vinyl ketone)	1.06	2-10	0.19

71.0847	C5H11+	pentanol fragment + pentene	1.4	2-10	0.46
73.0277	C3H5O2+	acrylic acid**	0.288	2-10	0.067
73.0638	C4H9O+	butanal + methyl ethyl ketone	0.596	2-10	0.13
74.0609	C3H8NO+		0.154	2-10	0.044
75.0431	C3H7O2+	propionic acid	1.02	2-10	0.3
75.9946	C2H3ClN+		0.007	Outdoor < LOD	0.002
76.9793	C2H2ClO+		0.008	Outdoor < LOD	0.002
77.0223	C2H5O3+	glycolic acid**	0.024	1-2	0.005
77.0421	C3H9S+	propanethiol	0.018	Outdoor < LOD	0.005
78.9941	C2H4OCl+		0.034	2-10	0.01
79.0203	C2H7OS+	2-thioethanol	0.047	2-10	0.016
79.0403	C2H7O3+		0.215	2-10	0.08
79.0521	C6H7+	benzene	0.207	2-10	0.068
81.0348	C5H5O+	furanoid fragment	0.733	<1	-0.12
83.0486	C5H7O+	furan	0.185	2-10	0.064
83.0847	C6H11+	alkyl fragment	1.78	>10	0.75
85.0279	C4H5O2+	furanone	0.08	Outdoor < LOD	0.043
85.064	C5H9O+	cyclopentanone + others	0.269	2-10	0.1
85.1005	C6H13+	hexanol fragment + hexene	0.512	2-10	0.2
87.0432	C4H7O2+	diacetyl + others	0.584	2-10	0.24
87.0788	C5H11O+	pentanal + C5 ketone	0.213	2-10	0.078
88.0759	C4H10NO+		0.038	2-10	0.012
89.0585	C4H9O2+	butyric acid	0.917	2-10	0.36
91.0214	C2H7O2Si+	dimethoxysilane	0.029	Outdoor < LOD	0.014
91.0414	C3H7O3+		0.077	Outdoor < LOD	0.039
91.053	C7H7+		0.097	Outdoor < LOD	0.062
93.0364	C6H5O+	aromatic fragment	0.312	2-10	0.14
93.069	C7H9+	toluene	0.564	2-10	0.24
94.998	C2H7S2+	dimethyl disulfide	0.036	Outdoor < LOD	0.016
95.0163	C2H7O2S+	dimethyl sulfone**	0.115	>10	0.053
95.049	C6H7O+	phenol	0.415	>10	0.2
95.084	C7H11+		0.176	>10	0.08
96.0446	C5H6NO+	4-pyridinol	0.171	>10	0.08

96.9948	CH5O3S+	methanesulfonic acid	0.268	Outdoor < LOD	0.14
97.0277	C5H5O2+	furfural	1.44	Outdoor < LOD	0.75
97.0636	C6H9O+	dimethyl furan	0.38	>10	0.19
97.1005	C7H13+		0.367	2-10	0.17
98.0612	C5H8NO+	furfurylamine	0.034	Outdoor < LOD	0.016
99.0074	C4H3O3+		0.012	1-2	-0.001
99.0434	C5H7O2+	furfuranol	0.085	2-10	0.015
99.0796	C6H11O+	cis-3-hexenal and others	0.407	2-10	0.12
100.077	C5H10NO+	2-piperidinone	0.066	2-10	0.021
101.023	C4H5O3+	succinic anhydride	0.028	Outdoor < LOD	0.004
101.059	C5H9O2+	4-OPA + others	0.377	2-10	0.15
101.095	C6H13O+	hexanal + C6 ketones	0.28	2-10	0.13
103.04	C4H7O3+	acetate anhydrate**	0.118	2-10	0.056
103.073	C5H11O2+	pentanoic acid	0.415	2-10	0.2
104.05	C7H6N+	benzonitrile	0.011	Outdoor < LOD	0.004
105.034	C4H9OS+	methional**	0.055	Outdoor < LOD	0.026
105.069	C8H9+	styrene	0.207	>10	0.1
107.049	C7H7O+	benzaldehyde	0.511	Outdoor < LOD	0.29
107.083	C8H11+	C8 aromatics	0.235	2-10	0.1
108.081	C7H10N+	dimethylpyridine	0.058	Outdoor < LOD	0.031
109.067	C7H9O+	cresol	0.101	2-10	0.051
109.1	C8H13+	6-MHO fragment	0.14	>10	0.074
111.044	C6H7O2+	benzenediol	0.095	2-10	0.049
111.08	C7H11O+		0.17	2-10	0.084
111.116	C8H15+	1-octen-3-ol fragment + others	0.711	2-10	0.37
113.023	C5H5O3+		0.017	<1	-0.008
113.059	C6H9O2+		0.055	2-10	0.021
113.095	C7H13O+		0.098	2-10	0.05
113.131	C8H17+	octanol frgment + others	0.039	2-10	0.02
114.092	C6H12NO+		0.011	Outdoor < LOD	0.006
115.039	C5H7O3+		0.044	Outdoor < LOD	0.019

115.075	C6H11O2+		0.181	2-10	0.085
115.11	C7H15O+	heptanal + C7 ketones	0.159	2-10	0.084
116.906	CCl3+	chloroform**	0.171	1-2	0.013
117.056	C5H9O3+		0.135	2-10	0.069
117.09	C6H13O2+	hexanoic acid	0.873	2-10	0.49
118.065	C8H8N+	indole	0.013	Outdoor < LOD	0.007
119.085	C9H11+		0.094	2-10	0.049
119.917	HCl3N+	trichloramine	0.013	1-2	0
121.031	C7H5O2+		0.027	Outdoor < LOD	0.015
121.064	C8H9O+	anisaldehyde + others	0.113	2-10	0.063
121.099	C9H13+		0.113	2-10	0.039
123.116	C9H15+		0.106	>10	0.067
125.024	C6H5O3+		0.009	Outdoor < LOD	0.007
125.06	C7H9O2+		0.034	Outdoor < LOD	0.019
125.096	C8H13O+		0.086	2-10	0.05
125.132	C9H17+		0.166	>10	0.1
127.111	C8H15O+	6-MHO + others	0.185	2-10	0.11
127.146	C9H19+	nonene	0.062	2-10	0.034
129.056	C6H9O3+		0.124	2-10	0.068
129.09	C7H13O2+		0.131	2-10	0.065
129.127	C8H17O+	C8 saturated carbonyl + 1-Octen-3-ol	0.295	2-10	0.15
131.105	C7H15O2+	heptanoic acid	0.095	2-10	0.059
133.065	C9H9O+	cinnamaldehyde	0.016	Outdoor < LOD	0.011
133.1	C10H13+		0.053	2-10	0.032
135.045	C8H7O2+		0.02	2-10	0.01
135.082	C9H11O+		0.044	2-10	0.024
135.116	C10H15+	1,4-diethylbenzene	0.08	2-10	0.04
136.022	C7H6NS+	benzothiazole	0.032	2-10	0.017
136.077	C8H10NO+	2-aminoacetophenone	0.01	Outdoor < LOD	0.006
137.06	C8H9O2+	4-anisaldehyde + others	0.062	2-10	0.038
137.132	C10H17+	monoterpenes	1.35	2-10	0.61
139.075	C8H11O2+	2-methoxy-4-methylphenol (creosol)	0.041	2-10	0.024
139.111	C9H15O+		0.149	2-10	0.071

139.145	C10H19+		0.066	2-10	0.037
141.055	C7H9O3+	methoxymethylfurfural	0.011	Outdoor < LOD	0.006
141.092	C8H13O2+		0.034	Outdoor < LOD	0.02
141.127	C9H17O+	nonenal + others	0.084	2-10	0.055
141.162	C10H21+	1-decene	0.082	2-10	0.054
143.071	C7H11O3+		0.051	2-10	0.026
143.107	C8H15O2+		0.142	2-10	0.086
143.142	C9H19O+	C9 saturated carbonyl	2.2	2-10	1.5
145.05	C6H9O4+		0.009	Outdoor < LOD	0.005
145.122	C8H17O2+	octanoic acid	0.1	2-10	0.067
146.977	C6H5Cl2+		0.009	Outdoor < LOD	0.005
147.077	C10H11O+		0.014	Outdoor < LOD	0.008
149.096	C10H13O+		0.095	2-10	0.067
149.133	C11H17+	neopentylbenzene	0.043	2-10	0.027
151.112	C10H15O+		0.067	2-10	0.046
151.145	C11H19+		0.037	2-10	0.024
153.056	C8H9O3+	vanillin + others	0.047	2-10	0.025
153.127	C10H17O+	citral + others	0.656	2-10	0.4
155.089	C9H15S+	pentylthiopene	0.032	2-10	0.019
155.107	C9H15O2+		0.048	2-10	0.031
155.14	C10H19O+	monoterpene alcohols	0.051	2-10	0.035
155.177	C11H23+		0.051	2-10	0.036
157.086	C8H13O3+		0.058	2-10	0.043
157.157	C10H21O+	C10 saturated carbonyl	0.186	2-10	0.14
159.101	C8H15O3+		0.015	Outdoor < LOD	0.009
159.134	C8H19O2+		0.033	Outdoor < LOD	0.025
160.999	C7H4ClF2+	parachlorobenzotrifluoride	0.01	Outdoor < LOD	0.006
161.153	C9H21O2+		0.008	Outdoor < LOD	0.005
163.076	C10H11O2+		0.009	1-2	0.004
163.112	C11H15O+		0.019	2-10	0.013
163.151	C12H19+	1,3,5-triethylbenzene	0.014	Outdoor < LOD	0.009
165.091	C10H13O2+		0.017	2-10	0.011
165.163	C12H21+		0.02	Outdoor < LOD	0.013

167.071	C9H11O3+	veratraldehyde (fragerance)	0.018	2-10	0.011
167.104	C10H15O2+		0.025	2-10	0.017
167.177	C12H23+		0.011	Outdoor < LOD	0.007
169.122	C10H17O2+	pinonaldehyde + others	0.027	2-10	0.019
169.158	C11H21O+		0.022	2-10	0.016
169.194	C12H25+		0.057	2-10	0.037
171.172	C11H23O+	C11 saturated carbonyl	0.072	2-10	0.058
175.148	C13H19+		0.05	>10	0.042
177.163	C13H21+		0.02	Outdoor < LOD	0.016
179.179	C13H23+		0.018	Outdoor < LOD	0.014
183.174	C12H23O+		0.013	Outdoor < LOD	0.01
183.208	C13H27+		0.013	2-10	0.007
185.119	C10H17O3+		0.015	2-10	0.009
185.152	C11H21O2+		0.019	2-10	0.013
185.188	C12H25O+	C12 saturated carbonyl	0.052	2-10	0.043
189.131	C13H17O+		0.01	Outdoor < LOD	0.007
189.161	C14H21+		0.02	Outdoor < LOD	0.018
191.179	C14H23+		0.053	Outdoor < LOD	0.052
193.161	C13H21O+		0.006	Outdoor < LOD	0.005
193.193	C14H25+		0.017	Outdoor < LOD	0.016
195.176	C13H23O+		0.006	Outdoor < LOD	0.004
195.207	C14H27+		0.007	Outdoor < LOD	0.006
197.15	C12H21O2+		0.012	Outdoor < LOD	0.01
197.224	C14H29+		0.014	Outdoor < LOD	0.012
199.17	C12H23O2+		0.457	2-10	0.36
203.179	C15H23+		0.016	Outdoor < LOD	0.014
205.195	C15H25+	sesquiterpenes	0.049	2-10	0.043
207.178	C14H23O+		0.021	Outdoor < LOD	0.022
207.203	C15H27+		0.02	Outdoor < LOD	0.02
209.224	C15H29+		0.008	Outdoor < LOD	0.008

211.239	C15H31+		0.012	Outdoor < LOD	0.011
213.152	C12H21O3+		0.01	Outdoor < LOD	0.008
213.22	C14H29O+	C14 saturated carbonyl	0.017	Outdoor < LOD	0.014
215.165	C12H23O3+		0.078	<1	0
217.181	C16H25+		0.029	1-2	0.017
218.189	C15H24N+		0.007	Outdoor < LOD	0.005
219.176	C15H23O+		0.008	Outdoor < LOD	0.008
219.207	C16H27+	C16 aromatics + others	0.015	Outdoor < LOD	0.016
221.155	C14H21O2+	chromanol + others	0.027	Outdoor < LOD	0.029
221.19	C15H25O+		0.01	Outdoor < LOD	0.011
221.221	C16H29+		0.012	Outdoor < LOD	0.012
223.067	C6H19O3Si3+	siloxane D3	0.064	Outdoor < LOD	0.074
223.095	C12H15O4+	diethyl phthalate	0.02	Outdoor < LOD	0.024
223.24	C16H31+		0.006	Outdoor < LOD	0.006
225.257	C16H33+		0.011	Outdoor < LOD	0.011
227.035	C13H7O4+		0.009	Outdoor < LOD	0.01
227.235	C15H31O+	pentadecanal	0.005	Outdoor < LOD	0.006
231.161	C12H23O4+		0.01	Outdoor < LOD	0.012
231.177	C16H23O+		0.024	Outdoor < LOD	0.026
233.225	C17H29+	C17 aromatics + others	0.017	Outdoor < LOD	0.018
235.208	C16H27O+	callicarpenal (bug repellent)	0.028	2-10	0.03
243.219	C18H27+		0.007	Outdoor < LOD	0.008
245.226	C18H29+		0.015	2-10	0.014
247.241	C18H31+	C18 aromatics + others	0.017	2-10	0.018
249.257	C18H33+		0.008	Outdoor < LOD	0.009
259.241	C19H31+		0.015	2-10	0.013
261.257	C19H33+		0.016	2-10	0.016
263.272	C19H35+		0.008	Outdoor < LOD	0.008

271.249	C20H31+		0.015	Outdoor < LOD	0.017
273.258	C20H33+		0.013	2-10	0.012
275.273	C20H35+		0.011	2-10	0.01
277.288	C20H37+		0.006	1-2	0.004
297.081	C8H25O4Si4+	siloxane D4	0.036	Outdoor < LOD	0.053
371.091	C10H31O5Si5+	siloxane D5	0.743	>10	1.5
445.086	C12H37O6Si6+	siloxane D6	0.051	>10	0.11

Table 4.8.2 Emissions (mg per mop) and relative 95% confidence intervals (%) from bleach mopping. Table is sorted by emissions, high to low. Compound assignments with double asterisk are tentative (**).

Ion Formula	Compound Assignment	Emission (mg per mop)	Rel. 95% CI (%)
NH3Cl+	chloramine	16	29
H2Cl2N+	dichloramine	9.5	38
HCl3N+	trichloramine	4.2	27
CH5O+	methanol	1.1	59
C2H5O+	acetaldehyde	1	26
CHClN+	cyanogen chloride	1	20
CHCl2+		0.91	17
C3H7O+	acetone + propanal	0.78	41
CH3O2+	formic acid	0.35	89
CCl3+	chloroform**	0.23	20
C2H7S2+	dimethyl disulfide	0.21	27
C4H9O+	butanal + methyl ethyl ketone	0.21	46
CH4Cl2N+		0.18	23
C2H4N+	acetonitrile	0.18	60
C4H7O+	unsaturiated carbonyl (e.g., methyl vinyl ketone)	0.17	39
C2H4OCl+		0.14	22
C5H5O+	furanoid fragment	0.14	61
C12H23O2+		0.12	86
C7H7O+	benzaldehyde	0.12	37
C6H13O2+	hexanoic acid	0.12	75
C3H7O2+	propionic acid	0.1	84
C2H7O2S+	dimethyl sulfone**	0.1	32
CH5O3S+	methanesulfonic acid	0.088	20
C3H8NO+		0.083	44
C6H11+	alkyl fragment	0.077	59
CH4NOS+	n-sulfinyl methanamine	0.071	38
C2H6NO+	acetamide	0.069	60
C8H15+	1-octen-3-ol fragment + others	0.062	91
CH3O3+		0.054	52
C6H5O+	aromatic fragment	0.053	95
C5H11O+	pentanal + C5 ketone	0.05	52
C6H9O4+		0.05	98
C3H5O2+	acrylic acid**	0.047	48
C8H17O+	C8 saturated carbonyl + 1-Octen-3-ol	0.046	97

C5H11+	pentanol fragment + pentene	0.042	90
C8H8N+	indole	0.039	46
C7H15O2+	heptanoic acid	0.038	64
C6H11O+	cis-3-hexenal and others	0.038	80
C10H21O+	C10 saturated carbonyl	0.034	39
C2H7OS+	2-thioethanol	0.033	32
C4H5O3+	succinic anhydride	0.032	68
C5H9O+	cyclopentanone + others	0.03	90
C2H2ClO+		0.025	40
C8H9O+	anisaldehyde + others	0.024	36
C5H10NO+	2-piperidinone	0.024	33
C8H17O2+	octanoic acid	0.024	92
C2H4NO3+		0.023	21
C5H7O+	furan	0.022	39
C6H9O3+		0.022	87
C4H7O3+	acetate anhyidrate**	0.021	86
C8H10NO+	2-aminoacetophenone	0.02	36
C6H5Cl2+		0.02	48
C7H5O2+		0.02	36
C4H9OS+	methional**	0.019	56
C7H6NS+	benzothiazole	0.019	53
C7H7+		0.019	53
C10H15+	1,4-diethylbenzene	0.018	46
C4H6N+	pyrrole	0.017	48
C6H7+	benzene	0.017	61
C3H7O3+		0.017	76
C5H7O3+		0.016	73
C6H12NO+		0.016	49
C16H25+		0.015	92
C7H4ClF2+	parachlorobenzotrifluoride	0.015	36
C7H10N+	dimethylpyridine	0.014	58
C4H10NO+		0.014	67
C2H7O2Si+	dimethoxysilane	0.013	34
C2H3ClN+		0.013	28
C8H7O2+		0.013	87
C5H7O2+	furfuranol	0.013	90
C7H13O2+		0.013	88
C6H9O2+		0.012	93
C2H5O3+	glycolic acid**	0.012	34
C5H5O3+		0.011	44
CH6NS+		0.011	29

C5H8NO+	furfurylamine	0.011	50
C4H5O2+	furanone	0.011	95
C6H5O3+		0.01	43
C4H4NO3+	nitrofuran	0.01	34
C6H7O2+	benzenediol	0.01	90
C8H5O2+		0.01	30
C7H11O3+		0.009	43
C7H13O+		0.009	88
C10H11O2+		0.009	63
C3H4N+	acrylonitrile**	0.008	34
C8H19O2+		0.008	68
CH5O2+	methane diol	0.008	41
C7H6N+	benzonitrile	0.007	62
C4H3O3+		0.007	92
C9H9O+	cinnamaldehyde	0.006	98
C9H11+		0.006	84
C3H9S+	propanethiol	0.005	53
C7H9O3+	methoxymethylfurfural	0.005	64
C8H15O3+		0.005	57
C9H7O2+		0.005	42
C12H23O+		0.003	91
C13H17O+		0.003	75

Table 4.8.3 Emissions (mg per mop) and relative 95% confidence intervals (%) from natural product mopping. Table is sorted by emissions, high to low. Compound assignments with double asterisk are tentative (**).

Formula	Chemical ID	Emission (mg per mop)	Rel. 95% CI (%)
C10H17+	monoterpenes	12	22
C10H17O+	citral + others	1.2	22
C7H11+		0.53	21
C14H23O+		0.44	26
C10H19O+	monoterpene alcohols	0.35	20
C5H5O+	furanoid fragment	0.32	36
C6H11+	alkyl fragment	0.26	33
C8H9O2+	4-anisaldehyde + others	0.22	25
C7H9+	toluene	0.18	36
C7H7+		0.18	56
C15H27+		0.17	25
C12H23O2+		0.15	94
C10H19+		0.15	24
C16H27O+	callicarpenal (bug repellent)	0.15	63
C4H7O+	unsaturiated carbonyl (e.g., methyl vinyl ketone)	0.14	54
C9H15O+		0.12	29
C8H15+	1-octen-3-ol fragment + others	0.11	74
C5H9+	isoprene	0.1	84
C11H23+		0.1	26
C10H13O2+		0.099	46
C10H15+	1,4-diethylbenzene	0.088	30
C6H7+	benzene	0.084	40
C5H11+	pentanol fragment + pentene	0.082	96
C12H23O3+		0.07	36
C8H15O+	6-MHO + others	0.069	27
NH3Cl+	chloramine	0.067	27
C8H17O+	C8 saturated carbonyl + 1-Octen-3-ol	0.067	82
C8H11+	C8 aromatics	0.065	35
C8H13+	6-MHO fragment	0.063	37
C9H13+		0.06	57
C6H7O+	phenol	0.059	71
C5H7+	alkyl fragment	0.058	27
C6H9O+	dimethyl furan	0.054	77
C9H15O2+		0.053	27
C3H7O3+		0.053	54

C7H13+		0.048	47
C7H11O+		0.04	73
C8H15O2+		0.036	76
C7H7O+	benzaldehyde	0.036	79
C15H25+	sesquiterpenes	0.036	51
C8H17O2+	octanoic acid	0.035	69
C5H7O+	furan	0.033	28
C5H9O+	cyclopentanone + others	0.032	95
C8H9+	styrene	0.031	75
C10H21O+	C10 saturated carbonyl	0.028	67
C16H25+		0.025	93
C9H15S+	pentylthiopene	0.024	49
C14H21+		0.024	35
C8H13O+		0.019	30
C10H15O+		0.019	85
C12H21O2+		0.017	24
C5H11O+	pentanal + C5 ketone	0.017	70
C11H17+	neopentylbenzene	0.017	53
C9H19+	nonene	0.015	94
C10H17O2+	pinonaldehyde + others	0.015	40
C9H11O+		0.014	48
C4H5O+	furan	0.014	64
C7H10N+	dimethylpyridine	0.014	58
C8H9O3+	vanillin + others	0.013	61
C2H7O2Si+	dimethoxysilane	0.013	60
CHCl2+		0.012	37
C7H9O+	cresol	0.011	62
C6H9O2+		0.011	90
C10H13+		0.01	79
C12H21O3+		0.009	62
C11H19+		0.009	60
C8H10NO+	2-aminoacetophenone	0.008	32
C12H21+		0.007	73
C15H24N+		0.006	61
C8H15O3+		0.006	85
C11H21O+		0.006	89
C15H29+		0.005	51
C16H31+		0.005	76
C8H17+	octanol frgment + others	0.004	98
C4H5+	alkyl fragment	0.004	72

C12H19+	1,3,5-triethylbenzene	0.003	81
C3H9S+	propanethiol	0.002	93
C3H4N+	acrylonitrile**	0.002	64
C18H33+		0.001	93

Table 4.8.4 Emissions (mg per event) and relative 95% confidence intervals (%) from stir fry cooking. Table is sorted by emissions, high to low. Compound assignments with double asterisk are tentative (**).

Ion Formula	Compound Assignment	Emission (mg)	Rel. 95% CI (%)
C2H7O+	ethanol	200	22
CH5O+	methanol	13	23
C2H5O2+	acetic acid	10	99
C2H5O+	acetaldehyde	5.1	29
C3H7O+	acetone + propanal	3.8	32
C10H17O+	citral + others	1.8	48
C3H5O+	acrolein + propionic acid fragment	1.7	60
C4H9O+	butanal + methyl ethyl ketone	1.6	17
C5H9+	isoprene	1.1	29
C6H11+	alkyl fragment	0.89	51
C10H17+	monoterpenes	0.82	21
C5H11O+	pentanal + C5 ketone	0.77	24
C4H7O+	unsaturiated carbonyl (e.g., methyl vinyl ketone)	0.51	52
C7H13O+		0.41	53
C7H11O+		0.38	46
C3H7O2+	propionic acid	0.35	43
C7H11+		0.34	52
C5H5O2+	furfural	0.28	34
C4H7O2+	diacetyl + others	0.27	36
CH5S+	methanethiol	0.27	26
C5H11+	pentanol fragment + pentene	0.23	38
C3H5O2+	acrylic acid**	0.21	27
C5H9O+	cyclopentanone + others	0.19	38
C6H7+	benzene	0.18	30
C8H15+	1-octen-3-ol fragment + others	0.17	75
C6H7O2+	benzenediol	0.16	47
C6H13O+	hexanal + C6 ketones	0.15	46
C2H6NO+	acetamide	0.15	53
C6H9O2+		0.14	28
C8H15O+	6-MHO + others	0.14	47
C4H5O+	furan	0.14	29
C6H9O+	dimethyl furan	0.13	30
C7H9+	toluene	0.13	73
C5H7O+	furan	0.11	31
C6H7O+	phenol	0.11	35

C8H13+	6-MHO fragment	0.11	48
C6H11O+	cis-3-hexenal and others	0.11	36
C7H13+		0.11	54
C9H15O+		0.098	52
CH3O3+		0.086	58
C8H9O+	anisaldehyde + others	0.085	40
C8H17O+	C8 saturated carbonyl + 1-Octen-3-ol	0.084	56
C5H9O2+	4-OPA + others	0.077	58
C3H8NO+		0.066	44
C2H7S2+	dimethyl disulfide	0.066	68
C7H7O+	benzaldehyde	0.065	79
C7H15O2+	heptanoic acid	0.064	73
C8H11+	C8 aromatics	0.062	43
C10H21O+	C10 saturated carbonyl	0.061	43
C5H7O2+	furfuranol	0.06	42
C10H19O+	monoterpene alcohols	0.06	45
C6H13+	hexanol fragment + hexene	0.058	59
CH5O3S+	methanesulfonic acid	0.056	38
C2H4N+	acetonitrile	0.055	53
C8H13O+		0.051	54
C15H25+	sesquiterpenes	0.048	30
C5H7+	alkyl fragment	0.045	36
C8H15O2+		0.045	57
NH3Cl+	chloramine	0.044	59
C8H9+	styrene	0.043	49
C10H15+	1,4-diethylbenzene	0.043	40
C2H7O2S+	dimethyl sulfone**	0.043	59
C7H15O+	heptanal + C7 ketones	0.043	47
C4H10NO+		0.042	25
C5H5O3+		0.042	36
C9H15O2+		0.041	79
C7H7+		0.039	81
C9H19+	nonene	0.037	39
C6H12NO+		0.037	46
C9H13+		0.036	33
CHCl2+		0.035	25
C10H19+		0.035	30
C5H9O3+		0.034	93
C4H5O2+	furanone	0.033	55
C9H11+		0.033	46
C6H11O2+		0.033	84
CH5O2+	methane diol	0.032	28

C8H17O2+	octanoic acid	0.031	75
C7H13O2+		0.03	79
C11H23+		0.029	28
H2O2N+	nitrous acid	0.029	59
C8H25O4Si4+	siloxane D4	0.029	67
C8H11O2+	2-methoxy-4-methylphenol (creosol)	0.028	78
C3H7O3+		0.028	27
C7H7O3+		0.028	40
C7H5O2+		0.026	25
C16H25+		0.026	65
C8H9O3+	vanillin + others	0.025	42
C4H5+	alkyl fragment	0.025	41
C16H35O+		0.024	56
C11H21O+		0.024	66
C4H9OS+	methional**	0.024	54
C8H17+	octanol frgment + others	0.023	53
C9H17+		0.022	95
C10H17O2+	pinonaldehyde + others	0.022	37
C8H9O2+	4-anisaldehyde + others	0.019	53
C7H9O2+		0.018	29
C2H7O2Si+	dimethoxysilane	0.018	19
C10H15O+		0.018	67
C11H19+		0.018	72
C4H5O3+	succinic anhydride	0.017	81
C11H23O+	C11 saturated carbonyl	0.017	66
C11H17+	neopentylbenzene	0.017	46
C6H19O3Si3+	siloxane D3	0.016	78
C12H15O4+	diethyl phthalate	0.016	29
C2H7OS+	2-thioethanol	0.016	84
C12H25O+	C12 saturated carbonyl	0.016	52
C12H21O3+		0.015	43
C6H5O3+		0.015	40
C13H21+		0.014	61
C10H15O2+		0.014	38
C4H3O3+		0.014	45
C7H10N+	dimethylpyridine	0.013	30
C12H25+		0.012	70
C5H8NO+	furfurylamine	0.012	44
C8H19O2+		0.012	80
C18H31+	C18 aromatics + others	0.012	82
C5H7O3+		0.011	86
CHClN+	cyanogen chloride	0.011	69
C5H10NO+	2-piperidinone	0.011	72
C12H21+		0.01	40
C9H11O+		0.01	35

C10H13+		0.01	84
C16H27+	C16 aromatics + others	0.01	48
C4H6N+	pyrrole	0.01	53
C18H29+		0.01	51
C8H15O3+		0.009	80
C15H23+		0.009	61
C14H29O+	C14 saturated carbonyl	0.009	52
C15H27+		0.009	93
C12H21O2+		0.009	66
C2H4OCl+		0.008	76
CH6NS+		0.008	27
C17H29+	C17 aromatics + others	0.008	64
C3H4N+	acrylonitrile**	0.007	24
C13H23+		0.007	92
C3H9S+	propanethiol	0.007	43
C14H21O2+	chromanol + others	0.007	84
C12H23+		0.007	78
C15H25O+		0.007	94
C11H15O+		0.007	77
C12H23O+		0.006	52
C2H5O3+	glycolic acid**	0.006	55
C17H35+		0.006	63
C18H27+		0.006	70
C15H31O+	pentadecanal	0.005	88
C13H7O4+		0.005	81
C13H23O+		0.005	33
C16H29+		0.005	80
C13H21O+		0.005	60
C14H27+		0.005	65
C10H17O3+		0.004	86
C12H21O+		0.004	84
C8H19O2+		0.004	55
C16H31+		0.004	70
C8H10NO+	2-aminoacetophenone	0.004	84
C15H25O2+		0.004	59
C16H23O+		0.004	40
C19H35+		0.004	94
C12H19+	1,3,5-triethylbenzene	0.003	79
CH4NOS+	n-sulfinyl methanamine	0.003	46
C18H35+		0.003	83
C2H3ClN+		0.002	98
C7H4ClF2+	parachlorobenzotrifluoride	0.002	92

Table 4.8.5 Per-person emission rates for ion signals across all occupancy experiments (μg person^{-1} h^{-1}). Compound assignments with double asterisk are tentative (**).

Mass	Formula	Chemical ID	Low PCP morning (μg person^{-1} h^{-1})	Low PCP Afternoon (μg person^{-1} h^{-1})	Normal PCP (μg person^{-1} h^{-1})	High PCP morning (μg person^{-1} h^{-1})	High PCP afternoon (μg person^{-1} h^{-1})
27.0238	C2H3+	alkyl fragment	0.67	0.51	1.3	-	1.2
28.0182	CH2N+	hydrogen cyanide	1.2	-	0.25	1.5	-
28.0304	C2H4+	alkyl fragment	0.2	0.4	0.43	0.23	0.77
33.0333	CH5O+	methanol	46	310	-	-	170
41.0382	C3H5+	alkyl fragment	15	15	19	12	7.3
42.0336	C2H4N+	acetonitrile	10	60	3.4	9.8	3.5
43.0537	C3H7+	propanol fragment + propene	21	40	34	-	8.7
45.033	C2H5O+	acetaldehyde	-	42	41	0.98	150
47.0485	C2H7O+	ethanol	170	200	2600	1500	5400
48.0086	H2O2N+	nitrous acid	-	-	-	-	0.45
49.0162	CH5S+	methanethiol	-	0.68	-	-	0.62
51.9947	NH3Cl+	chloramine	-	-	-	0.12	0.49
53.0389	C4H5+	alkyl fragment	0.074	0.11	0.28	-	-
54.0333	C3H4N+	acrylonitrile**	0.18	0.33	-	-	0.54
57.0328	C3H5O+	acrolein + propionic acid fragment	0.62	9.4	-	-	11
59.0484	C3H7O+	acetone + propanal	450	550	380	390	510
60.0456	C2H6NO+	acetamide	3.2	18	5.8	2.3	19
63.0069	CH3O3+		-	3.2	-	-	1.7
64.0209	CH6NS+		-	0.16	-	0.084	-
67.0537	C5H7+	alkyl fragment	4.4	3.2	1.2	4.8	1.4
68.0503	C4H6N+	pyrrole	0.19	0.51	0.36	-	-
69.033	C4H5O+	furan	4.6	6.8	0.92	5.2	4.6
69.0691	C5H9+	isoprene	76	75	60	83	66
71.0485	C4H7O+	unsaturated carbonyl (e.g., methyl vinyl ketone)	15	19	13	22	18
71.0847	C5H11+	pentanol fragment + pentene	-	2	-	-	12
73.0277	C3H5O2+	acrylic acid**	-	0.31	-	-	-
73.0638	C4H9O+	butanal + methyl ethyl ketone	5.1	6.9	22	3.3	15
74.0609	C3H8NO+		-	0.11	-	-	0.21
75.0431	C3H7O2+	propionic acid	-	12	1.7	-	-
75.9946	C2H3ClN+		-	-	-	-	0.26
76.9793	C2H2ClO+		-	0.62	-	-	0.14

77.0223	C2H5O3+	glycolic acid**	0.42	2	1.1	2.5	1.3
77.0421	C3H9S+	propanethiol	0.25	0.087	0.43	0.38	0.54
78.0005	CH4NOS+	n-sulfinyl methanamine	0.25	-	-	-	0.21
78.9941	C2H4OCl+		-	0.63	-	-	-
79.0203	C2H7OS+	2-thioethanol	-	0.19	-	-	-
79.0521	C6H7+	benzene	-	1.4	1.7	-	3
81.0348	C5H5O+	furanoid fragment	-	0.39	-	-	-
82.9448	CHCl2+		0.24	0.28	0.27	1.8	38
83.0486	C5H7O+	furan	2	3.6	0.48	5	3.3
83.0847	C6H11+	alkyl fragment	25	26	-	42	10
85.0279	C4H5O2+	furanone	-	-	-	-	0.18
85.064	C5H9O+	cyclopentanone + others	-	2.6	-	-	3
85.1005	C6H13+	hexanol fragment + hexene	-	0.97	-	-	-
85.9549	H2Cl2N+	dichloramine	-	0.56	-	-	0.2
87.0432	C4H7O2+	diacetyl + others	-	0.63	-	-	5.5
87.0788	C5H11O+	pentanal + C5 ketone	-	3.7	-	-	6.5
88.0759	C4H10NO+		-	0.36	-	-	0.31
89.0585	C4H9O2+	butyric acid	-	9.9	-	-	24
90.0184	C2H4NO3+		0.26	-	-	-	0.68
91.0214	C2H7O2Si+	dimethoxysilane	0.52	1.2	0.37	2.9	1.4
91.0414	C3H7O3+		2.9	0.99	2.4	8.1	2.9
91.053	C7H7+		11	4.1	11	20	8.1
93.0364	C6H5O+	aromatic fragment	-	0.31	-	-	1.6
93.069	C7H9+	toluene	6.3	5.7	-	0.51	9.7
94.998	C2H7S2+	dimethyl disulfide	-	0.85	-	-	0.76
95.0163	C2H7O2S+	dimethyl sulfone**	-	1.9	0.22	-	4.1
95.049	C6H7O+	phenol	1.3	2.1	0.84	8.1	2.1
95.084	C7H11+		2.8	2.7	1.8	18	-
96.9948	CH5O3S+	methanesulfonic acid	-	0.67	-	-	0.27
97.0277	C5H5O2+	furfural	-	3.9	-	-	2.1
97.0636	C6H9O+	dimethyl furan	-	2.5	-	-	0.07
97.1005	C7H13+		3.8	5.6	-	6.4	6.7
98.0612	C5H8NO+	furfurylamine	-	0.46	0.6	-	0.33
99.0074	C4H3O3+		0.42	1.2	-	-	-
99.0434	C5H7O2+	furfuranol	-	-	0.3	-	0.54
99.0796	C6H11O+	cis-3-hexenal and others	-	1.3	9.8	-	1.6
99.9711	CH4Cl2N+		1.1	1.5	0.14	0.093	0.19
100.022	C4H6NS+		1.6	3.9	-	-	1.2
100.077	C5H10NO+	2-piperidinone	-	0.55	-	-	-

101.023	C4H5O3+	succinic anhydride	-	1.7	-	-	0.48
101.059	C5H9O2+	4-OPA + others	0.25	7.2	-	-	3
101.095	C6H13O+	hexanal + C6 ketones	0.15	3.2	-	-	2
103.04	C4H7O3+	acetate anhyidrate**	1.3	1.7	6.3	29	8.3
103.073	C5H11O2+	pentanoic acid	-	-	0.64	-	0.97
104.05	C7H6N+	benzonitrile	-	0.11	0.42	1.4	0.39
105.034	C4H9OS+	methional**	0.096	1.2	-	1.8	1.7
105.069	C8H9+	styrene	1.8	2.9	0.42	12	3.9
107.049	C7H7O+	benzaldehyde	-	3.1	-	-	3.2
107.083	C8H11+	C8 aromatics	2.6	4	-	3.5	1.5
108.081	C7H10N+	dimethylpyridine	-	-	-	-	0.25
109.067	C7H9O+	cresol	1.9	12	1.4	3.5	3.6
109.1	C8H13+	6-MHO fragment	15	20	9.1	12	11
111.08	C7H11O+		0.47	1.8	-	-	-
111.116	C8H15+	1-octen-3-ol fragment + others	-	4.1	-	-	-
113.023	C5H5O3+		-	0.52	-	-	0.44
113.059	C6H9O2+		-	-	1.4	-	0.73
113.095	C7H13O+		0.52	-	-	-	-
113.131	C8H17+	octanol frgment + others	-	0.83	-	0.19	0.78
114.02	C4H4NO3+	nitrofuran	-	0.098	0.23	-	0.23
114.092	C6H12NO+		0.78	-	0.33	1	0.36
115.039	C5H7O3+		-	0.29	-	-	0.63
115.075	C6H11O2+		-	-	-	-	1.4
116.906	CCl3+	chloroform*	0.45	-	2.2	1.2	0.7
118.065	C8H8N+	indole	0.22	-	-	-	-
119.085	C9H11+		3.2	4.7	-	1.6	3.2
119.917	HCl3N+	trichloramine	-	0.26	-	-	0.68
121.031	C7H5O2+		1.5	1.2	2.6	9.4	4
121.064	C8H9O+	anisaldehyde + others	5.2	3.1	3.3	15	3.2
121.099	C9H13+		1.7	2.6	0.32	8.3	1.5
123.116	C9H15+		2.6	2.4	0.8	4.1	-
125.024	C6H5O3+		-	0.39	-	-	-
125.06	C7H9O2+		-	-	-	0.45	-
125.096	C8H13O+		0.75	3.7	2.1	0.59	0.71
125.132	C9H17+		3.4	3.5	0.22	0.49	0.98
127.111	C8H15O+	6-MHO + others	9.8	17	4.2	3.4	9.5
127.146	C9H19+	nonene	0.97	4.4	3.2	0.69	0.59
129.056	C6H9O3+		-	2.4	-	-	-
129.09	C7H13O2+		-	0.9	-	-	-

129.127	C8H17O+	C8 saturated carbonyl + 1-Octen-3-ol	-	1.4	-	-	2.7
131.105	C7H15O2+	heptanoic acid	-	2.1	-	-	0.48
133.022	C8H5O2+		0.58	1.1	-	-	0.15
133.065	C9H9O+	cinnamaldehyde	1.1	-	-	-	-
133.1	C10H13+		0.87	1.6	0.54	3.1	0.64
135.045	C8H7O2+		-	-	-	0.86	0.58
135.082	C9H11O+		0.47	-	-	1.1	1.4
135.116	C10H15+	1,4-diethylbenzene	0.78	1.4	-	3.7	0.77
136.022	C7H6NS+	benzothiazole	0.4	1.7	0.83	0.22	2.2
136.077	C8H10NO+	2-aminoacetophenone	-	0.22	0.92	0.73	0.23
137.06	C8H9O2+	4-anisaldehyde + others	1.4	1.3	-	4.8	0.93
137.132	C10H17+	monoterpenes	84	51	33	300	47
139.039	C7H7O3+		0.55	7.4	7	61	39
139.075	C8H11O2+	2-methoxy-4-methylphenol (creosol)	3.1	2.9	6.7	35	5.9
139.111	C9H15O+		-	2.9	3.1	9.8	4.6
139.145	C10H19+		2.7	3.3	3.6	11	1.9
141.055	C7H9O3+	methoxymethylfurfural	0.28	0.13	-	1.4	-
141.092	C8H13O2+		-	1.5	0.52	-	0.71
141.127	C9H17O+	nonenal + others	1.6	1.1	-	1	-
141.162	C10H21+	1-decene	-	1.1	1.2	1.8	-
143.071	C7H11O3+		-	0.46	-	0.64	1.9
143.107	C8H15O2+		2.3	5	-	-	2.6
143.142	C9H19O+	C9 saturated carbonyl	49	60	6.8	8.5	12
145.05	C6H9O4+		-	7.5	-	-	0.18
145.122	C8H17O2+	octanoic acid	-	0.69	-	-	-
146.977	C6H5Cl2+		-	3.2	-	-	0.37
147.047	C9H7O2+		-	-	0.13	1.8	-
147.136	C8H19O2+		-	0.44	0.15	-	-
149.096	C10H13O+		-	1.8	-	2.1	1
149.133	C11H17+	neopentylbenzene	0.58	1.4	0.38	1.9	0.28
151.112	C10H15O+		1.2	1.5	0.76	6.7	1.9
151.145	C11H19+		1.2	1	1.4	4.6	2.3
153.056	C8H9O3+	vanillin + others	2.1	4.6	26	27	8.6
153.127	C10H17O+	citral + others	19	6.8	170	390	100
155.089	C9H15S+	pentylthiopene	0.43	-	-	1.8	0.69
155.107	C9H15O2+		1.7	2	-	1.3	-

155.14	C10H19O+	monoterpene alcohols	4.6	2.8	2.4	22	1.1
155.177	C11H23+		-	1.5	0.59	5.6	-
157.086	C8H13O3+		-	1.7	-	-	1.8
157.157	C10H21O+	C10 saturated carbonyl	15	20	14	15	17
159.101	C8H15O3+		0.89	1.7	-	2.5	1.8
159.134	C8H19O2+		-	0.53	-	-	0.16
160.999	C7H4ClF2+	parachlorobenzotrifluoride	-	-	-	0.85	-
161.153	C9H21O2+		-	-	0.21	-	-
163.076	C10H11O2+		0.23	0.09	0.58	0.35	0.38
163.112	C11H15O+		-	0.18	-	1.9	1.4
163.151	C12H19+	1,3,5-triethylbenzene	-	0.2	-	0.88	0.16
165.091	C10H13O2+		0.88	0.48	0.44	0.32	0.86
165.163	C12H21+		0.88	0.79	0.15	1	0.7
167.071	C9H11O3+	veratraldehyde (fragerance)	0.46	0.49	0.24	0.9	0.49
167.104	C10H15O2+		-	0.61	-	-	0.2
167.177	C12H23+		-	0.32	0.6	0.33	0.19
169.122	C10H17O2+	pinonaldehyde + others	-	-	0.4	-	-
169.158	C11H21O+		0.72	-	0.46	0.14	-
169.194	C12H25+		-	0.2	-	-	0.63
171.172	C11H23O+	C11 saturated carbonyl	2.3	3.9	0.2	-	2.1
175.148	C13H19+		0.073	1.2	-	-	-
177.057	C10H9O3+		0.44	0.38	0.14	1	0.42
177.163	C13H21+		4.2	4.4	2.7	3.5	5.5
179.179	C13H23+		0.41	0.98	0.22	0.68	0.7
181.118	C11H17O2+		-	0.19	-	0.36	0.49
181.156	C12H21O+		-	0.25	0.17	-	0.27
181.193	C13H25+		0.11	-	-	0.073	0.44
183.174	C12H23O+		0.5	1.1	0.93	1.2	-
183.208	C13H27+		-	0.34	-	0.29	0.69
185.119	C10H17O3+		-	0.11	-	0.74	0.4
185.152	C11H21O2+		-	0.085	-	1.2	0.53
185.188	C12H25O+	C12 saturated carbonyl	1.7	0.9	0.25	1.5	2.1
189.131	C13H17O+		0.9	0.73	0.85	3.1	1.6
189.161	C14H21+		0.32	0.94	0.13	1.5	1
190.087	C11H12NO2+		-	0.41	14	25	0.57
191.179	C14H23+		-	0.79	-	1.4	1.3
193.118	C12H17O2+		0.58	-	0.45	2.6	1.9
193.161	C13H21O+		0.41	0.2	-	2.5	0.68

193.193	C14H25+		0.68	0.76	0.46	2.1	1.4
195.176	C13H23O+		1.4	1.5	0.99	1.6	1.3
195.207	C14H27+		0.25	0.85	-	-	0.59
197.15	C12H21O2+		0.21	-	-	2	0.76
197.224	C14H29+		0.85	0.27	-	-	0.52
199.17	C12H23O2+		-	-	-	-	2.8
203.179	C15H23+		0.93	0.79	0.41	1.9	1.1
204.103	C12H14NO2+		-	0.34	11	23	2.8
205.195	C15H25+	sesquiterpenes	3.6	5.8	3.7	22	4.6
207.178	C14H23O+		1.2	1.5	1.1	11	2.3
207.203	C15H27+		0.31	0.78	0.52	4.3	0.72
209.224	C15H29+		0.29	0.3	-	0.36	0.47
211.239	C15H31+		0.36	-	0.12	0.42	-
213.152	C12H21O3+		0.81	-	0.35	1.2	1
213.22	C14H29O+	C14 saturated carbonyl	-	-	-	-	0.79
217.181	C16H25+		1.9	2.4	-	1.6	2.1
218.189	C15H24N+		0.66	0.24	-	0.85	-
219.176	C15H23O+		-	0.67	0.47	0.84	1.1
219.207	C16H27+	C16 aromatics + others	0.093	0.97	0.32	1.5	0.6
221.155	C14H21O2+	chromanol + others	0.82	-	-	3.8	1
221.19	C15H25O+		0.65	0.99	0.87	1.7	-
221.221	C16H29+		-	0.086	-	0.96	0.61
223.067	C6H19O3Si3+	siloxane D3	1.5	0.97	-	42	5.5
223.095	C12H15O4+	diethyl phthalate	-	0.95	-	13	0.86
223.24	C16H31+		0.4	0.4	-	0.25	0.4
225.257	C16H33+		-	0.51	-	2	1.4
227.035	C13H7O4+		-	0.46	0.29	1.1	0.36
227.174	C17H23+		-	-	0.69	6.1	2
227.235	C15H31O+	pentadecanal	0.23	0.59	-	1.4	-
231.161	C12H23O4+		-	0.5	0.43	0.65	-
231.177	C16H23O+		-	1.1	0.17	0.48	0.16
233.225	C17H29+	C17 aromatics + others	1.5	0.39	0.65	1.9	1.4
235.208	C16H27O+	callicarpenal (bug repellent)	18	13	5.3	37	18
237.181	C15H25O2+		0.7	0.23	0.27	1.1	0.34
237.255	C17H33+		-	0.43	0.23	1.1	0.6
239.27	C17H35+		-	0.17	0.47	-	0.18
241.2	C18H25+		-	0.63	-	0.46	0.33
243.219	C18H27+		-	0.7	-	-	0.12
243.264	C16H35O+		1.5	3.8	0.85	1.8	-
245.226	C18H29+		0.47	1.9	-	1.8	1.1

247.241	C18H31+	C18 aromatics + others	0.3	0.79	1.8	2.4	0.76
249.257	C18H33+		0.83	0.28	0.97	0.5	0.17
251.165	C15H23O3+		0.29	1.4	2.2	20	6.9
251.271	C18H35+		-	0.39	0.21	1.6	0.12
259.241	C19H31+		-	0.58	-	1.9	0.6
261.257	C19H33+		0.77	0.12	0.23	-	1.2
263.166	C16H23O3+		0.45	1.4	0.9	10	9.9
263.272	C19H35+		-	0.39	-	1.6	0.2
271.249	C20H31+		-	0.25	-	0.072	0.69
273.258	C20H33+		-	0.56	-	0.57	0.63
275.273	C20H35+		-	1	-	-	-
277.288	C20H37+		-	-	-	0.63	-
297.081	C8H25O4Si4+	siloxane D4	2.3	0.97	3.4	160	2.5
371.091	C10H31O5Si5+	siloxane D5	340	8.2	2900	16000	-
445.086	C12H37O6Si6+	siloxane D6	5.1	5.5	130	270	19

5. Future Work

5.1. Indoor Air as Outdoor Pollutant

The introduction of this dissertation showed how atmospheric chemistry techniques are being applied to indoor air, and that this work fits into the larger project to "bring atmospheric chemistry home." While our understanding of indoor VOCs is far from complete, the thread of this research must again venture outdoors.

The past 50 years has seen a dramatic reduction in US vehicular VOC emissions.[1] As these emissions declined, a gap in emission inventories has widened, attributable to volatile chemical products (VCPs), cooking emissions, and other indoor sources emitted to the outdoors.[2] McDonald *et al*. (2018) present estimates that VCPs contribute ~50% of the petrochemical VOC sources in industrialized cities. Despite the successful interventions to reduce VOC emissions from transportation and other regulated sources, air pollution in major metropolitan areas still regularly exceeds air quality standards. To understand and model these air pollution events, we must understand the emissions of VOCs. As emissions from traditional sources of VOCs continue to decline due to technology and regulation, this gap between emissions inventories and observed concentrations will continue to grow. Preliminary data presented in this chapter shows that indoor VOCs emitted outdoors can be a substantial source contributing to urban air pollution.

In addition to the experiments reported in Chapter 4, a second set of HOMEChem experiments referred to as "layered" experiments were conducted as well. Rather than repetitions of activities or occupancy, layered experiments were designed to replicate a normally occupied day or a thanksgiving holiday. For the normally occupied day 3 occupants entered the test house in the morning and remained inside until the evening, cooking 3 meals and mopping once. For a thanksgiving holiday, 4 occupants entered the house in the morning and prepared a large meal. In the afternoon, 10+ guests entered the house to eat dinner.

Emissions from the house to the outdoors are given by:

$$M = \rho V A \Delta t (C_{in} - C_{out}) \quad (1)$$

Where ρ (mg mm^{-3}) is the gas density at 20 °C of the species emitted as calculated from the molar mass of the compound and the ideal gas law, V is the mixed volume of the house (235,000 L), A is the ACR (h^{-1}), Δt (h) is the time interval over which the emission occurs, and C_{in} and C_{out} are the indoor and outdoor mixing ratios, respectively (ppb).

One indication of the importance of indoor emissions to the outdoors is seen by comparing biogenic emissions to residential emissions. Emissions from the house are normalized to the house area (120 m^2), as well as the mass of carbon emitted rather than the total mass. A normal layered day gives a total emission of 0.8 mg C m^{-2} h^{-1}, while the mock thanksgiving holiday gives 1.5 mg C m^{-2} h^{-1}. This range of total C emissions is remarkably similar to emissions measured above a California pine forest, which ranged from 0.7-1.4 mg C m^{-2} h^{-1}.[8] Monoterpene emissions from the normal layered day were 0.04 mg C m^{-2} h^{-1}, a factor of 5 lower than the 0.2

mg C m^{-2} h^{-1} reported from the pine forest.[8] However, the large monoterpene emissions from cooking herbs and citrus during thanksgiving experiments led to 0.2 mg C m^{-2} h^{-1} of emissions, matching the biogenic rate. This comparison to biogenic emissions is of course limited: on a layered day 0.03 mg m^{-2} h^{-1} of D5 siloxane is emitted while we would expect none from a forest.

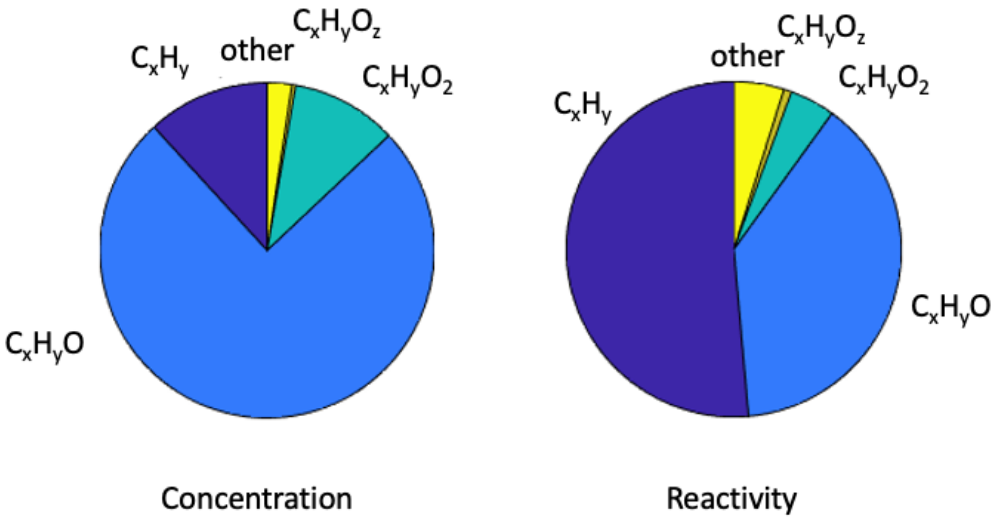

Figure 5.1.1 Relative contribution of VOCs to concentration and reactivity during a layered experiment. Large amounts of ethanol account for high concentrations of CxHyO while small amounts of monoterpene lead to the large reactivity of CxHy.

OH reactivity, secondary organic aerosol (SOA) formation potential, and ozone formation potential are all used to assess the air quality impact of VOC emissions. Of these, OH reactivity is the easiest to calculate, and is used here to infer the impact of indoor VOCs emitted outdoors. OH reactivity due to VOCs, R_{VOC} (s^{-1}), is given by:

$$R_{VOC} = \sum k_{VOC+OH} \cdot [VOC] \quad (2)$$

Where k_{VOC} (cm^3 $molec^{-1}$ s^{-1}) is the reaction rate constant for OH with a specific compound, and [VOC] is the concentration of that compound (molec cm^{-3}). For reported VOC signals for which we have high confidence in the compound assignment, reaction rate constants from previous kinetics studies are used.[9–13] For compounds with a chemical formula assignment that matches one or more chemical formulas in the NIST chemical kinetics data-base, the median reaction rate constant is chosen.[14] Finally, for VOC signals with no match in the database, a generic value of k_{OH} is used (1.82 x 10^{-11} cm^3 $molec^{-1}$ s^{-1}).[15]

The unoccupied HOMEChem test house has an average R_{VOC} of 38 s^{-1}, four times higher than the corresponding outdoor value of 9 s^{-1}. The ratio of indoor:outdoor reactivity is smaller than the ratio of indoor:outdoor concentrations, indicating that on average indoor compounds are less reactive than outdoor compounds but their large concentration leads to the larger reactivity. This is expected given the high percentage of oxygenated compounds found indoors. The largest

contributor to unoccupied indoor R_{VOC} is monoterpenes, contributing 6 s^{-1} (15%) of the reactivity (treated as limonene, k_{OH} = 1.61 x 10^{-10} cm^3 $molec^{-1}$ s^{-1}).[11]

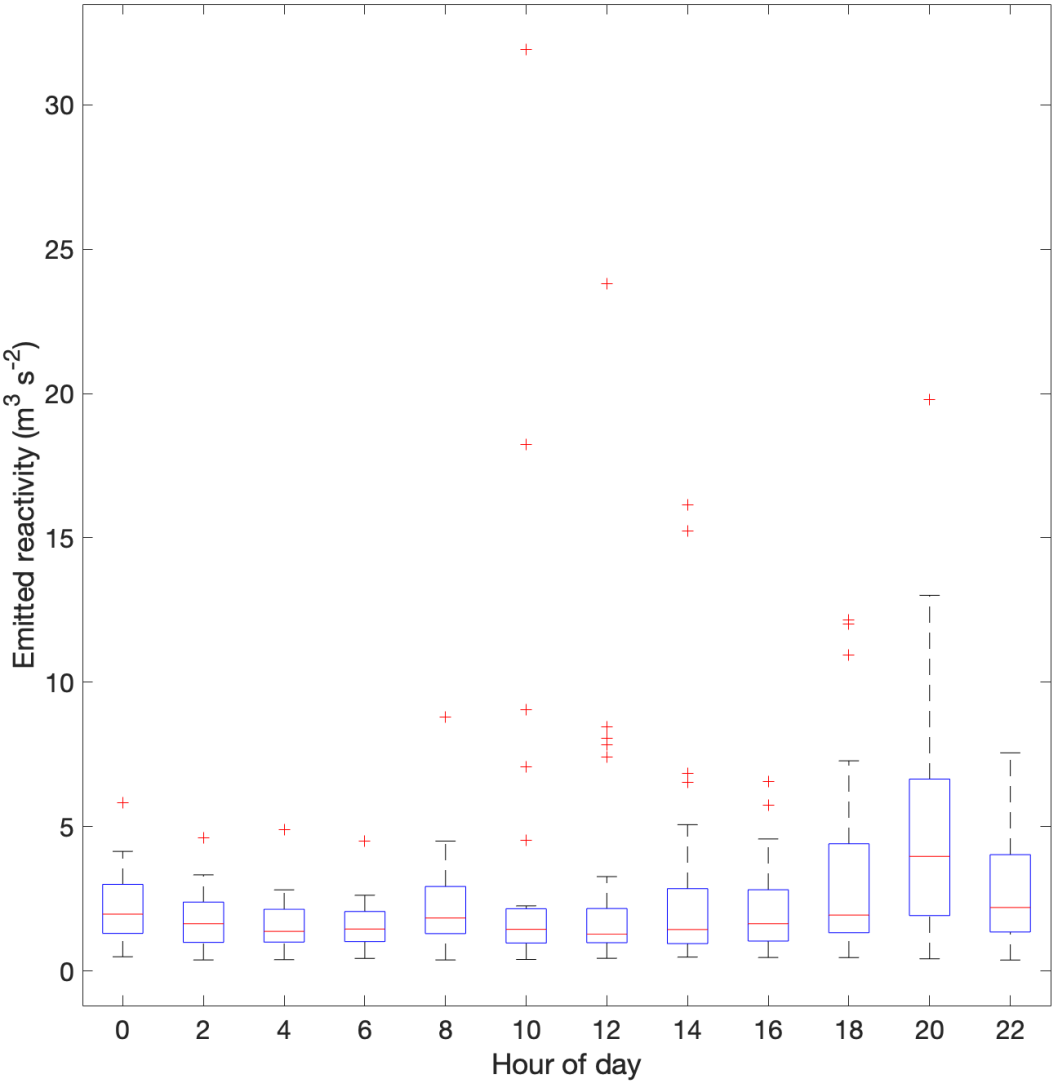

Figure 5.1.2: Emitted reactivity from the normally occupied residence studied in Liu *et al.* (2019). The 5 week campaign has been binned by time of day.

The layered day has an average R_{OH} of 120 s^{-1}, an order of magnitude greater than outdoor R_{OH} and three times greater than indoor unoccupied R_{OH}. Figure 5.1.1 shows a comparison of the relative composition of concentration and R_{OH} of the layered day. Despite their relatively small concentration, compounds comprised of just carbon and hydrogen make up over half of the reactivity. Monoterpenes, a subset of this class, are again the largest single source of R_{OH}, responsible for 26% of R_{OH} but making up only 1.3% of the total indoor VOC concentration. The second largest source of R_{OH} is ethanol. In contrast to monoterpenes it is found in high abundance, making up more than half of the VOC signal in the house. This large concentration

allows ethanol to overcome it's relatively slow rate of reaction with OH, and is responsible for one-fifth of the total indoor R_{OH}.

As we saw in Chapter 4, ethanol is the major emission from HOMEChem cooking experiments. Increases in urban ethanol concentrations have been attributed partially to the rise of ethanol as a fuel additive, but expected emissions from transportation cannot completely account for observed concentrations.[16] McDonald *et al*. (2018) find that transportation emissions only make up 20% total ethanol emissions in Los Angeles, and attribute the rest of the emissions to VCPs.[2] The data from HOMEChem and Liu *et al*. (2019) both point to residential cooking as a large and previously unconsidered source of ethanol that deserves more study.[17]

In their study of VOC emissions from a normally occupied residence, Liu *et al*. (2019) demonstrated that ~50% of all indoor VOC species observed by PTR-ToFMS were an order of magnitude higher in concentration than outdoors, and ~80% of observed VOCs were at least twice as high as outdoors.[17] Ventilation rates were fast enough that in just a few hours the indoor air exchanged completely with outdoor air.[18] Together these results suggest indoor VOC emissions are typically transported to the outdoors.

Using VOC concentration data from the field campaign described in Liu *et al*. (2019) we find indoor R_{OH} ranging from 40 s^{-1} to 120 s^{-1} in the living space over summer and winter measurements. Outdoor R_{OH} was always at least one order of magnitude lower, ranging from 2 to 4 s^{-1}. Detailed measurements of ventilation allows for the calculation of reactivity emissions, simply the volume flow rate out of the house multiplied by the indoor R_{OH} (giving the delightfully unintuitive units of m^{-3} s^{-2}). Figure 5.1.2 shows hourly averages of emitted reactivity over the 5 week winter sampling period.

The role of the occupant is clearly visible, with elevated emissions of reactivity in the morning and evening, correlated with cooking and demonstrating the impact of occupant activities. The large number of outliers further highlight the importance of the occupant, as each one indicates an event driven emission.

This analysis is still ongoing, with the immediate intention of combining data from the HOMEChem study with VOC and ventilation data from two normally occupied northern California homes. These three studies, combined with previous inventories of indoor VOCs and ventilation rates will allow us to constrain VOC emissions from residences, and comment on the impact to urban air pollution.

The next research step for this work is to expand the scale of measurements: mobile sampling from a van will provide VOC measurements with high spatial resolution, while a flux tower operating in the same spatial domain will directly measure VOC fluxes from a large swath of residences. Finally, airborne measurements over urban areas can provide city wide flux measurements, with speciation to compare back to smaller scales. With these multiscale observations, it will be feasible to determine the magnitude of residential VOC emissions contributing to regional urban air pollution, and their relative importance compared to other sources.

5.2. Continued Work Indoors

While the trajectory of the study of VOC emissions leads outdoors, the study of indoor oxidants is far from complete.

Our work measuring the nitrate radical indoors shows that NO_3 *can* be an important indoor oxidant, however this is one study of a manipulated environment over a short time frame. We are left to speculate that certain conditions, i.e. high outdoor ozone and NO_x, will lead to large amounts of indoor NO_3 chemistry. It seems prudent that the next step in determining the role of indoor NO_3 chemistry is to confirm the presence of NO_3 in unmanipulated indoor environments, with a focus on polluted areas.

An interesting wrinkle of the NO_3 experiments was that in the home where the measurements took place NO released from the natural gas heating system prevented the buildup of NO_3. Similarly, during the manipulation experiments indoor concentrations of NO_3 began to grow only after the NO released from the combustion stove was depleted. As we showed in Chapter 2, competition between NO and VOC reactions determine the influence of NO_3. This competition may be changing as new residential construction moves away from natural gas appliances and towards electrification. Berkeley, for instance, limits the use of natural gas in new construction.[14] However the effects are not immediately obvious: with insufficient ozone, NO attenuates NO_3 chemistry. With excess ozone, NO is a precursor to NO_3 formation.

On a broad level, if we wish to increase our understanding of the importance of NO_3 indoors we must increase our understanding of the other oxidants with which it competes. While more studied than NO_3, the OH radical has few indoor measurements. Promising work on indoor relevant OH production pathways has shown that OH levels indoors can lead to significant oxidation.[15–18] The Cl radical may also take on an increased importance indoors especially during bleach cleaning.[19,20] Ozone is the most characterized indoor oxidant, but the work in Chapter 3 shows there are still discoveries to be made.

An excellent body of literature on the ozonolysis of skin oil led to the work in Chapter 3, and more field measurements of skin oil oxidation product VOCs will help us determine typical indoor concentrations. However, because the products are released directly from the occupant (as well as skin oil infused furnishings and clothing), exposure to these VOCs may be greater than exposures determined from bulk air concentrations. Some products, such as 4-OPA, are known irritants so exposure analysis could be a step to improved perceived indoor air quality. Additionally, the presence of multiple generations of ozonolysis products presents an opportunity to track the oxidation "age" of indoor spaces. Both 6-MHO and 4-OPA act as tracers of skin oil ozonolysis, with 6-MHO able to be further consumed by ozone. The ratio of the two products may prove a useful tool in assessing the state of ozonolysis in indoor air.

As mentioned in Chapter 3, the mechanism describing the humidity dependence of heterogeneous ozonolysis is not specific to squalene. While the large number of unsaturated bonds separating small moieties may exaggerate the effect, we expect to see it replicated in reactions with other surface bound unsaturated organics. If this holds true, manipulating relative humidity may strongly influence the VOC concentration and composition indoors. This could be tested by manipulating ozone and humidity levels in recently occupied indoor spaces so as to

capture the full chemical spectrum that builds up on indoor surfaces. Not nearly enough evidence exists to prescribe changes to indoor humidity, however the results warrant more study of humidity effects on ozonolysis.

5.3. References

1. Warneke C, De Gouw JA, Holloway JS, et al. Multiyear trends in volatile organic compounds in Los Angeles, California: Five decades of decreasing emissions. *J Geophys Res Atmos*. 2012;117.

2. McDonald BC, De Gouw JA, Gilman JB, et al. Volatile chemical products emerging as largest petrochemical source of urban organic emissions. *Science (80-)*. 2018;359:760-764.

3. Bouvier-Brown NC, Schade GW, Misson L, Lee A, McKay M, Goldstein AH. Contributions of biogenic volatile organic compounds to net ecosystem carbon flux in a ponderosa pine plantation. *Atmos Environ*. Published online 2012.

4. Atkinson R, Baulch DL, Cox RA, et al. Evaluated Kinetic, Photochemical and Heterogeneous Data for Atmospheric Chemistry: Supplement V: IUPAC Subcommittee on Gas Kinetic Data Evaluation for Atmospheric Chemistry. *J Phys Chem Ref Data*. 1997;26:521-784.

5. Atkinson R, Winer AM, Pitts JN. Estimation of night-time N2O5 concentrations from ambient NO2 and NO3 radical concentrations and the role of N2O5 in night-time chemistry. *Atmos Environ*. 1986;20:331-339.

6. Gill KJ, Hites RA. Rate constants for the gas-phase reactions of the hydroxyl radical with isoprene, α- and β-pinene, and limonene as a function of temperature. *J Phys Chem A*. 2002;106:2538-2544.

7. Atkinson R, Aschmann SM, Winer AM, Carter WPL. Rate constants for the gas phase reactions of OH radicals and O3 with pyrrole at 295 ± 1 K and atmospheric pressure. *Atmos Environ*. 1984;18:2105-2107.

8. Xiao R, Zammit I, Wei Z, Hu WP, MacLeod M, Spinney R. Kinetics and Mechanism of the Oxidation of Cyclic Methylsiloxanes by Hydroxyl Radical in the Gas Phase: An Experimental and Theoretical Study. *Environ Sci Technol*. 2015;49:13322-13330.

9. J. A. Manion, R. E. Huie, R. D. Levin, D. R. Burgess Jr., V. L. Orkin, W. Tsang, W. S. McGivern, J. W. Hudgens, V. D. Knyazev, D. B. Atkinson, E. Chai, A. M. Tereza, C.-Y. Lin, T. C. Allison, W. G. Mallard, F. Westley, J. T. Herron, R. F. Hampson DHF. NIST Chemical Kinetics Database, NIST Standard Reference Database 17, Version 7.0 (Web Version), Release 1.6.8, Data version 2015.09. National Institute of Standards and Technology.

10. Park JH, Goldstein AH, Timkovsky J, et al. Active atmosphere-ecosystem exchange of the vast majority of detected volatile organic compounds. *Science (80-)*. Published online 2013.

11. De Gouw JA, Gilman JB, Borbon A, et al. Increasing atmospheric burden of ethanol in the United States. *Geophys Res Lett*. Published online 2012.

12. Liu Y, Misztal PK, Xiong J, et al. Characterizing sources and emissions of volatile organic compounds in a northern California residence using space-and time-resolved measurements. *Indoor Air*. 2019;29:630-644.

13. Liu Y, Misztal PK, Xiong J, et al. Detailed investigation of ventilation rates and airflow patterns in a northern California residence. *Indoor Air*. 2018;28:572-584.

14. Planning and Development Department Office of Energy Sustainability. *City of Berkeley Natural Gas Prohibition & Reach Code for Electrification*.; 2019.

15. Gomez Alvarez E, Amedro D, Afif C, et al. Unexpectedly high indoor hydroxyl radical concentrations associated with nitrous acid. *Proc Natl Acad Sci*. 2013;110:13294-13299.

16. Weschler CJ, Shields HC. Production of the hydroxyl radical in indoor air. *Environ Sci Technol*. 1996;30:3250-3258.

17. Weschler CJ, Shields HC. Measurements of the hydroxyl radical in a manipulated but realistic indoor environment. *Environ Sci Technol*. 1997;31:3719-3722.

18. Carslaw N, Fletcher L, Heard D, Ingham T, Walker H. Significant OH production under surface cleaning and air cleaning conditions: Impact on indoor air quality. *Indoor Air*. 2017;27:1091-1100.

19. Schwartz-Narbonne H, Wang C, Zhou S, Abbatt JPD, Faust J. Heterogeneous Chlorination of Squalene and Oleic Acid. *Environ Sci Technol*. Published online 2019.

20. Wong JPS, Carslaw N, Zhao R, Zhou S, Abbatt JPD. Observations and impacts of bleach washing on indoor chlorine chemistry. *Indoor Air*. 2017;27:1082-1090.